

Master's thesis

NTNU
Norwegian University of Science and Technology

Kristine Eriksen Eia

Characterisation of pyroxene and olivine in the Tellnes deposit

With focus on types, occurrences and physical
properties for separation

Master's thesis in MGEOL - Bedrock and Resource Geology

Supervisor: Kurt Aasly

July 2020



Norwegian University of
Science and Technology

Kristine Eriksen Eia

Characterisation of pyroxene and olivine in the Tellnes deposit

With focus on types, occurrences and physical properties for separation

Master's thesis in MGEOL - Bedrock and Resource Geology
Supervisor: Kurt Aasly
July 2020

Norwegian University of Science and Technology



Norwegian University of
Science and Technology



Norwegian University of
Science and Technology

Characterisation of pyroxene and olivine in the Tellnes deposit

- Focus on types, occurrences and physical properties for separation

Kristine Eriksen Eia

MGEOL Bedrock and resource geology

Supervisor: Kurt Aasly, NTNU

Co-supervisors: Rune Berg-Edland Larsen, NTNU
Marte Kristine Tøgersen, Titania AS
Åsa Barstad, Titania AS

Submission: July 2020

Norwegian University of Science and Technology
Department of Geoscience and Petroleum

ABSTRACT

The Tellnes deposit is one of the worlds largest ilmenite deposits. The orebody was detected by aeromagnetic surveying in 1954 and has been continuously mined by Titania AS since 1960. Titania produces an ilmenite rich concentrate of 44% TiO₂, including a magnetite- and a sulphide concentrate. The concentrate is used as a raw material for the production of a white titanium oxide pigment.

The ore show chemical and mineralogical variations, which can be challenging in relation to the processing of the ore. Ore mixing are mainly based on the content of TiO₂ and Cr₂O₅, but there is an increasing focus on alteration zones and associated minerals as well as variations of pyroxene and olivine. The mineral processing is based on gravitational and magnetic methods, thus, the specific gravity and magnetic properties are essential criteria for how a mineral behaves through the process and if it ends up in concentrate or tailings. Pyroxene and olivine can be challenging in gravity and magnetic separation, due to the minerals' high specific gravity and magnetic properties and may therefore be separated into the concentrate instead of the tailings. This may be a consequence of a high content of iron or related to poor liberation.

This thesis presents a detailed study of the pyroxene and the olivine in the Tellnes deposit with the focus on types, occurrences and physical properties for separation. Thin section microscopy and EPMA-analyses have been used to investigate chemical and mineralogical properties for olivine and pyroxene. Drill core sections have been crushed, ground and processed through gravity and magnetic separation, with continuous mineralogical and chemical analyses to investigate how the different types of pyroxene and olivine behaves through gravity and magnetic separation.

Results show rather small chemical variations among the olivine and the pyroxenes. Liberation and association data shows that olivine and pyroxene occurs as liberated or as composite grains, often associated with magnetite or ilmenite in stronger magnetic concentrates. It has therefore been suggested that the reason why olivine and pyroxene may end up in the concentrate is a combination of poor mineral liberation and magnetic properties.

SAMMENDRAG

Tellnesforekomsten er en av verdens største ilmenittforekomster. Forekomsten ble oppdaget ved flymagnetometriske målinger i 1954 og har vært i kontinuerlig drift av Titania AS siden 1960. Titania produserer et ilmenittrikt konsentrat på 44% TiO₂, inkludert et magnetitt- og et sulfidkonsentrat. TiO₂-konsentratet blir brukt som råmateriale for produksjonen av et hvitt titandioksidpigment.

Malmen på Tellnes har kjemiske og mineralogiske variasjoner som kan skape utfordringer i oppredningsverket. Per i dag styres malmblandinger hovedsakelig basert på TiO₂-innhold og Cr₂O₅-innhold, men der er også et økende fokus på omvandlingssoner og mineraler assosiert med disse samt variasjoner av oliven og pyroksen. Oppredningen er basert på gravitative- og magnetiske metoder og mineralenes egenvekt og magnetiske egenskaper vil derfor påvirke hvordan de oppfører seg gjennom prosessen og om de ender opp i konsentratet eller avgangen. Pyroksen og oliven kan skape problemer i tyngdekraft- og magnetseparasjon på grunn av mineralenes høye egenvekt og magnetiske egenskaper. Dette kan være en konsekvens at et høyt jerninnhold eller skyldes dårlig frimaling.

Oppgaven presenterer et detaljert studie av pyroksen og oliven i Tellnesmalmen, med fokus på variasjoner, fordelingen i bruddet, og hvordan mineralene oppfører seg i oppredningsprosessen. Mikroskopering og EPMA-analyser har blitt brukt for å undersøke de kjemiske- og mineralogiske egenskapene til pyroksen og oliven. For å undersøke hvordan de ulike typene pyroksen og oliven oppfører seg i tyngdekraft- og magnetseparasjon har 6 kjerneprøver blitt knust, malt og prosessert.

Resultatene viser forholdsvis små kjemiske variasjoner i oliven og pyroksen i de analyserte kjerneprøvene. Frimalings- og assosiasjonsdata viser at oliven og pyroksen i de sterkt magnetiske konsentratene forekommer som frimalede korn eller som halvkorn med enten magnetitt eller ilmenitt. Det er derfor foreslått at grunnen til at uønskede mengder oliven og pyroksen går i konsentratet er en kombinasjon av magnetiske egenskaper og dårlig frimaling.

ACKNOWLEDGEMENTS

I would like to start off by giving a special thanks to my supervisor Kurt Aasly, IGP, NTNU. I am very grateful for all the help and guidance I have been given throughout this work, despite him being on the other side of the world. Also a special thanks to co-supervisor Rune Berg-Edland Larsen.

I would like to offer a special thanks to Titania AS, with co-supervisors Marte Kristine Tøgersen and Åsa Barstad, for funding and giving me the opportunity to work with such an interesting project. I'm very grateful for all help and support I have been given. The Norwegian Laboratory for Mineral and Materials Characterisation, MiMaC, NFR project number 269842/F50, is acknowledged for the analyses performed on EPMA and Automated Mineralogy. I wish to thank Ben Snook for his help and guidance with the SEM-analyses, and Kristian Drivenes for running the EPMA-analyses.

A special thanks to Kjetil Rehaug-Sletvold at the Mineral Processing Laboratory, IGP, NTNU, for helping me with the mineral processing, and Erik Larsen, for help and valuable discussions. I would also extend my thanks to Torill Sørlokk and Laurentius Tijhuis at the Chemical/Mineralogical Laboratory.

I think we can all agree on that these past few months have been rough! Significant measures was introduced by the Government due to the Covid-19 outbreak and late nights with friends at the study hall were replaced with something comparable to isolation. However, the internet made it possible to stay in contact and since we could not be there for each other physically, digitally was the second best. I would therefore like to thank my good friends, I could not have done this without you and you have made these last years unforgettable. I would also like to thank my family and my great roommates Tiril and Aksel. Lastly I would like to thank my father, for his encouragement and support, it means a lot.

TABLE OF CONTENTS

ABSTRACT	III
SAMMENDRAG.....	V
ACKNOWLEDGEMENTS.....	VII
LIST OF FIGURES	XI
LIST OF TABLES	XIII
ABBREVIATIONS	XV
1 INTRODUCTION	1
1.1 MOTIVATION.....	1
1.2 AIMS OF THE STUDY	2
1.3 TITANIA AS	2
1.4 THE PRODUCTION OF TiO ₂	2
1.5 THE PROCESSING OF THE TELLNES ORE	3
2 REGIONAL GEOLOGY.....	7
2.1 THE ROGALAND ANORTHOSITE PROVINCE	7
2.2 THE ÅNA-SIRA MASSIF	8
2.3 GEOLOGY OF THE TELLNES DEPOSIT	9
2.3.1 <i>MAIN TELLNES ORE</i>	14
2.3.2 <i>SKOGESTAD AREA</i>	16
3 METHODS	17
3.1 SAMPLING.....	17
3.2 OPTICAL MICROSCOPY	21
3.3 SCANNING ELECTRON MICROSCOPY - SEM	22
3.4 ELECTRON PROBE MICROANALYSIS - EPMA	23
3.5 PROCESS DESCRIPTION	24
3.5.1 <i>COMMINUTION</i>	24
3.6 SHAKING TABLE SEPARATIONS - NTNU	25
3.7 SHAKING TABLE SEPARATIONS - TITANIA	25
3.8 WET HIGH-INTENSITY MAGNETIC SEPARATION	26
4 RESULTS.....	29
4.1 MINERALOGICAL DESCRIPTIONS	29
4.1.1 <i>SILICATES</i>	29
4.1.2 <i>OXIDES</i>	39
4.1.3 <i>SULPHIDES</i>	41
4.2 MINERAL PROCESSING	43
4.3 SHAKING TABLE SEPARATIONS IGP, NTNU	44
4.4 SHAKING TABLE SEPARATIONS TITANIA	47
4.5 WET HIGH-INTENSITY MAGNETIC SEPARATION	50
4.5.1 <i>STRONG MAGNETIC CONCENTRATE 148 AMPERE</i>	53
4.5.2 <i>MAGNETIC CONCENTRATE 348 AMPERE</i>	53
4.5.3 <i>MAGNETIC CONCENTRATE 548 AMPERE</i>	54
4.5.4 <i>WEAK MAGNETIC CONCENTRATE 778 AMPERE</i>	55
4.5.5 <i>NON-MAGNETIC MATERIAL</i>	56
5 DISCUSSION	57
5.1 MINERALOGICAL VARIATIONS	57
5.2 SHAKING TABLE SEPARATIONS	59
5.1 MAGNETIC PROPERTIES VERSUS LIBERATION	61
6 CONCLUSION.....	65
7 FURTHER WORK	66

REFERENCES.....	67
APPENDIX A – DRILL CORE SECTIONS	69
APPENDIX B – THIN SECTION SCANS	72
APPENDIX C – EPMA-ANALYSES	79
APPENDIX D – SEM ANALYSES	94
APPENDIX E – SEM ELEMENT MAPS.....	95

LIST OF FIGURES

Figure 1. Simplified flow sheet of the mineral processing at Tellnes. Figure provided by Titania AS.....	4
Figure 2. The cross section of the different facilities at Titania AS. Figure provided by Titania AS.	5
Figure 3. Geological map of the Rogaland Anorthosite Province. Vt: Vettaland dyke; Vs:Værslund dyke; Vb: Varberg dyke; L: Lomland dyke; K: Koldal intrusion; Hl: Håland dyke; S: Storgangen deposit; Bs: Bøstølen intrusion; Bf: Pegmatite norite of the Blåfjell deposit; T': Tellnes deposit; T: Tellnes dyke; Hg: Hogstad layered intrusion. From Duchesne (2001)	7
Figure 4. Geological map of the Tellnes deposit, with associated dikes. From Krause <i>et al.</i> (1985).....	11
Figure 5. The placement of the Tellnes deposit in relation to the Åna-Sira Massif and the Jøssingfjord (11)....	12
Figure 6. An overview of the open pit at Tellnes. The main ore extends from section S-1350 to section S-600, whilst the Skogestad area extends from section 6 to section -3.5.....	14
Figure 7. (A) The location of the cross section on the map of the Tellnes deposit. (B) The cross section of section 800, showing the spatial distribution of the different zones in a vertical profile section. The bold lines are drill hole collars with numbers indicating depth. UMC = Upper Marginal Zone, UCZ = Upper Central Zone, LMZ = Lower Marginal Zone, LCZ = Lower Central Zone. Figure modified after Charlier <i>et al.</i> (2006).	15
Figure 8. The figure gives the spatial distribution of the chosen drill hole collars in the open pit. All collars are located within the Skogestad area of the pit. The respective coordinates, sample interval and chemical and mineralogical data is given in table x. and table x., respectively.....	18
Figure 9. A) Coarse-grained orthopyroxene, with brown iron-oxide exsolution lamellas and inclusions of ilmenite in PPL (thin section 0.5V-3N). B) Picture A) in XPL. Abbreviations: Opx – orthopyroxene, Ilm – ilmenite, Pl – plagioclase.....	31
Figure 10. Orthopyroxene (grey) with white exsolution lamellas. The figure shows the points set for EPMA-analyses, with the corresponding chemical analyses given in Table 7.....	33
Figure 11. A) Orthopyroxene partly altered to clinopyroxene in PPL (thin section 3,5V-1S). B) Picture A) in XPL. Abbreviations: Opx – orthopyroxene, Cpx – clinopyroxene, Pl – plagioclase, Ilm – ilmenite	35
Figure 12. A) Olivine, plagioclase, biotite and ilmenite in PPL (drill core -3.5V-2N). B) Picture A) in XPL. Abbreviations: Opx – orthopyroxene, Cpx – clinopyroxene, Pl – plagioclase, Ilm – ilmenite, Bt – biotite.	36
Figure 13. Ilmenite and magnetite with straight spinel exsolution lamellae in transmitted lightning (drill core -3.5V-2N). Abbreviations: Ilm – ilmenite, Mag – magnetite.	40
Figure 14. Various sulphides in transmitted lightning (drill core 3.0V-4N). Abbreviations: Ccp – chalcopyrite, Po – pyrrhotite, Pn – pentlandite.	42
Figure 15. Flow sheet of the mineral processing.....	43
Figure 16. Modal mineralogy (analysed by XRD) of the strong magnetic products (148 ampere) from WHIMS. Values are given in wt% and normalized to 100%.....	53
Figure 17. Modal mineralogy (analysed by XRD) of the magnetic products (348 ampere) from WHIMS. Values are given in wt% and normalized to 100%.....	54
Figure 18. Modal mineralogy (analysed by XRD) of the magnetic products (548 ampere) from WHIMS. Values are given in wt% and normalized to 100%.....	54
Figure 19. Modal mineralogy (analysed by XRD) of the weak magnetic products (778 ampere) from WHIMS. Values are given in wt% and normalized to 100%.....	55
Figure 20. Modal mineralogy (analysed by XRD) of the non-magnetic products from WHIMS. Values are given in wt% and normalized to 100%.....	56
Figure 21. A) Coarse-grained orthopyroxene, with inclusions of ilmenite and biotite in PPL (thin section 3.5V-1S). B) Picture A) in XPL. Abbreviations: Opx – orthopyroxene, ilm – ilmenite, Pl – plagioclase.	58
Figure 22. A) Coarse-grained orthopyroxene, with brown iron-oxide exsolution lamellas and inclusions of ilmenite in PPL (thin section 3.0V-4N). B) Picture A) in XPL. Abbreviation: Opx – orthopyroxene.....	58

LIST OF TABLES

Table 1. The average chemical composition of the Tellnes ore after (Dybdahl, 1960).....	13
Table 2. An overview of the chosen drill core sections for the making of polished thin sections. Including the XYZ-coordinates for the respective drill hole collars and the chemical content by XRF-analyses provided by Titania, all values are given in wt%.....	19
Table 3. An overview of the chosen drill core sections for the making of polished thin sections. Including the XYZ-coordinates for the respective drill hole collars and the modal mineralogical content by XRD-analyses provided by Titania, all values are given in wt% and normalized to 100 %.....	20
Table 4. Crushed drill core sections chosen for mineral processing. 9 of the samples corresponds to the sample interval as chosen for polished thin section production, whilst 3 are from the following sample interval and 1 is from the preceding.....	21
Table 5. Samples and section types chosen for SEM-analyses conducted at IGP, NTNU.....	23
Table 6. Average chemical composition (wt% oxides) of the 12 analysed orthopyroxenes, retrieved from EPMA-data.....	30
Table 7. Average chemical composition (wt% oxides) of 6 analysed Fe-Oxide lamellas in orthopyroxene, retrieved from EPMA-data. Figure x. show the location of the analysed lamellas.....	32
Table 8. Average chemical composition (wt% oxides) of 3 clinopyroxenes, retrieved from EPMA-data.....	34
Table 9. Average chemical composition (wt% oxides) of 5 olivines, retrieved from EPMA-data.....	36
Table 10. Average chemical composition (wt% oxides) of the two mica-varieties, retrieved from EPMA-data.....	37
Table 11. Average chemical composition (wt% oxides) of plagioclase, retrieved from EPMA-data.....	38
Table 12. Average chemical composition of ilmenite and spinel exsolution lamellas (wt%). Data retrieved from EPMA-analyses performed on 4 ilmenite grains and 2 spinel lamellas.....	40
Table 13. Average chemical composition (wt%) of the analysed sulphides, retrieved from EPMA-data.....	41
Table 14. Overview of samples, with the respective running time, feed-, concentrate-, middling-, and tailings size from the shaking table analyses performed at IGP, NTNU. The shaking table separations were run with an average feed flow rate of 2.87 kg/h, 200 L/h wash water and 270 L/h water for feed distribution.....	44
Table 15. Analyses of the modal mineralogy by XRD of the products from the gravity separation performed with a shaking table at the Mineral Processing Laboratory, IGP, NTNU. Each sample is separated into; concentrate, middling and tailings. Table 14. gives an overview of the respecting sample sizes. Analyses were performed at Titania and all values are normalized and given in wt%.....	45
Table 16. Bulk chemical analyses by XRF of the products from gravity separation, performed with a shaking table at the Mineral Processing Lab, IGP, NTNU. Each sample is separated into; concentrate, middling and tailings. Table 14. gives an overview of the respecting sample sizes. Analyses were performed at Titania and values are given in wt%.....	46
Table 17. Overview of samples, with the respective running time, feed-, concentrate-, middling-, and tailings size from the shaking table analyses performed at Titania. The shaking table separations were run with an average feed flow rate of 13.17 kg/h. Sample 1-6 were run with a water flow of 600 L/h, sample 7-8; 650 L/h and sample 13-14; 850 L/h.....	47
Table 18. Analyses of the modal mineralogy by XRD of the products from the gravity separation performed with a shaking table at Titania. Each sample is separated into; concentrate, middling and tailings. Table 17. gives an overview of the respecting sample sizes. Analyses were performed at Titania and all values are normalized and given in wt%.....	48
Table 19. Bulk chemical analyses by XRF of the products from gravity separation, performed with a shaking table at Titania. Each sample is separated into; concentrate, middling and tailings. Table 17. gives an overview of the respecting sample sizes. Analyses were performed at Titania and values are given in wt%.....	49
Table 20. Results from Wet-High-Intensity Magnetic Separation (WHIMS) with the respective sample size per field strengths; 148, 348, 548, 778 ampere.....	50
Table 21. Analyses of the modal mineralogy by XRD of the products from magnetic separation. Table 20. gives an overview of the respecting sample sizes. All values are normalized and given in wt%.....	51
Table 22. Bulk chemical analyses by XRF of the products from magnetic separation. Table 20. gives an overview of the respecting sample sizes. Values are given in wt%.....	52
Table 23. Comparison of the average chemical composition (wt% oxides) of the two different types of orthopyroxenes, retrieved from EPMA-data.....	58
Table 24. Shaking table feeds with the respective ilmenite, orthopyroxene, clinopyroxene and olivine content (wt%), modal mineralogy analysed by XRD.....	59
Table 25. Shaking table concentrates with the respective ilmenite, orthopyroxene, clinopyroxene and olivine content (wt%), modal mineralogy analysed by XRD.....	60

ABBREVIATIONS

COORD Coordinate

EPMA Electron Probe Microanalysis

HGMS High Gravity Magnetic Separator

IGP Department of Geoscience and Petroleum (Norwegian: Institutt for geovitenskap og petroleum)

LIMS Low Intensity Magnetic Separator

NTNU Norwegian University of Science and Technology (Norwegian: Norges teknisk-naturvitenskapelige universitet)

PPL Plane Polarised Light

SEM Scanning Electron Microscope

WHIMS Wet High-Intensity Magnetic Separation

XPL Cross Polarised Light

XRD X-ray Diffraction

XRF X-ray Fluorescence

1 INTRODUCTION

1.1 MOTIVATION

The Tellnes ore deposit, operated by Titania AS, show chemical and mineralogical variations, which can be challenging in relation to the processing of the ore. The mineral processing is based on gravitational and magnetic methods, thus, the specific gravity and magnetic properties are essential criteria for how a mineral behaves through the process and if it ends up in concentrate or tailings.

As of today, ore mixing are mainly based on the content of TiO_2 and Cr_2O_5 , but there is an increasing focus on alteration zones and associated minerals as well as variations of pyroxene and olivine in the deposit. Pyroxene and olivine can be challenging in gravity and magnetic separation, due to the minerals' high specific gravity and magnetic properties. As a consequence, these minerals may be separated into the concentrate instead of the tailings. This may be due to a high content of Fe, but can also be related to poor liberation. A particle containing ilmenite and pyroxene will have a high specific gravity and may therefore be challenging in relation to the concentrate quality.

The amount of olivine and pyroxene a blast can contain before it affects the quality of the concentrate has been previously investigated and a limit of 15% has been defined, based only on operational experience. The different variants of orthopyroxene, clinopyroxene and olivine, based on chemical composition can also affect how particles containing these minerals behave both in gravity and magnetic separation. It is therefore necessary with further investigations to define a total limit or a separate limit for each mineral. It is also of interest to investigate if there are spatial variations that must be taken into account in production planning.

1.2 AIMS OF THE STUDY

This Master's project were carried out at NTNU in collaboration with Titania AS. The project intents to define the chemical and mineralogical properties for olivine and pyroxene, giving a spatial distribution, by drill core analysis, microscopy and with the use of various analysing tools.

Process mineralogy will be used to observe the performance of the different variations of pyroxene and olivine through gravity and magnetic separation. Malvik (2014) defines process mineralogy as following: "Process mineralogy relates the physical, chemical, mineralogical and textural properties of the mineral raw materials to their behaviour in the process, to product quality and the utilization of the mineral products". Drill cores will be processed through crushing, grinding and separated with gravitational and magnetic methods, with continuous mineralogical and chemical analyses. The end products will be analysed with a Scanning Electron Microscopy (SEM) investigating modal mineralogy, mineral classification, mineral associations, locking and liberation.

1.3 TITANIA AS

Titania AS is a Norwegian mining company, founded in 1902, and one of the world's largest producers of ilmenite concentrate. They operate the Tellnes ore deposit, which is the second most important ilmenite deposit in the world, after Lake Tio deposit, Canada (Duchesne, 1999). Titania AS is owned by the American company Kronos Worldwide Inc (former National Lead Ltd.). The ore deposit is located at Hauge i Dalane in Sokndal municipality in Rogaland county, Southwest Norway. Titania produces an ilmenite rich concentrate of 44% TiO_2 , including magnetite- and sulphide concentrates as by-product from the processing of the ore. The concentrate is used as a raw material for the production of a white titanium oxide (TiO_2) pigment.

1.4 THE PRODUCTION OF TiO_2

The production of a white TiO_2 -pigment constitutes over 90% of the world's TiO_2 -consumption, only a small part (ca. 5%) is produced as titanium metal. The white TiO_2 pigment has excellent light refractive properties, which gives the pigment good opacity and clear colours. It is a non-reactive material with no harmful health or environmental effects (NGU, 2015a). The pigment is primarily used in paints, paper, and plastic as well as in

cosmetics, such as in sunscreen, and as a food additive (E-171). Titanium metal has a relatively low weight, high strength, resistant against corrosion and can endure very high temperatures. Titanium alloys are therefore widely used in the aerospace industry and in high corrosion environments (Kofstad & Pedersen, 2019).

1.5 THE PROCESSING OF THE TELLNES ORE

The ore is extracted from the open pit at Tellnes and transported by articulated haulers from the pit to the primary crusher where the ore is reduced to pieces of 20-30 cm. A simplified flow sheet of the mineral processing is given in Figure 1. From the primary crusher the material goes into two silos before being transported on conveyor belts to Hommedal. At Hommedal the material goes through additional crushing followed by wet grinding in ball mills.

The ball mill product (<390 µm) goes to low-intensity magnetic separation (LIMS) separating out magnetite. The magnetite from LIMS goes through several LIMS- steps and flotation before the final product is sent to the drying facility by Jøssingfjord. Tailings from LIMS and flotation goes to sulphide flotation. The non-magnetic fraction from the first LIMS-separation is further separated with three different methods; spirals, magnetic separation and flotation. The material is first separated with primary cyclones, which separates the material into a coarse and a fine fraction. The coarse fraction goes to spirals in the gravity separation plant, whilst the fine fraction goes to HGMS and flotation.

In the gravity separation plant the coarse fraction is further divided into a second coarse and a fine fraction. The spirals consists of roughers, cleaners and scavengers. The ilmenite concentrate is transported from the processing plant at Hommedal through pipelines approximately 4 km to the drying plant by Jøssingfjord, where the final part of the process takes place.

At the drying plant the ilmenite concentrate undergoes an acid leaching process and reverse flotation, to reduce the content of sulphides and oil residues. In the flotation process tall oil, paraffin and sulphuric acid is used to give the ilmenite the necessary surface treatment. Figure 2. shows a cross section of the facilities at Titania AS and how they are connected.



Flytskjema - Mineralseparering

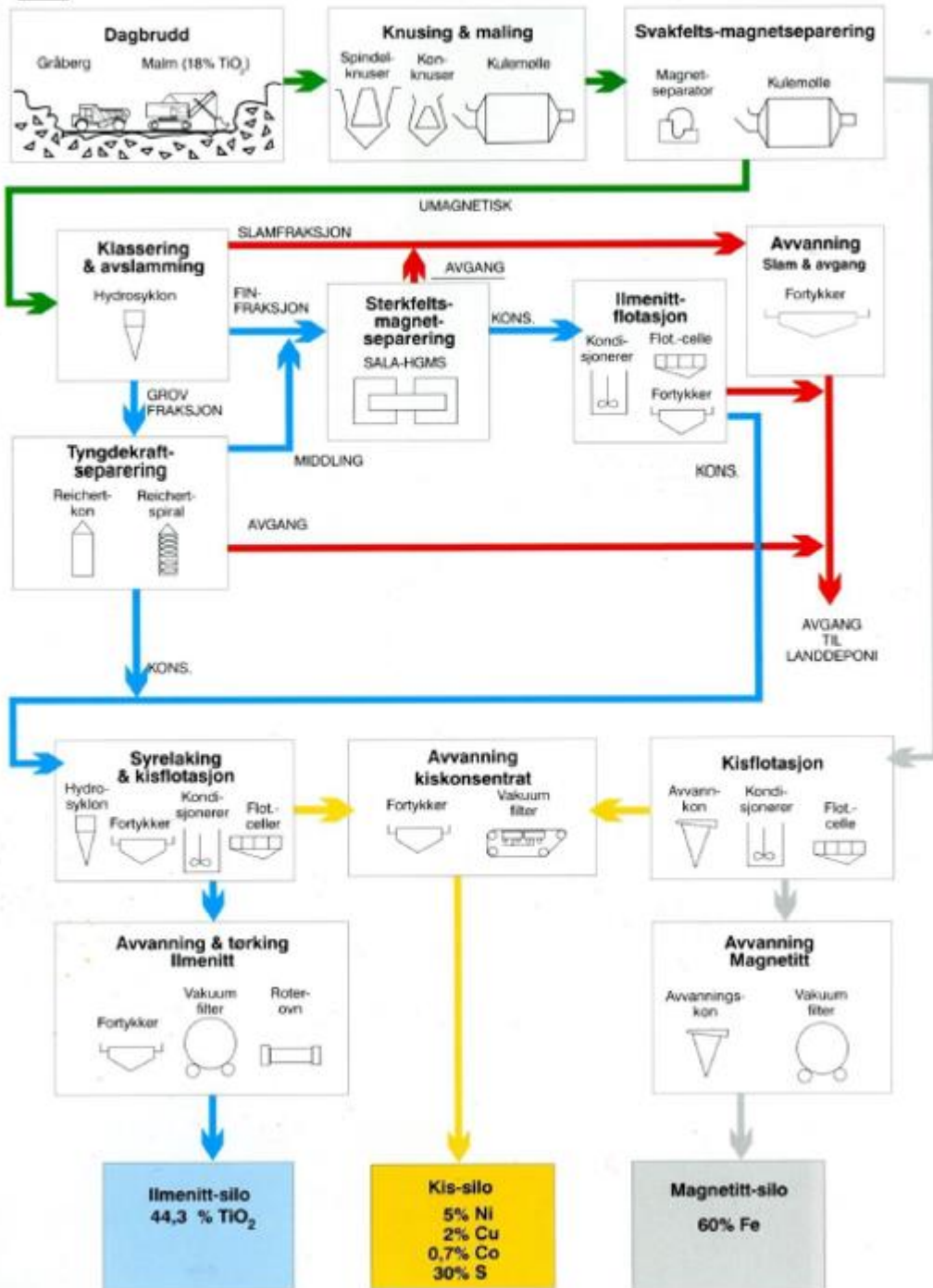


Figure 1. Simplified flow sheet of the mineral processing at Tellnes. Figure provided by Tellnes AS.

THE TELLNES PLANT

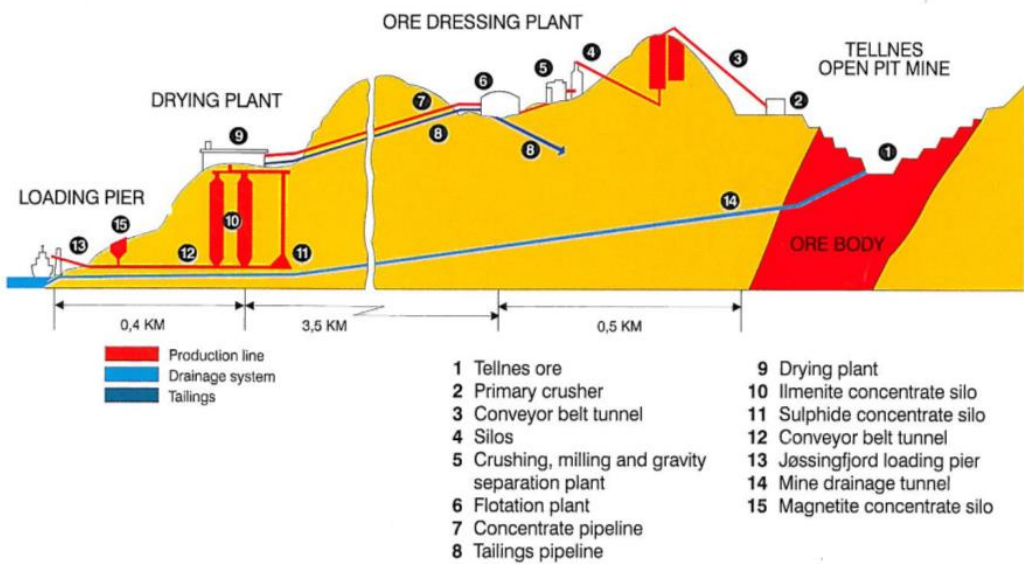


Figure 2. The cross section of the different facilities at Titania AS. Figure provided by Titania AS.

2 REGIONAL GEOLOGY

2.1 THE ROGALAND ANORTHOSITE PROVINCE

The Rogaland Anorthosite Province (also referred to as the Egersund Igneous Complex) is an igneous province located in the southwestern part of the exposed Sveconorwegian orogenic belt in Rogaland-Vest-Agder (Duchesne, 2001). The province is made up of three large anorthositic massifs; The Egersund-Ogna Massif, Håland-Helleren Massif and the Åna-Sira Massif. The latter will be described further in the next section. Including a large layered lopolith, the Bjerkreim-Sokndal layered intrusion, two smaller leuconoritic bodies (Hidra and Garsaknatt) and to the south three acidic intrusives; the Farsund charnockite, the Lyngdal granodiorite and the Kleivan granites (Maijer & Padget, 1987). Figure 3. gives a geological map of the Rogaland anorthosite province.

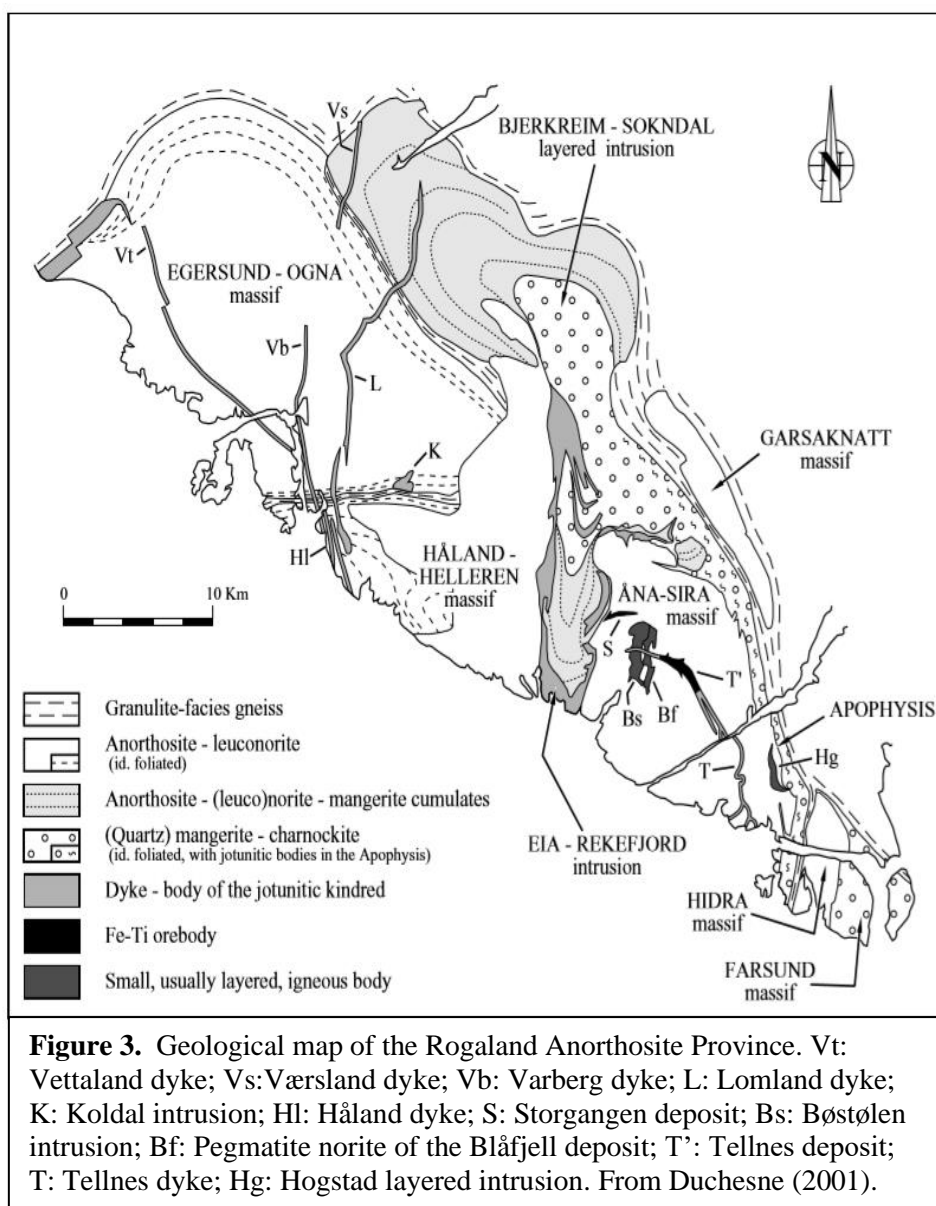


Figure 3. Geological map of the Rogaland Anorthosite Province. Vt: Vettaland dyke; Vs: Værsland dyke; Vb: Varberg dyke; L: Lomland dyke; K: Koldal intrusion; HI: Håland dyke; S: Storgangen deposit; Bs: Bøstølen intrusion; Bf: Pegmatite norite of the Blåfjell deposit; T': Tellnes deposit; T: Tellnes dyke; Hg: Hogstad layered intrusion. From Duchesne (2001).

2.2 THE ÅNA-SIRA MASSIF

The Åna-Sira Anorthosite Massif is located in the south-east of the province and covers an area of about 200 km². It is mostly made up of coarse-grained andesine anorthosite and leuconorite as well as several intrusions of norite, norite-ilmenite, mangerite and jotunite (Krause *et al.*, 1985; Krause & Pedall, 1980; Zeino-Mahmalat & Krause, 1976). U-Pb dating performed by Schärer *et al.* (1996) estimates an emplacement age of 932 ± 3 Ma.

Andesine anorthosite consists of more than 90% plagioclase with 40-50% An and about 3% Or. Minor constituents are orthopyroxene, clinopyroxene, ilmenite, biotite and accessory apatite as well as sulphides such as pyrrhotite, pyrite and secondary magnetite (Krause & Pedall, 1980; Zeino-Mahmalat & Krause, 1976).

The Massif is structurally characterized by Krause *et al.* (1985) as a brachy-anticlinorium, folded along non-linear N-S axes with an additionally domed crest. It is surrounded by the layered Bjerkreim-Sokndal layered intrusion in the north and west, from which Åna-Sira is cut by several intrusions, the Hidra Anorthosite/Leuconorite in the east and forms the coastal border to the North Sea in the south (Krause *et al.*, 1985). The location of the Åna-Sira Massif in relation to the Rogaland Anorthosite Province is shown in Figure 3.

Åna-Sira essentially hosts the largest and most important Fe-Ti ore-deposits in the Rogaland Anorthosite Province in addition to several smaller deposits. The main deposits are the Tellnes-, Storgangen- and the Blåfjell deposits. The Tellnes deposit is the only one being currently operated, but both Storgangen and the Blåfjell deposit have been operated in the past. Blåfjell was mined as an iron ore during two periods, from 1863-1865 and 1869-1876, where a total of 90 000 t were exported mainly to England. Storgangen were mined in the period from 1916-1965 for the production of an ilmenite concentrate for the pigment industry (17-19% TiO₂) and a magnetite concentrate. The total production yielded more than 10 Mt of concentrate. The Tellnes deposit has been continuously mined since 1965 for the production of ilmenite concentrate for the pigment industry (44%). Tellnes has an annual production of approximately 850 000 t ilmenite (KRONOS, n.d.) in addition to a magnetite- and a sulphide-concentrate.

They are representing three different geological, petrological and mineralogical types (Krause *et al.*, 1985). The Blåfjell-ore is coarse-grained, containing thick, close to monomineralologic

layers of ilmenite, whilst the Storgangen and the Tellnes deposit are medium and fine-grained respectively (NGU, 2015b; 2017).

2.3 GEOLOGY OF THE TELLNES DEPOSIT

The Tellnes Deposit has been described and interpreted by several after its discovery in 1954. Petrographic and mineralogic descriptions are given in both (Gierth & Krause, 1973), (Krause *et al.*, 1985), (Wilmart *et al.*, 1989), (Dybdahl, 1960) and (Charlier *et al.*, 2006).

The Tellnes Deposit is an ilmenonite body, situated in the central part of the Åna-Sira Anorthosite Massif, approximately 4 km NE of Jøssingfjord. The orebody was detected by aeromagnetic surveying in 1954 with the production starting 6 years later. The orebody is shaped as a trough and extends in NW-SE direction with a length of approximately 2700 m and a width of 400 m in the central part of the orebody, reaching a depth of at least 60 m below sea level (Dybdahl, 1960; Gierth & Krause, 1973). Figure 4. show a geological map of the deposit. The placement of the deposit in relation to the Åna-Sira Massif and the Jøssingfjord is shown in Figure 5.

The orebody was intruded into the surrounding anorthosite, which is evidenced by sharp contacts, intrusive breccias, xenoliths of anorthosite and several apophyses cutting into the anorthosite (Wilmart *et al.*, 1989). The orebody extends into the main Tellnes dyke on both ends, which is 5 to 10 m thick and ranges in composition from jotunite to quartz mangerite. Two distinct faults cuts the ore, The Hommedal and the Tellnesvatn fault including several smaller fracture systems, see Figure 4. Both the ore and the surrounding anorthosite are intersected by several WNW-ESE diabase dykes.

The orebody is dated by Schärer *et al.* (1996) to 920 ± 3 Ma, whilst the Tellnes dyke is dated to 931 ± 5 , indicating that these were not comagmatic, although both units were emplaced in the same dyke structure (Schärer *et al.*, 1996). Another factor supporting this theory is the difference in Sr-isotope ratios between the orebody and the dyke Wilmart 1989. The deposit is interpreted as a noritic cumulate, emplaced as a crystal mush, lubricated by a Fe-Ti rich intercumulus liquid. The high ilmenite content is mainly due to a mechanical sorting during emplacement (Duchesne, 1999). The crystal mush is assumed to be intruded into a weakness

zone, a local extensional faulting environment, emplacing it in the same structure as the Tellnes dyke (Diot *et al.*, 2003).

The ore is defined as an ilmenonorite. A norite is in general a coarse-grained igneous rock, mainly consisting of calcic plagioclase and orthopyroxene. It is generally similar to gabbro, but is predominantly composed of orthopyroxene, whilst gabbro is composed of clinopyroxene. Ilmenonorite is an ilmenite-rich norite, with the pyroxene varieties of high magnesian enstatite or an iron-bearing intermediate hypersthene (Strekeisen, n.d.). The ore is fine-grained, equigranular, dark in colour, with nearly black grains of ilmenite, surrounded by lighter grains of plagioclase and pyroxene. The average modal composition of the ore is: (vol%) plagioclase 53.2%, ilmenite 28.6%, orthopyroxene 10.2%, biotite 3.9%, magnetite 0.7% up to 2.5% and accessories 3.4%. There are observed up to 24 different accessory minerals such as; apatite, augite, olivine, aluminous spinel, hematite and different kinds of sulphides, such as pyrite, pyrrhotite, chalcopyrite, pentlandite and millerite (Krause *et al.*, 1985). Table 1. show the average chemical composition of the ore.

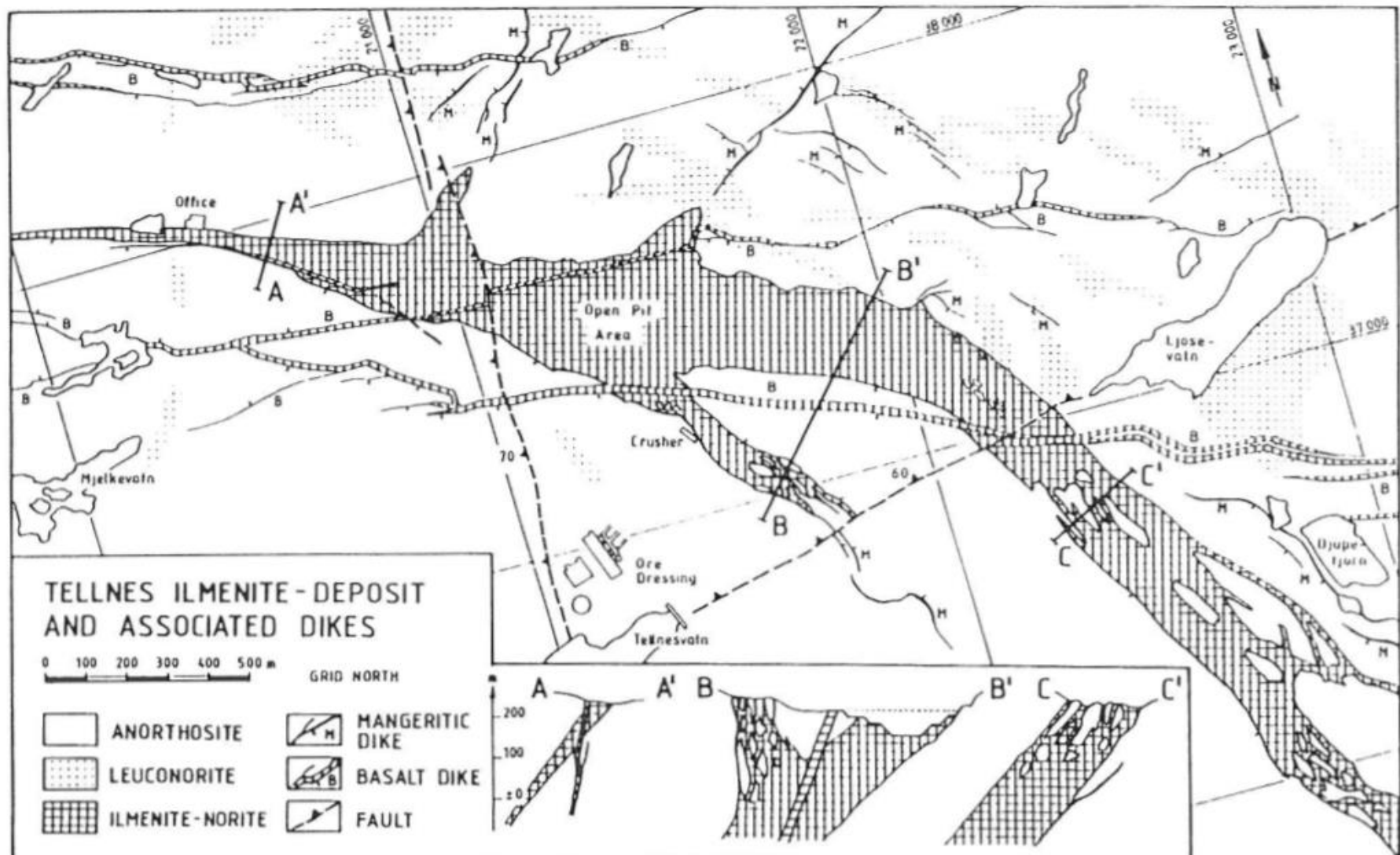


Figure 4. Geological map of the Tellnes deposit, with associated dikes. From Krause *et al.* (1985).

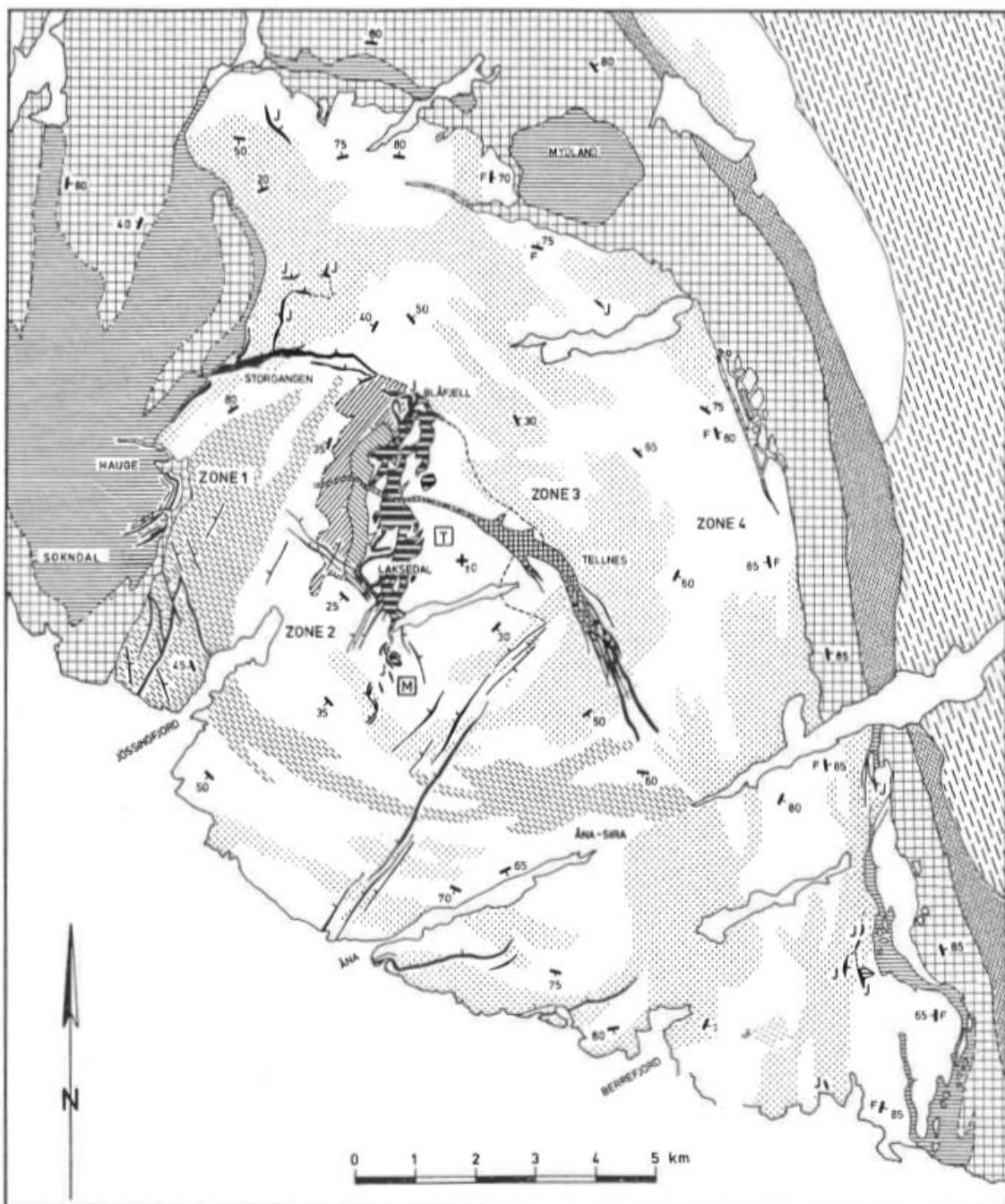


Figure 5. The placement of the Tellnes deposit in relation to the Åna-Sira Massif and the Jøssingfjord (11)

1: Charnockitic migmatites and gneisses; 2: Banded noritic-charnockitic gneisses; 3: Anorthosite; 4: Leuconorite; 5: Rhythmic bedding of anorthosite and leuconorite; 6-8: Noritic internides; 6: Layered intrusion of Bøstølen, poorly stratified upper part; 7: Layered intrusion of Bøstølen, stratified lower part; 8: Norite-pegmatite body of Blåfjell-Måkevatnet; 9: Noritic externides (Lopolith of Bjerkreim-Sokndal); 10: Norite, ilmenite-norite (J) and ilmenite (J) dikes; 11: Ilmenite-norite body of Tellnes; 12: Mangeritic externides (Lopolith of Bjerkreim-Sokndal); 13: Igneous layering and secondary foliation (F) From Krause & Pedall, (1980).

Table 1. The average chemical composition of the Tellnes ore after (Dybdahl, 1960).

SiO ₂	30.37 %
TiO ₂	18.40 %
FeO	17.43 %
Fe ₂ O ₃	7.25 %
FeS ₂	0.60 %
Al ₂ O ₃	11.70 %
MgO	6.13 %
CaO	4.39 %
MnO	0.18 %
P ₂ O ₅	0.20 %
K ₂ O	0.60 %
Na ₂ O	2.40 %

The plagioclase (An₄₅₋₄₂) is euhedral and commonly slightly bent and locally granulated. The orthopyroxene (En₇₇₋₇₅) varies between a Mg-rich enstatite and a Fe-bearing intermediate hypersthene. Exsolution lamellas of clinopyroxene and ilmenite are common as well as clinopyroxene rims in some grains. Ti-rich biotite are often associated with ilmenite and the majority of the hematite occurs as exsolution lamellas. Some of the ilmenite grains has needle shaped exsolutions of aluminous spinel, which are also common in magnetite (Krause *et al.*, 1985).

The mineralogical and chemical composition is fairly uniform throughout the deposit. There is chemical zoning across the orebody and there is a several metres wide marginal zone along the margins where the content of ilmenite is lower. A small zone of coarse-grained norite can often be observed at the sharp contact to the anorthosite (Gierth & Krause, 1973).

The mineralogy is relatively constant with more than 80% of any sample made up of plagioclase, orthopyroxene and ilmenite, however, with varying modal proportions. The Tellnes deposit is essentially a three phase cumulate of plagioclase, orthopyroxene and ilmenite with local cumulus olivine (Schiellerup *et al.*, 2003).

The Tellnes ore is divided into two different areas; the main ore and the Skogestad area. Figure 6. gives an overview of the open pit at Tellnes. There are distinctive mineral and chemical variations between the two areas, which will be further explained in the next sections.

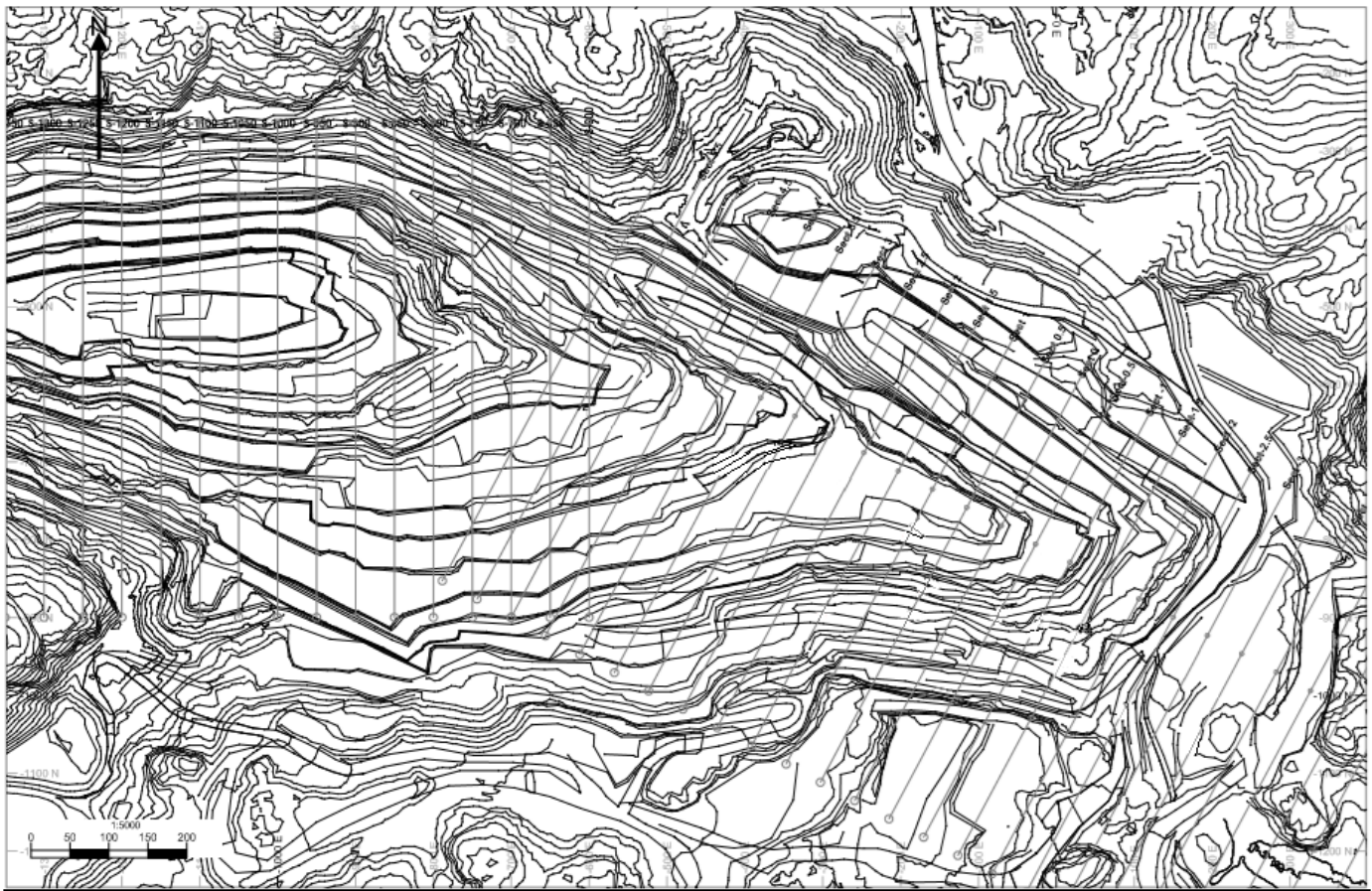


Figure 6. An overview of the open pit at Tellnes. The main ore extends from section S-1350 to section S-600, whilst the Skogestad area extends from section 6 to section -3.5.

2.3.1 MAIN TELLNES ORE

Extensive work has been done by (Kullerud, 2003; 2005; 2007; 2008) to understand the chemical content and variation throughout the Tellnes ore. The main ore, as described earlier, has chemical zoning, reflecting the variations in the modal content of the ore-forming minerals. Kullerud (2003) divides the orebody into 4 zones; the upper marginal zone (UMZ), the upper central zone (UCZ), the lower central zone (LCZ) and the lower marginal zone (LMZ) based on these variations.

The UMZ is situated between the UCZ and the contact to the anorthosite. According to Kullerud (2003) the UMZ shows low contents of ilmenite but high contents of plagioclase and Mg-Fe silicates, such as orthopyroxene, clinopyroxene and olivine. The UCZ constitutes the upper part of the intrusion. The content of ilmenite and the Mg-Fe silicates is generally high, with a lower content of plagioclase. The LMZ is situated between the LCZ and the contact to

the anorthosite. The ilmenite-content is lower whereas the content of plagioclase, orthopyroxene and clinopyroxene is higher. The LCZ shows the highest content of ilmenite and an intermediate content of plagioclase. The zone is low in Mg-Fe silicates with olivine being absent (Kullerud, 2003). Figure 7., modified after Charlier *et al.* (2006), shows the spatial distribution of the different zones in a vertical profile section.

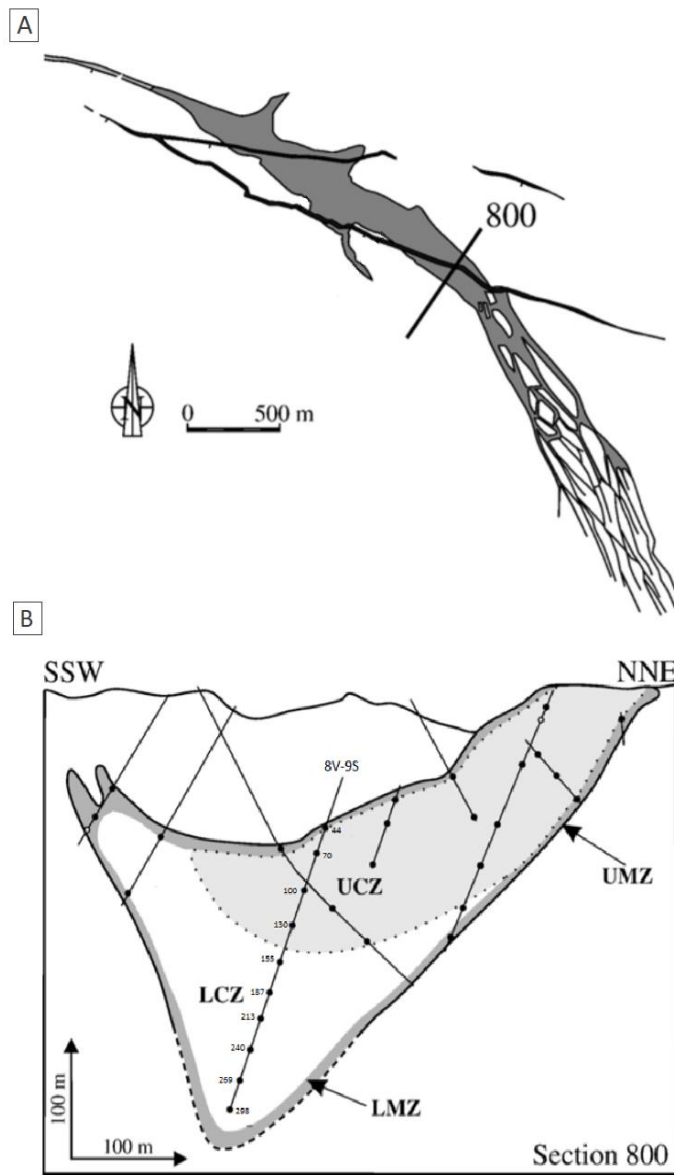


Figure 7. (A) The location of the cross section on the map of the Tellnes deposit. (B) The cross section of section 800, showing the spatial distribution of the different zones in a vertical profile section. The bold lines are drill hole collars with numbers indicating depth. UMC = Upper Marginal Zone, UCZ = Upper Central Zone, LMZ = Lower Marginal Zone, LCZ = Lower Central Zone. Figure modified after Charlier *et al.* (2006).

2.3.2 SKOGESTAD AREA

An internal rapport done by Kullerud (2005) show a group of Fe-rich samples in the Skogestad area with a composition that is distinctly different from the majority of the samples of the Tellnes ore. In addition, the concentrations of TiO_2 and Cr_2O_3 relative to FeO are lower compared to the main part of the ore. Based on the difference in chemical composition Kullerud (2008) have divided the Skogestad ore into 4 ore types, strictly based on the FeO and TiO_2 -content;

Type 1. Can generally be classified as chemically equivalent to the main Tellnes ore. Of the 4 types, type 1. have the highest content of TiO_2 and FeO .

Type 2. Classified as an intermediate between type 1. and type 3., without any clear chemical boundary. However the MgO and Cr_2O_3 -content in ilmenite differs from the main ore with a higher content of MgO and a lower content of Cr_2O_3 . The TiO_2 -content is higher than 13 wt%.

Type 3. Has a chemical composition which differs distinctively from the main ore. The content of MgO in ilmenite is significantly higher and the Cr_2O_3 is lower. Such as type 2., the TiO_2 -content is higher than 13 wt%. The content of magnetite and Fe-Mg silicates, such as olivine and orthopyroxene are also higher.

Type 4. The TiO_2 -content in type 4. is generally lower than 13 wt% and therefore not qualified as ore.

Type 2., 3. and 4. show a lower content than type 1. of Al_2O_3 , CaO , Na_2O generally controlled by the plagioclase content. Type 2., 3. and 4. has also a noticeably high content of magnetite, P, K and Mg. The P is from apatite, the K from biotite, whilst Mg constitutes as a main element in several minerals (Kullerud, 2008).

3 METHODS

3.1 SAMPLING

The Tellnes deposit shows local mineralogical variations within the deposit. Sampling is therefore based on the difference in mineralogy and chosen on the basis of XRD- and XRF-analysis performed at Titania. A total of 18 out of 40 available drill core sections were chosen for the making of polished thin sections. A complete list of the available drill core sections, including drill hole collar coordinates and XRD-data, provided by Titania are listed in Appendix A, Table A 2. An equivalent list with XRF-data is given in Table A 1.

Sections were selected with the emphasis of selecting the drill cores with the highest content of various minerals, such as the drill core with the highest content of ilmenite or the highest content of olivine and so on. A complete overview of the chosen drill core sections including XRF-data and XRD-data provided by Titania and the respective drill hole collars is given in Table 2. and Table 3., respectively.

The chosen drill cores are all drilled within the time period from 2004 to 2007. The spatial distribution of the drill hole collars is given in Figure 8. All samples are named after the corresponding drill core. The ore is divided into profile lines with the two first numbers indicating along which profile line it was drilled. Which means that drill core -2,5V-1L, was drilled along the -2,5V profile line. The next number and letter indicates the drill core number and the direction of drilling. 1L is therefore the first hole drilled along the specific profile line and was drilled vertically. The L stands for “loddrett” in Norwegian, meaning vertical. In addition to vertical drilling some cores are drilled in direction either to the north (N) or to the south (S).

For mineral processing, the intention was to process crushed drill core sections from the same drill cores as selected for the making of thin sections. Of 18 only 13 samples were found at the drill core storage at Titania. Of which 9 were from the exact same sample interval, whilst 4 were from either the prior or later sample interval. An overview of the drill core sections chosen for the mineral processing are given in Table 4.

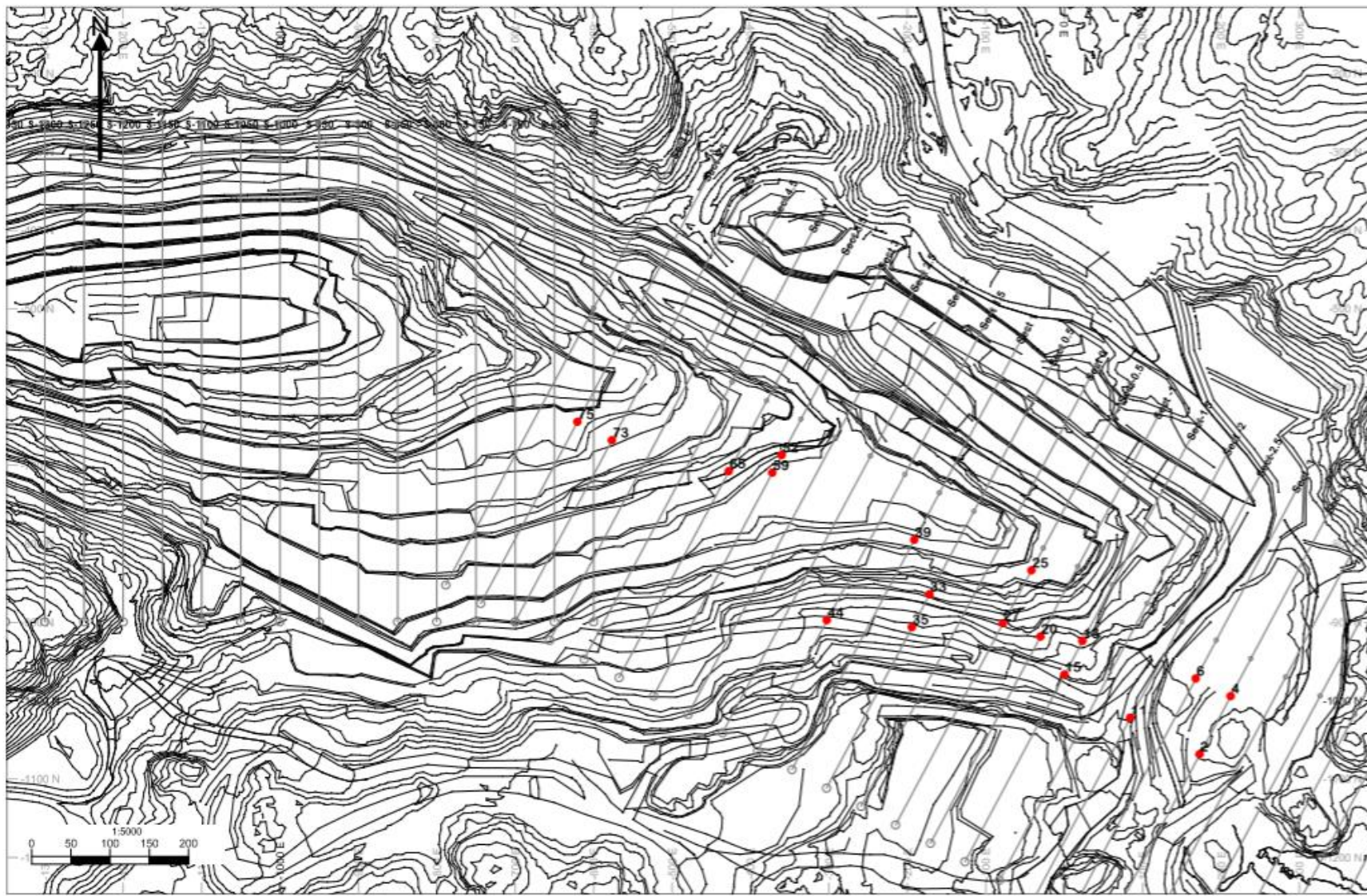


Figure 8. The figure gives the spatial distribution of the chosen drill hole collars in the open pit. All collars are located within the Skogestad area of the pit. The respective coordinates, sample interval and chemical and mineralogical data is given in table x. and

Table 2. An overview of the chosen drill core sections for the making of polished thin sections. Including the XYZ-coordinates for the respective drill hole collars and the chemical content by XRF-analyses provided by Titania, all values are given in wt%.

Sample Number	Exploration core	Length drill core (m)	X-COORD	Y-COORD	Z-COORD (m. a. sea level)	%Magn sm																					
						TiO ₂	P ₂ O ₅	S	Cr ₂ O ₃	Fe	SiO ₂	V ₂ O ₃	CaO	MgO	Al ₂ O ₃	MnO	K ₂ O	Na ₂ O	Zn	Ni	Cu	Co	Sr	Zr	Nb	Pb	
2	-3,5V-2N	71.0-71.2	173.2	-1068.98	213	16.523	0.301	0.231	0.034	17.727	31.982	0.083	3.983	8.929	11.009	0.160	0.738	1.866	0.019	0.031	0.019	0.015	0.041	0.019	< 0.0001	0.001	3.479
4	-3,5V-2N	191.0-191.2	212.68	-994.98	126	15.956	0.399	0.100	0.043	14.529	34.743	0.077	4.981	5.898	13.760	0.130	0.940	2.473	0.016	0.024	0.013	0.011	0.054	0.023	< 0.0001	0.001	0.663
6	-3,0V-1N	181.0-181.2	168	-972.46	150	17.434	0.252	0.140	0.056	16.376	33.675	0.088	4.519	7.477	12.516	0.131	0.737	2.000	0.018	0.026	0.016	0.012	0.050	0.021	< 0.0001	0.001	3.791
11	-2,5V-1L	71.0-71.2	84.66	-1022.5	192	14.549	0.377	0.254	0.031	16.665	34.180	0.074	4.560	7.190	11.986	0.159	0.730	2.101	0.020	0.030	0.018	0.016	0.047	0.021	< 0.0001	0.001	4.200
13	-1,5V-1N	66.0-66.2	23.68	-924.36	226.5	14.971	0.407	0.176	0.024	17.537	34.745	0.080	3.748	8.047	9.950	0.182	0.891	1.756	0.020	0.027	0.015	0.016	0.033	0.021	< 0.0001	0.001	0.339
15	-1,5V-1L	88.0-88.2	0.74	-967.4	184.5	17.196	0.223	0.358	0.039	17.886	31.302	0.084	4.058	7.726	11.367	0.162	0.571	1.903	0.019	0.038	0.023	0.017	0.044	0.020	< 0.0001	0.001	3.223
20	-1,0V-1N	129.0-129.2	-29.9	-918.6	149	17.496	0.292	0.305	0.038	18.369	30.332	0.087	3.861	8.126	10.692	0.165	0.628	1.808	0.020	0.037	0.023	0.017	0.041	0.021	< 0.0001	0.001	3.463
25	-0,5V-2N	114.0-114.2	-41.6	-834.3	170.5	17.086	0.351	0.117	0.048	15.279	34.053	0.084	4.909	5.467	13.694	0.126	0.906	2.440	0.017	0.029	0.014	0.013	0.053	0.022	< 0.0001	0.001	0.331
27	-0,5V-3N	189.0-189.2	-77.7	-902	121	17.310	0.293	0.240	0.037	18.191	30.926	0.087	4.008	8.162	11.038	0.164	0.630	1.891	0.020	0.033	0.020	0.016	0.042	0.020	< 0.0001	0.001	3.493
33	0,5V-3N	89.1-89.25	-171.18	-864.7	213	15.682	0.376	0.192	0.025	18.805	33.899	0.086	3.752	8.384	8.861	0.227	0.769	1.467	0.023	0.023	0.011	0.013	0.029	0.023	< 0.0001	0.000	0.359
35	0,5V-1L	132.0-132.2	-193.66	-906.9	158	15.051	0.197	0.132	0.044	14.434	35.565	0.075	5.254	5.873	14.350	0.127	0.670	2.483	0.016	0.024	0.016	0.012	0.059	0.014	< 0.0001	0.001	2.781
39	1,0V-2N	166.0-166.2	-190.9	-795.5	130.5	17.685	0.367	0.170	0.046	16.347	32.250	0.086	4.438	6.458	12.396	0.140	0.910	2.038	0.017	0.036	0.018	0.013	0.048	0.019	< 0.0001	0.001	0.134
44	1,5V-2N	225.0-225.2	-302.16	-897.85	104.5	21.377	0.184	0.149	0.066	18.783	28.568	0.105	3.931	6.433	10.965	0.161	0.596	1.799	0.018	0.033	0.016	0.013	0.046	0.020	< 0.0001	0.000	3.181
52	2,5V-2N	168.0-168.2	-359.8	-687.16	137	14.031	0.325	0.131	0.025	16.041	36.642	0.071	4.491	6.750	11.759	0.175	0.802	2.141	0.019	0.023	0.013	0.013	0.042	0.026	< 0.0001	0.001	0.296
59	3,0V-4N	127.0-127.2	-371.9	-709.95	131.5	17.586	0.246	0.229	0.038	18.226	30.705	0.089	3.826	8.791	10.565	0.162	0.673	1.762	0.019	0.033	0.019	0.016	0.040	0.020	< 0.0001	0.001	3.229
65	3,5V-1S	123.0-123.2	-427.45	-707.75	132	20.186	0.185	0.434	0.048	20.910	27.552	0.102	2.934	10.034	8.234	0.188	0.484	1.195	0.022	0.056	0.032	0.019	0.029	0.023	< 0.0001	0.000	3.373
73	5,0V-5N	128.0-128.2	-576.3	-668.06	106.5	31.196	0.107	0.165	0.087	26.686	15.929	0.146	1.644	8.711	4.700	0.220	0.252	0.567	0.024	0.058	0.017	0.019	0.016	0.027	0.000	0.001	1.704
75	6,3V-1L	84.0-84.2	-620.56	-644.84	103	18.083	0.221	0.115	0.052	16.128	31.882	0.089	4.599	6.034	12.896	0.137	0.604	2.188	0.016	0.027	0.015	0.013	0.052	0.016	< 0.0001	0.001	1.848

Table 3. An overview of the chosen drill core sections for the making of polished thin sections. Including the XYZ-coordinates for the respective drill hole collars and the modal mineralogical content by XRD-analyses provided by Titania, all values are given in wt% and normalized to 100 %.

Sample Number	Exploration core	Length drill core (m)	X-COORD	Y-COORD (m. a. sea level)	Z-COORD																
					Ilmenite	Hematite	Rutile	Magnetite	Pyrite	Orthopyroxene	Clinopyroxene	Plagioclase	Olivine	Biotite	Phlogopite	Quartz	Calcite	Apatite	Spinel	Antigorite	
2	-3,5V-2N	71.0-71.2	173.2	-1068.98	213	31.40	2.18	0.22	2.64	0.04	14.48	2.69	39.68	4.30	0.57	0.60	0.23	0.08	0.07	0.12	0.71
4	-3,5V-2N	191.0-191.2	212.68	-994.98	126	27.18	4.33	0.24	0.55	0.01	12.48	2.05	51.25	0.00	0.72	0.67	0.19	0.06	0.04	0.03	0.20
6	-3,0V-1N	181.0-181,2	168	-972.46	150	30.90	2.36	0.23	3.01	0.05	15.92	2.00	41.11	2.64	0.65	0.55	0.13	0.05	0.07	0.01	0.33
11	-2,5V-1L	71.0-71.2	84.66	-1022.5	192	26.16	2.02	0.28	3.72	0.10	21.76	2.90	41.13	0.00	0.54	0.53	0.18	0.11	0.10	0.14	0.33
13	-1,5V-1N	66.0-66.2	23.68	-924.36	226.5	27.57	3.98	0.31	0.63	0.15	28.46	2.45	35.13	0.00	0.48	0.27	0.12	0.06	0.10	0.07	0.25
15	-1,5V-1L	88.0-88.2	0.74	-967.4	184.5	30.99	2.18	0.22	2.73	0.04	16.98	2.40	41.10	1.96	0.53	0.38	0.10	0.04	0.10	0.13	0.13
20	-1,0V-1N	129.0-129.2	-29.9	-918.6	149	30.84	2.46	0.23	2.66	0.02	15.71	1.99	37.61	6.74	0.57	0.33	0.11	0.10	0.09	0.12	0.43
25	-0,5V-2N	114.0-114.2	-41.6	-834.3	170.5	27.98	3.97	0.32	0.00	0.06	9.73	1.70	52.38	0.00	0.90	1.14	0.63	0.04	0.10	0.14	0.92
27	-0,5V-3N	189.0-189.2	-77.7	-902	121	29.31	2.38	0.22	2.24	0.03	14.50	2.31	41.32	6.29	0.62	0.39	0.20	0.07	0.08	0.07	0.00
33	0,5V-3N	89.1-89.25	-171.18	-864.7	213	27.87	3.80	0.37	0.96	0.04	28.21	2.40	34.60	0.00	0.57	0.66	0.12	0.11	0.07	0.10	0.10
35	0,5V-1L	132.0-132.2	-193.66	-906.9	158	25.44	2.13	1.01	1.45	0.19	9.98	2.10	54.57	0.00	0.44	0.69	0.35	0.07	0.11	0.18	1.29
39	1,0V-2N	166.0-166.2	-190.9	-795.5	130.5	30.42	4.43	0.19	0.00	0.07	14.19	1.67	45.90	0.19	0.71	0.56	0.52	0.12	0.09	0.17	0.77
44	1,5V-2N	225.0-225.2	-302.16	-897.85	104.5	39.76	4.04	0.25	1.18	0.08	11.14	1.51	39.44	0.00	0.76	0.65	0.24	0.07	0.11	0.14	0.64
52	2,5V-2N	168.0-168.2	-359.8	-687.16	137	24.26	3.15	0.34	0.41	0.05	24.96	3.01	42.85	0.00	0.04	0.20	0.22	0.13	0.12	0.06	0.22
59	3,0V-4N	127.0-127.2	-371.9	-709.95	131.5	31.12	2.69	0.22	3.07	0.00	13.93	2.10	40.44	4.88	0.38	0.61	0.13	0.06	0.05	0.03	0.30
65	3,5V-1S	123.0-123.2	-427.45	-707.75	132	37.41	3.60	0.13	2.92	0.04	20.32	1.77	30.21	1.70	0.64	0.49	0.16	0.04	0.05	0.16	0.37
73	5,0V-5N	128.0-128.2	-576.3	-668.06	106.5	57.53	7.16	0.10	1.31	0.03	12.86	0.37	15.02	4.69	0.02	0.16	0.04	0.00	0.06	0.10	0.55
75	6,3V-1L	84.0-84.2	-620.56	-644.84	103	28.51	3.57	0.12	1.12	0.06	13.63	1.78	48.88	1.00	0.03	0.25	0.21	0.10	0.08	0.05	0.60

Table 4. Crushed drill core sections chosen for mineral processing. 9 of the samples corresponds to the sample interval as chosen for polished thin section production, whilst 3 are from the following sample interval and 1 is from the preceding.

Sample number	Exploration core	Length drill core (m)	
6	-3,0V-1N	181.0-181.2	Corresponding sample interval
11	-2,5V-1L	71.0-71.2	Corresponding sample interval
15	-1,5V-1L	88.0-88.2	Corresponding sample interval
20	-1,0V-1N	129.0-129.2	Corresponding sample interval
27	-0,5V-3N	189.0-189.2	Preceding sample interval (182.5–185.5 m)
35	0,5V-1L	132.0-132.2	Corresponding sample interval
39	1,0V-2N	166.0-166.2	Following sample interval (167.3–170.3 m)
44	1,5V-2N	225.0-225.2	Following sample interval (225.15–228.15 m)
52	2,5V-2N	168.0-168.2	Following sample interval (168.8–171.8 m)
59	3,0V-4N	127.0-127.2	Corresponding sample interval
65	3,5V-1S	123.0-123.2	Corresponding sample interval
73	5,0V-5N	128.0-128.2	Corresponding sample interval
75	6,3V-1L	84.0-84.2	Corresponding sample interval

3.2 OPTICAL MICROSCOPY

18 polished thin sections were studied in both transmitted and reflected light using a Nikon Eclipse E600 microscope, at the Electron microscopy laboratory, IGP, NTNU. Pictures were captured with a SPOT Insight CMOS camera.

In transmitted lighting both plane- (PPL) and cross polarization (XPL) were applied; for mineral identification, observation of mineral associations, texture and microstructures of isotropic and anisotropic minerals. Reflected lighting was used to study opaque minerals, mainly iron oxides and sulphides, with focus on mineral identification, observation of mineral associations, microstructures and textures. The mineralogy in the thin sections are relatively comparable, all thin sections contains silicates, iron-oxides and sulphides.

A thorough study of the thin sections in reflected and transmitted light were essential in selecting thin sections for SEM- and EPMA-analyses.

Selected thin sections were scanned in PPL, XPL and reflected light, using an Olympus BX51 microscope equipped with a Olympus UC90 camera and the Olympus Stream software. Scans were mainly used in preparation for EPMA-analyses, marking grains and setting points, due to Covid-19 making it impossible to participate in the set up of the analyses. The scanned thin sections can be found in Appendix B.

3.3 SCANNING ELECTRON MICROSCOPY - SEM

All SEM-analyses were performed at the Electron microscopy Laboratory, IGP, NTNU using a Zeiss Sigma 300 field emission SEM with a Schottky field emitter and the software Zeiss Mineralogic 1.6 for quantitative mineralogical analyses. A total of 12 polished ore sections were analysed. Table 5. gives an overview of the analysed samples.

The intents of the SEM-analyses of the polished ore sections were to analyse the modal mineralogy, mineral classification, associations, locking and liberation.

Analyses were performed in 2 rounds; 8+4 polished ore sections. A complete sample list is given in Table 5. The field scanning were done pixel by pixel, with a mapping step length of 10 µm. The acceleration voltage was 20 kV, with the working height set to 8,5 mm. The aperture size was 120 µm with 89x magnification. The EDS analysis per pixel was at a minimum of 0,005 s, and a minimum of 1500 counts.

Table 5. Samples and section types chosen for SEM-analyses conducted at IPG, NTNU.

Sample number	Sample name		Section type
A	-2,5V-1L	348 Ampere	Polished ore section
B	-2,5V-1L	778 Ampere	Polished ore section
C	-1,5V-1L	548 Ampere	Polished ore section
D	-1,5V-1L	Non-magnetic	Polished ore section
E	0,5V-1L	348 Ampere	Polished ore section
F	0,5V-1L	548 Ampere	Polished ore section
G	3,5V-1S	148 Ampere	Polished ore section
H	3,5V-1S	548 Ampere	Polished ore section
I	5,0V-5N	348 Ampere	Polished ore section
J	5,0V-5N	548 Ampere	Polished ore section
K	6,3V-1L	348 Ampere	Polished ore section
L	6,3V-1L	548 Ampere	Polished ore section

3.4 ELECTRON PROBE MICROANALYSIS - EPMA

Due to the COVID-19 outbreak, I was not able to participate in the execution of the EPMA-analyses. The analyses were performed at the Electron microscopy Laboratory, IGP, NTNU, by Kristian Drivenes using a JEOL JXF-8530F PLUS with a Schottky field emitter. 2 thins sections; 3,5V-1S and 3,0V-4N, were chosen with the aim to get high precision quantitative chemical analyses of the orthopyroxene and olivine chemistry.

The analyses includes point analyses of 18 mineral grains. All analyses were performed with an acceleration voltage of 15 kV and a beam current of 100 nA.

Biotite was analysed using a defocused beam diameter of 3 µm, a beam current of 10 nA and an acceleration voltage of 15 kV. Peak and background counting times were 5-30 s depending on element and mineral. The reference materials used included albite (Na), diopside (Mg, Si, Ca), fluorite (F), almandine (Al), chromite (Cr), sanidine (K), magnetite (Fe), rutile (Ti), rhodonite (Mn) and tugtupite (Cl).

Olivine and pyroxene were analysed using a defocused beam diameter of 1 μm , a beam current of 10 nA and an acceleration voltage of 15 kV. The reference materials used included albite (Na), diopside (Mg, Si, Ca), almandine (Fe), chromite (Cr), sanidine (K, Al), rutile (Ti), rhodonite (Mn), pentlandite (Ni), zircon (Zr), monazite (Ce) and pure metal references (V, Zn, Co).

Ilmenite was analysed using a defocused beam diameter of 1 μm , a beam current of 10 nA and an acceleration voltage of 15 kV. The reference materials used included rutile, (Ti), magnetite (Fe), chromite (Cr, Mg, Al), rhodonite (Mn), pentlandite (Ni) and pure metal references (V, As, Zn).

Plagioclase was analysed using a defocused beam diameter of 5 μm , a beam current of 10 nA and an acceleration current of 15 kV. The reference materials used included albite (Na, Al), diopside (Si, Ca, Mg), rutile (Ti), plagioclase (Sr), sanidine (K, Ba), magnetite (Fe) and rhodonite (Mn).

3.5 PROCESS DESCRIPTION

The following section describes the processing steps; crushing, grinding, screening, shaking table separation and magnetic separation, done in the processing of the 12 selected crushed drill core sections.

3.5.1 COMMINUTION

All comminution were executed at the Mineral Processing Laboratory, IGP, NTNU. All 12 samples were crushed in a Retsch Jaw Crusher BB 200 with no gap width and a feed rate of $\approx 50 \text{ kg/h}$. The grinding of the 6 samples were carried out wet with a batch-ball mill. The milling chamber is made of steel and has an inner diameter of 35 cm and a height of 10 cm. The ball charge was approximately 8 kg of steel balls with varying size. The charge size were approximately 2 kg of sample material and 2 L of water and the grinding time was 15 minutes. After grinding the samples were dried at approximately 110°C.

3.5.1.1 Screening

Screening were performed dry at two different stages in the process by using a SWECO vibratory separator. The +425 µm fraction were screened out in preparation for grinding, whilst the -62 µm fraction were screened out after grinding.

3.6 SHAKING TABLE SEPARATIONS - NTNU

A total of 6 samples were processed with a batch-size shaking table at the Mineral Processing Laboratory, IGP, NTNU. All samples were processed with the exact same degree of inclination of the table top, length of stroke and water flow.

The particle size in each sample were between 425 µm and 62 µm. Naturally, each sample has a different particle size distribution and mineral content, and thus behave differently on the table. The samples were separated in 3 products; a concentrate, middling and tailings. The feed flow rate was in average 2,87 kg/h, the water flow of wash water was 200 L/h and the water used for feed distribution was 270 L/h. For each run, the splitter between the concentrate launder and the middling launder were adjusted after where the segregation of the dark and light particles appeared.

A stopwatch was used to take the run time for each sample. The stopwatch was started when the sample material had properly fanned out on the table and the different product streams were visible. Hence, a small amount of sample material were lost, but this had no effect on the end results. The run time for each sample varies, due to the difference in sample size, but in average ≈27,6 minutes. An overview of the samples, with the respective feed sizes, running times and end products from separation is given in Section 4.4 Table 14.

Post separation, each product was first decanted then vacuum filtrated to filtrate out as much liquid as possible to reduce the drying time. All separation products were then carefully dried at approximately 110°C.

3.7 SHAKING TABLE SEPARATIONS - TITANIA

Significant mineralogical variations can occur within a blast. Shaking table tests of drill cuttings can be used to simulate how the different ore qualities will behave through the gravity separation process. Providing helpful information in planning of mixing ratio and

settings in the gravity separation process. 14 samples of drill cuttings, all sampled from within the same “salve” were processed, with the goal to observe how large the mineralogy varies within a salve and how it affects how each sample behaves on the shaking table. The tests were performed at Titania AS with a lab-size Deister shaking table concentrator.

Prior to the shaking table separations, all samples were crushed, screened wet, dried, and run through a magnetic roll separator to separate out magnetite. In each sample the particle sizes were between 212 µm and 63 µm. All samples were processed with the exact same degree of inclination of the table top length of stroke and feed flow rate. For each run, the splitter between the concentrate launder and the middling launder were adjusted after where the segregation of the dark and light particles appeared. The samples were separated in 3 products; concentrate, middling and tailings.

The feed flow rate was set to 13.17 kg/h. The water flow in each run was kept as consistent as possible but changes were made during the tests. Sample 1-6 were run with a water flow of approximately 600 L/h, sample 7-8 were run with a water flow of approximately 650 L/h, whilst sample 13 and 14 were, by mistake, run with a water flow of 850 L/h. Running the shaking table with a water flow of 850 L/h instead of 650 L/h did not affect the end result, which shows that 650 L/h is an adequate flow.

A stopwatch was used to take the run time for each sample and was started when the sample material had properly fanned out on the table and the different product streams were visible. The run time for each sample varies, due to the difference in sample size, but in average \approx 6,35 minutes. An overview of the samples, with the respective feed sizes, running times and end products from separation is given in Section 4.5, Table 17. Post separation, each sample was first decanted then dried at approximately 160°C.

3.8 WET HIGH-INTENSITY MAGNETIC SEPARATION

Wet high-intensity magnetic separation was carried out at the Mineral Processing Laboratory, IGP, NTNU. The 6 samples, concentrates from shaking table separations, were separated using a SLon, a vertically pulsating high-gradient magnetic separator (VPHGMS), manufactured by Outotec.

The purpose of magnetic separation is to simulate Titania's magnetic separation step, analysing the mineralogical content at each field strength, to investigate the content and variations of pyroxene and olivine.

Prior to the separation, sample -2,5V-1L was tested with increasing field strengths to get an indication for at which field strengths ilmenite will be separated out at and at which field strengths a concentrate comparable to Titania's is achieved. The sample were tested with a 2 mm steel rod matrix, at the field strengths; 0,05, 0,1, 0,3, 0,5, 0,7, 0,9, 1,0 Tesla. The sample were mixed with water and fed as a slurry. The waterflow was 588 L/h with a stroke length of 0,8 cm and 200 pulsations per minute.

Each magnetic fraction were then analysed with a handheld XRF to get a quick indication of the mineral content. On the basis of the XRF-analyses 4 field strengths were chosen; 0,1, 0,3, 0,5 and 0,7 Tesla which corresponds to a current of 148, 348, 548 and 778 ampere, respectively.

The test sample were tested a couple of times and necessary adjustments were done. The test sample is therefore separated with the same settings as the rest of the samples.

The separations were done in 4 steps, resulting in 5 products; 148 ampere, 348 ampere, 548 ampere, 778 ampere and a non-magnetic product, which is the product that did not get attracted to the matrix at 778 ampere (0,7 Tesla). The separations were done with a 3 mm steel rod matrix, corresponding to a maximum particle size of 1.5 mm, with a stroke length of 3,0 cm and 200 pulsations per minute. The samples were fed as a slurry with a waterflow of 588 L/h.

Each separation product, were named with the current at which the product were separated at. Table 20. in Section 4.6 gives an overview of the samples with the respective product sizes for each separation product and the non-magnetic product. Post separation, each product was decanted and vacuum filtrated then dried at approximately 110°C.

4 RESULTS

4.1 MINERALOGICAL DESCRIPTIONS

A combination of several analytical methods, described in Section 3, were used to assess and identify the mineral assemblage. The following sections give a mineralogical description of the most predominant minerals in the 18 thin sections. Optical characteristics such as colour, mineral texture, structures in addition to associations will be described for each mineral.

Whilst data from EPMA-analyses will provide the elemental content for each mineral.

Mineral abbreviations are based on the abbreviation list provided by Whitney and Evans (2010)

4.1.1 SILICATES

4.1.1.1 ORTHOPYROXENE

Orthopyroxene in addition to plagioclase, is the most predominant silicate mineral in the ore, thus found in all thin sections. The orthopyroxene typically occurs with two crystal habits; coarse grained, subhedral, prismatic crystals and medium to fine grained, sub- to euhedral, tabular crystals. The grain boundaries varies from straight to lobate. The crystals occur singly or in orthopyroxene aggregates. Commonly associated with ilmenite, plagioclase, biotite, olivine, clinopyroxene and sulphides.

In PPL the colour is pale cream to white, with varying pleochroism from light green to light brown pink. In XPL the interference colours are mainly up to 1st order yellow, with a few exceptions of 1st order pink. A distinctive feature for the orthopyroxene are the iron-oxide exsolution lamellas shown in Figure 9, these will be discussed further in section 4.1.1.2. However, a small number of orthopyroxenes occurs without the exsolution lamellas in some of the thin sections.

Most of the orthopyroxene grains contains inclusions of ilmenite, whilst some larger grains also contains inclusions of biotite and plagioclase, hinting of a poikilitic texture. The ilmenite inclusions typically has a rounded oval shape and ilmenite located at the grain boundary often creates a caries texture. Serpentization occurs in some of the thin sections, mainly along grain boundaries and/or in fractures. Partial alteration to clinopyroxene can be observed in

some of the thin sections, often along smaller parts of the grain boundary, but also occurs within the mineral grain.

The main chemical constituents are; FeO, MgO and SiO₂ with smaller amounts of Al₂O₃, CaO, MnO and TiO₂. The chemical analyses show limited variation among the main and minor constituents, see Table 6. The MgO content correlates weakly positive with the Al₂O₃-content and weakly negative with the FeO-content.

The Mg-Fe-Ca-ratio shows an En_{62.8-64.6}Fs_{34.0-34.6}Wo_{1.4-2.4} orthopyroxene, which corresponds chemically to an enstatite. All orthopyroxene A mineral formula was calculated from the averages of the chemical data provided by the EPMA-analyses;



A complete overview of the chemical composition can be found in Appendix C, Table C 1.

Table 6. Average chemical composition (wt% oxides) of the 12 analysed orthopyroxenes, retrieved from EPMA-data.

	MgO	FeO	Al ₂ O ₃	CaO	MnO	TiO ₂	SiO ₂
Wt% Oxides	27.029	15.456	1.850	0.598	0.280	0.180	53.757
	26.962	14.954	1.909	0.817	0.274	0.177	53.965
	26.802	14.764	1.956	1.125	0.261	0.169	53.848
	26.963	15.043	1.926	0.776	0.282	0.196	53.964
	26.822	14.870	1.951	1.361	0.280	0.184	54.197
	27.000	15.143	1.904	0.699	0.276	0.173	54.086
	27.084	15.110	1.966	0.764	0.272	0.175	54.175
	27.165	14.862	1.986	1.066	0.280	0.188	54.163
	27.603	14.532	1.950	0.622	0.270	0.156	54.435
	26.808	15.090	2.032	1.114	0.276	0.190	54.112
	27.050	15.016	2.014	1.035	0.278	0.185	54.142
	27.351	14.976	1.926	0.789	0.272	0.176	54.163

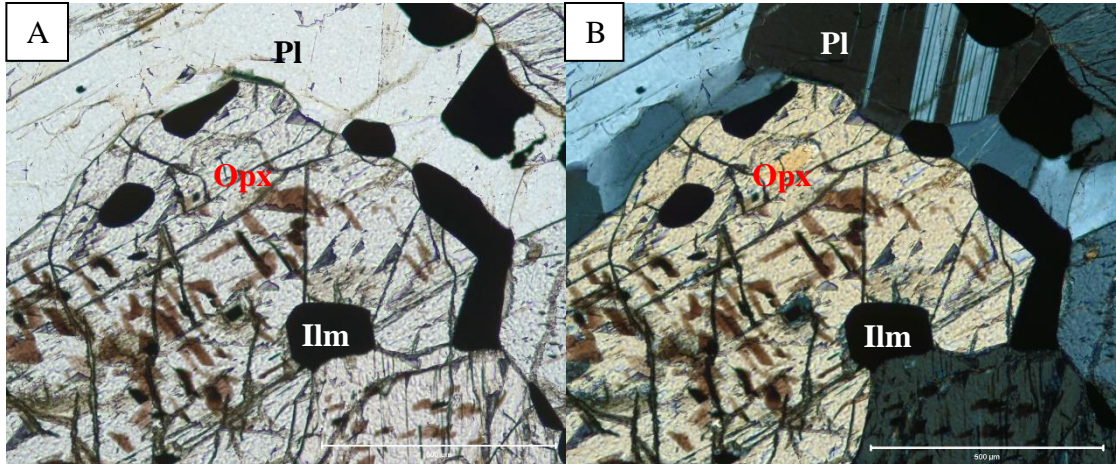


Figure 9. A) Coarse-grained orthopyroxene, with brown iron-oxide exsolution lamellas and inclusions of ilmenite in PPL (thin section 0.5V-3N). B) Picture A) in XPL.
Abbreviations: Opx – orthopyroxene, Ilm – ilmenite, Pl – plagioclase.

4.1.1.2 IRON-OXIDE LAMMELLAS IN ORTHOPYROXENE

The exsolution lamellas in orthopyroxene are in Raith, Raase and Reinhardt's "Guide to Thin Section Microscopy" (2012) described as "Oriented precipitation of ilmenite platelets in orthopyroxene" (Raith, Raase & Reinhardt, 2012, p.54). EPMA-analyses were performed on a few lamellas but it should be specified that as the lamellas are quite small and thin, it is challenging to get a representative analysis without any mixing from the orthopyroxene. Figure 10. shows the points set for the analyses, with the corresponding chemical composition in Table 7.

Inclusion 3-6. shows fairly comparable chemical compositions, with the main constituents MgO, FeO, SiO₂ and minor Al₂O₃. This composition corresponds more to an orthopyroxene, and it can be assumed that the analyses were overlapped by the orthopyroxene.

However, inclusion 1. and 2. chemically stands out. They can be compared based on the main constituents; MgO, Al₂O₃, K₂O, FeO, TiO₂ and SiO₂, but the elemental ratio is different. Inclusion 1. has a high FeO-content (53.470) but chemically don not correspond to an ilmenite due to the low content of TiO₂ (5.010 wt%). Inclusion 2. has a lower FeO-content (11.200 wt%) and a higher TiO₂-content (11.530 wt%), but does not either correspond chemically to an ilmenite.

Looking at the thickness of the lamellas in figure x. inclusion 1. might be the most representative analysis and the inclusion will therefore, hereby be recognized as iron-oxide lamellas.

Table 7. Average chemical composition (wt% oxides) of 6 analysed Fe-Oxide lamellas in orthopyroxene, retrieved from EPMA-data. Figure x. show the location of the analysed lamellas.

Number:	Point:	Oxides (wt%)										
		Na ₂ O	MgO	Al ₂ O ₃	SiO ₂	CaO	K ₂ O	Cr ₂ O ₃	V ₂ O ₃	FeO	TiO ₂	MnO
1	30V-4N-3-incl1	0.206	6.420	6.730	13.570	0.220	3.080	0.459	0.481	53.470	5.010	0.040
2	30V-4N-3-incl2	0.341	12.630	13.750	36.650	0.116	8.270	0.065	0.174	11.200	11.530	0.023
3	30V-4N-3-incl3	0.027	26.880	1.811	54.080	0.633	0.004	0.014	0.001	14.820	0.128	0.275
4	30V-4N-3-incl4	0.030	27.520	1.747	50.110	0.630	0.018	0.000	0.000	14.100	0.213	0.257
5	30V-4N-3-incl5	0.049	26.770	1.861	54.050	0.588	0.005	0.013	0.000	14.890	0.176	0.262
6	30V-4N-3-incl6	0.017	25.150	1.729	53.550	0.597	0.001	0.022	0.032	14.990	0.185	0.286

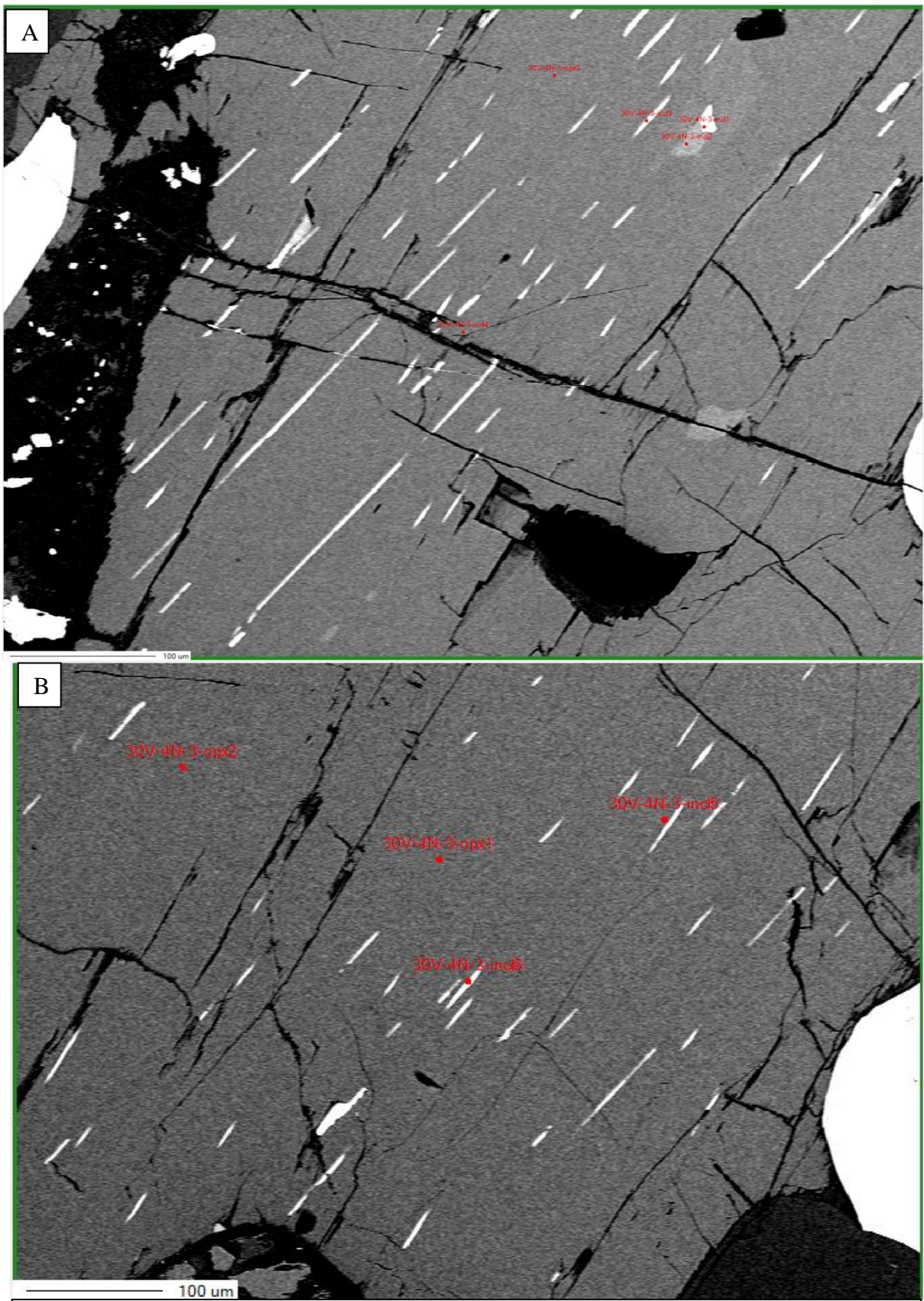


Figure 10. Orthopyroxene (grey) with white exsolution lamellas. The figure shows the points set for EPMA-analyses, with the corresponding chemical analyses given in Table 7.

4.1.1.3 CLINOPYROXENE

Clinopyroxene are observed in all thin sections. Clinopyroxene generally occurs as medium grained subhedral to anhedral crystals with straight to lobate grain boundaries. The clinopyroxene often occurs as partly altered orthopyroxene, Figure 11. Often in association with orthopyroxene, ilmenite, sulphides and plagioclase, with some having inclusions of ilmenite. Some grains contains dark thin, needle shaped exsolution lamellas.

Clinopyroxene are generally colourless in PPL, and only Fe-rich variants show pleochroism. Clinopyroxene can be separated from orthopyroxene in XPL due to 2nd order interference colours, most often yellow or blue.

Chemical analyses were performed on three clinopyroxene grains. The main constituents are; CaO, MgO, FeO, Al₂O₃ and SiO₂, with minimal chemical variation between the analysed grains, see Table 8. The mineral contains low contents <1% wt% of TiO₂, Na₂O and MnO. The Mg-Fe-Ca ratio shows an En_{43.1-43.6}Fs_{10.6-11.0}Wo_{45.4-45.9} clinopyroxene, which corresponds chemically to an augite. A mineral formula was calculated from data provided by EPMA-analyses based out of the 3 analysed clinopyroxenes;



A complete overview of the chemical composition can be found in Appendix C, Table C 2.

Table 8. Average chemical composition (wt% oxides) of 3 clinopyroxenes, retrieved from EPMA-data.

	CaO	MgO	FeO	Al ₂ O ₃	SiO ₂
Wt% Oxides	21.518	14.588	6.654	3.476	51.446
	21.503	14.838	6.576	3.477	51.836
	21.793	14.744	6.437	4.441	51.918

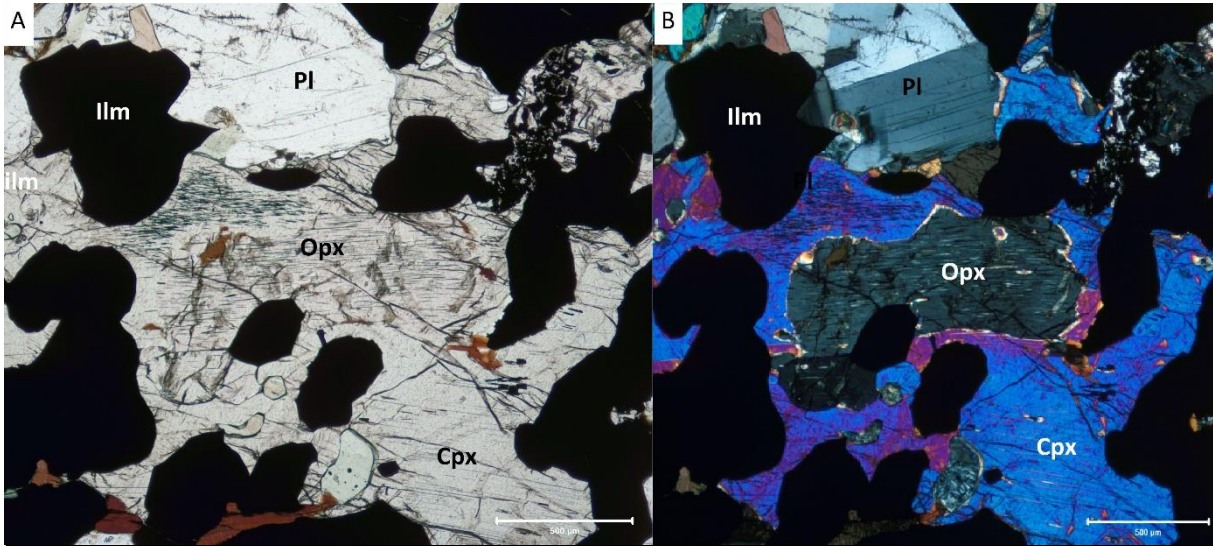


Figure 11. A) Orthopyroxene partly altered to clinopyroxene in PPL (thin section 3,5V-1S). B) Picture A) in XPL. Abbreviations: Opx – orthopyroxene, Cpx – clinopyroxene, Pl – plagioclase,

4.1.1.4 OLIVINE

Olivine MgFeSiO_4

Olivine is only observed in 10 out of 18 thin sections. Olivine typically occurs as medium grained, anhedral to subhedral, rounded, subequant crystals, with irregular microfractures and lobate grain boundaries. Occurring as single grains or as aggregates of grains. Commonly associated with plagioclase, often as inclusions, biotite, ilmenite and orthopyroxene, see Figure 12. Olivine is colourless in PPL, with no apparent pleochroism. In XPL the interference colours are up to 3rd order blues, greens, pinks and yellows. Serpentization often occurs at varying degrees around edges and in fractures.

The chemical analyses of olivine shows limited elemental variation among the main constituents; MgO, FeO and SiO₂, shown in Table 9. There is a slight variation of $\pm <2$ wt% FeO, which correlates equally negative with the MgO-content and positive with the MnO-content. MnO is the minor constituent and constitute in average 0.205 wt%.

The Mg-Fe ratio shows a Fo_{78.6-80.1}Fa_{19.9-21.4} olivine, which corresponds chemically in the olivine solid-solution series, more towards a forsterite than a fayalite. A mineral formula was calculated from data provided by EPMA-analyses based out of the 5 analysed olivines;



A complete overview of the chemical composition can be found in Appendix C, Table C 3.

Table 9. Average chemical composition (wt% oxides) of 5 olivines, retrieved from EPMA-data.

	MgO	FeO	SiO ₂	MnO
Wt% Oxides	40.909	19.000	38.882	0.202
	40.872	18.961	38.758	0.202
	40.599	19.672	38.880	0.214
	41.280	18.853	38.997	0.207
	41.653	18.503	39.247	0.199

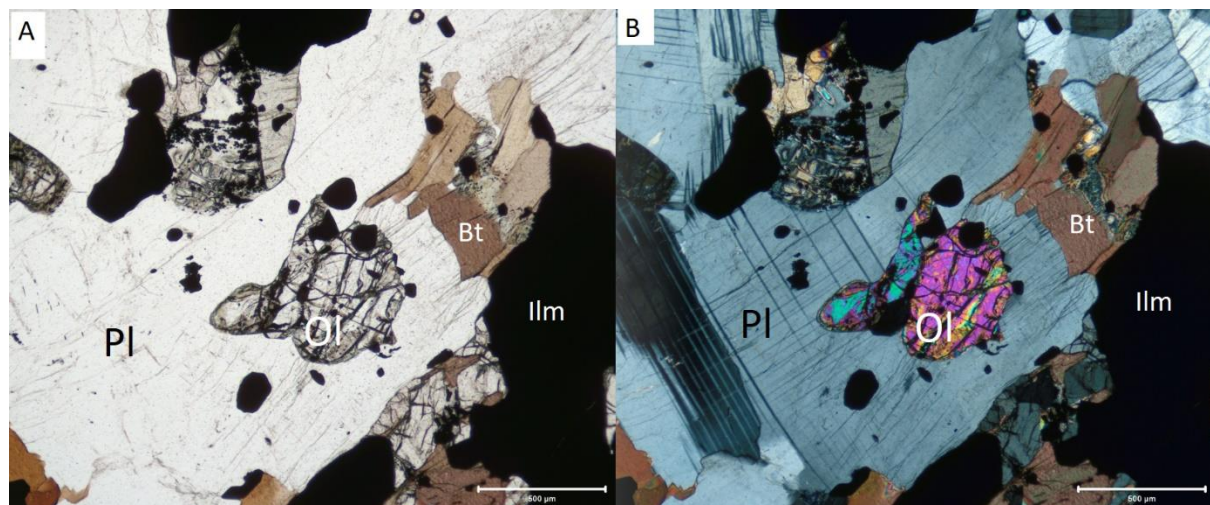


Figure 12. A) Olivine, plagioclase, biotite and ilmenite in PPL (drill core -3.5V-2N). B) Picture A) in XPL. Abbreviations: Opx – orthopyroxene, Cpx – clinopyroxene, Pl – plagioclase, Ilm – ilmenite, Bt – biotite.

4.1.1.5 BIOTITE

Biotite is observed in all thin sections. Crystals are in general medium- to fine grained, subhedral to euhedral, with a tabular shape. Biotite occur most often as single grains or as inclusions, but aggregates can be found. Inclusions of biotite are generally found associated with ilmenite, in orthopyroxene or plagioclase.

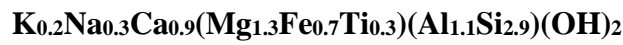
In PPL, biotite has a dark brown to a dark reddish brown colour, with a perfect cleavage, Figure 12. The biotite pleochroism is quite distinctive, with the colour being darkest when the cleavage direction is oriented parallel to the lower polarizer and lightest when the cleavage

direction is oriented perpendicular to the lower polarizer. In XPL biotite generally shows 3rd to 4th order interference colours, but are masked by strong mineral colours.

Chemical data provided by the EPMA-analyses show biotites of two different chemical compositions, which may indicate two different generations. The two different varieties can be distinguished in XPL by the interference colour, one variant (1) has a green, turquoise interference colour, whilst the other variant (2) is generally masked by the strong brown mineral colour.

In variant 1. the main constituents are Al_2O_3 , MgO , CaO , FeO , TiO_2 , Na_2O , K_2O , SiO_2 and OH , whilst the main constituents in variant 2. are MgO , Al_2O_3 , K_2O , FeO , TiO_2 , SiO_2 and OH . The average chemical composition of the two different varieties are shown in Table 10. Variety 1. contains in average 11.64 wt% CaO , whilst variety 2. is nearly depleted, with <0,01 wt% CaO . Variety 2. contains in average 9.89 wt% K_2O , whilst variety 1. contains <1.80 wt%. The varieties can therefore be divided into a K-rich mica (biotite) and Ca-rich mica.

Mineral formulas for both varieties was calculated from data provided by EPMA-analyses:



A complete overview of the chemical composition can be found in Appendix C, Table C 4.

Table 10. Average chemical composition (wt% oxides) of the two mica-varieties, retrieved from EPMA-data.

	Al_2O_3	MgO	CaO	FeO	TiO_2	K_2O	Na_2O	SiO_2
Wt% Oxides	12.789	11.996	11.638	10.932	5.371	1.667	2.379	40.198
	14.788	16.170	0.005	8.922	9.040	9.868	0.189	37.082

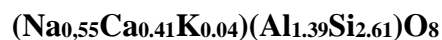
4.1.1.6 PLAGIOCLASE

Plagioclase is the most predominant silicate mineral in the ore. The plagioclase occurs as coarse- to medium grained with euhedral to anhedral crystal shapes. The crystals are tabular parallel to (010) and elongated parallel to the c-axis or a-axis. The grain boundaries varies from straight to lobate. Most crystal grains occurs in mineral aggregates but single grains occurs.

Plagioclase is colourless in PPL, with no apparent pleochroism. In XPL the interference colours are up to 1st order grey to white. Twinning is an distinctive feature for plagioclase. Polysynthetic twinning, both albite and pericline are found in all thin sections, in addition to carlsbad twinning found in most. A few grains do not show twinning. Plagioclase is often associated with ilmenite, biotite, olivine, orthopyroxene and clinopyroxene, see Figure 12 for an example. Rounded inclusions of ilmenite occurs most frequent.

The chemical analyses of plagioclase shows limited elemental variation among the main constituents; Al₂O₃, CaO, Na₂O and SiO₂, shown in Table 11. Minor constituents includes K₂O, SrO and FeO. The SiO₂-content correlates negative with the Al₂O₃- and CaO-content, whilst it correlates relatively positive with the Na₂O- and K₂O-content.

The An-Ab-Or ratio shows an An₄₁Ab₅₅Or₄ plagioclase. Chemically it plots in the intermediate andesine area of the plagioclase series. A mineral formula was calculated from data provided by EPMA-analyses based on the average of the analysed plagioclases;



A complete overview of the chemical composition can be found in Appendix C, Table C 5.

Table 11. Average chemical composition (wt% oxides) of plagioclase, retrieved from EPMA-data.

	Al ₂ O ₃	CaO	Na ₂ O	SiO ₂
Wt% Oxide	26.150	8.476	6.291	57.977

Ternary Ca-Na-K plot of plagioclase.

4.1.2 OXIDES

4.1.2.1 ILMENITE

Ilmenite is the most predominant oxide mineral in the ore and is one of the main constituents in each thin section. In reflected lighting, ilmenite have a light grey colour with a light grey pink bireflectance, see Figure 13, but appears opaque in transmitted lightning. It is medium to coarse grained, with subhedral to anhedral shapes. Larger grains occur commonly in granular ilmenite clusters, associated with plagioclase, pyroxene, biotite, magnetite and sulphides. Smaller, rounded inclusions of ilmenite are common in pyroxene, plagioclase and biotite. It also occurs as exsolution lamellas in orthopyroxene.

White exsolution lamellas of hematite are frequent in several grains. Needle shaped exsolution lamellas of spinel (pleonaste) are also found. The chemical composition retrieved from EPMA-analyses show limited variation in the TiO₂-concentration, however there is a slight variation of 5 wt% in the FeO-concentration, see table x. FeO shows a negative correlation with TiO₂. Minor elements such as MnO and V₂O₃ show only minor variations, whereas the MgO-content varies with around 1 wt%.

During the EPMA-analyses the points were set intentionally to avoid analysing the hematite lamellas, but it should be specified that as the lamellas are quite thin and often tightly spaced and there is always a risk that the analyses represents a mix between the lamellas and the surrounding ilmenite. A mineral formula was calculated based on the average chemical composition provided by EPMA-data;



A complete overview of the chemical composition, retrieved from the EPMA-analyses can be found in Appendix C, table C 6.

Table 12. Average chemical composition of ilmenite and spinel exsolution lamellas (wt%). Data retrieved from EPMA-analyses performed on 4 ilmenite grains and 2 spinel lamellas.

Oxides (wt%)	FeO	TiO ₂	MgO	MnO	V ₂ O ₃	
Ilmenite	47.530	48.032	3.000	0.324	0.336	
	48.103	48.017	2.007	0.323	0.304	
	46.920	48.546	3.118	0.316	0.335	
	46.425	49.308	3.125	0.342	0.293	
	43.100	49.150	2.990	0.339	0.309	
Oxides (wt%)	Al ₂ O ₃	MgO	FeO	ZnO	Cr ₂ O ₃	
Spinel	64.950	17.196	13.324	5.056	0.716	0.341

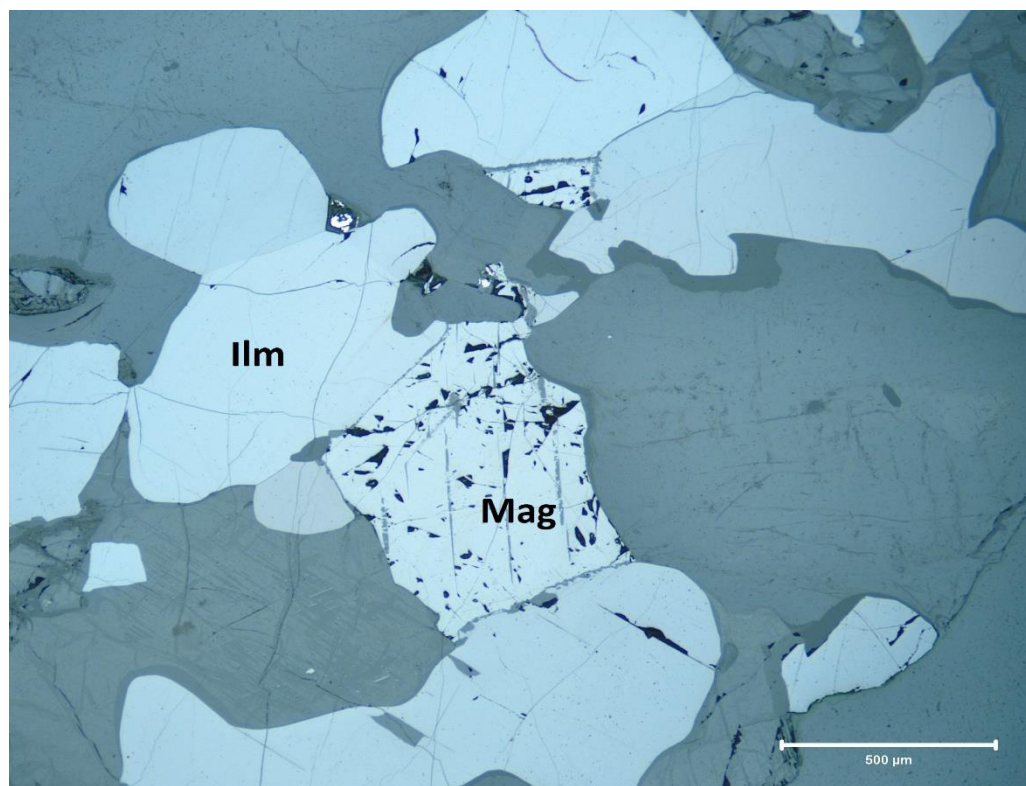


Figure 13. Ilmenite and magnetite with straight spinel exsolution lamellae in transmitted lightning (drill core -3.5V-2N). Abbreviations: Ilm – ilmenite, Mag – magnetite.

4.1.2.2 MAGNETITE

Magnetite Fe_3O_4

Magnetite were not specifically studied in this master's project and therefore no chemical analyses were done. Magnetite is an iron oxide found in almost all of the thin sections. In reflected lighting it has a grey colour, Figure 13., but appears opaque in transmitted lighting. The magnetite occur as medium grained, subhedral with straight to lobate grain boundaries. Associated with ilmenite, plagioclase, pyroxene and sulphides. Exsolution lamellae of spinel are common, see Figure 13.

4.1.3 SULPHIDES

Sulphides were not heavily studied in this master's project, but are still worth commenting on. Pyrite (FeS_2) were observed in all thin sections, most often in association with other various sulphides.

Pyrite is an iron sulphide, with a light yellow colour and a cubic shape, often triangular or rectangular, euhedral to subhedral. It is observed in association with orthopyroxene, plagioclase, ilmenite, magnetite and biotite and as an inclusion in plagioclase.

Pyrite is the predominant sulphide mineral but commonly partly replaced by chalcopyrite (CuFeS_2) with a varying content of pentlandite ($(\text{Fe},\text{Ni})_9\text{S}_8$) and pyrrhotite (Fe_{1-x}S), see Figure 14. Chemical analyses were only performed on three sulphide grains and will therefore give limited representative results, see Table 13.

The sulphides are a source of various minor elements such as cobalt (Co) in pyrite and pentlandite and pentlandite representing the main source of nickel (Ni) having an average concentration of approximately 36 wt%.

Table 13. Average chemical composition (wt%) of the analysed sulphides, retrieved from EPMA-data.

	Fe	Cu	Ni	Co	S
Pyrite	45.236	0.008	0.031	1.480	53.858
Pyrrhotite	58.867	0.272	1.047	0.040	39.527
Chalcopyrite	30.101	34.636	0.034	0.015	34.678
Pentlandite	28.915	0.112	36.360	1.231	33.060

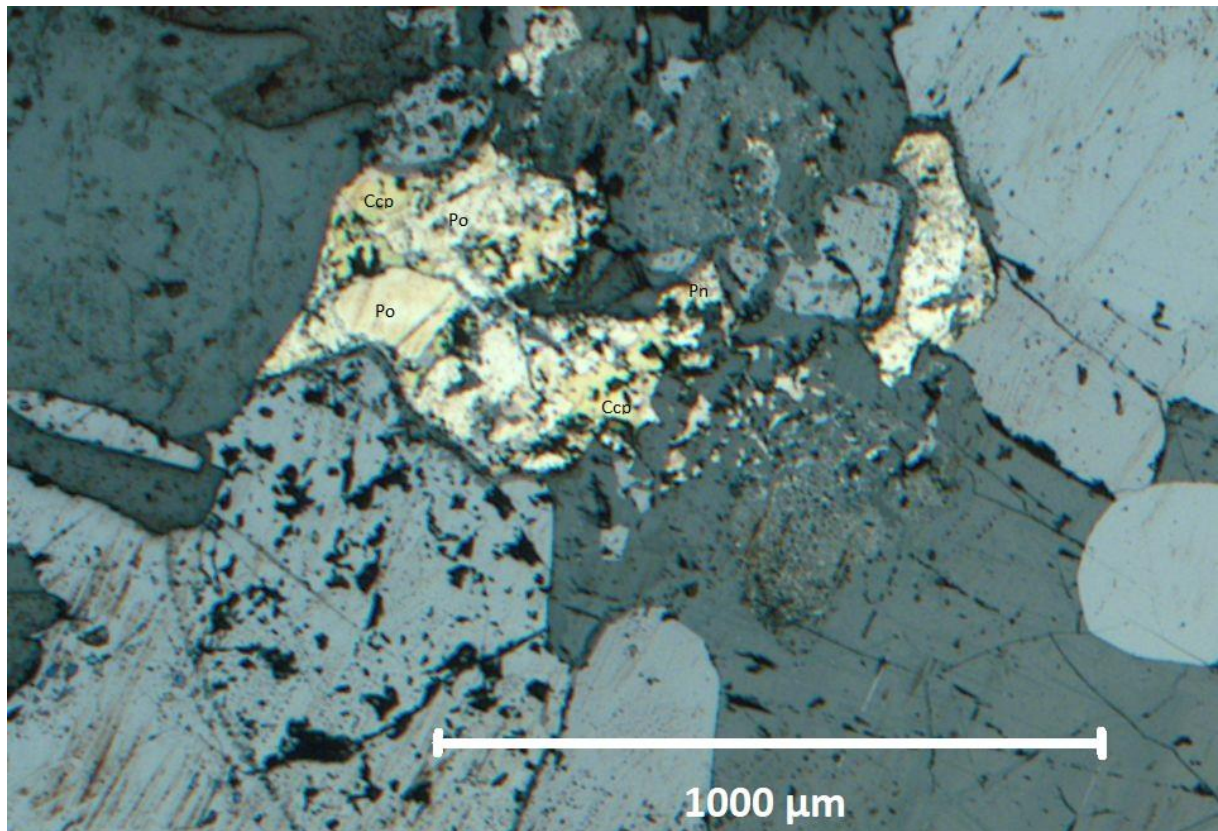


Figure 14. Various sulphides in transmitted lightning (drill core 3.0V-4N). Abbreviations: Ccp – chalcopyrite, Po – pyrrhotite, Pn – pentlandite.

4.2 MINERAL PROCESSING

The mineral processing were done in several steps including; crushing, grinding, screening, gravitational separation, and magnetic separation. Figure 15, gives a simplified flow sheet of the process. After crushing the initial 12 samples were cut down to 6 due to time constraints.

Flow sheet

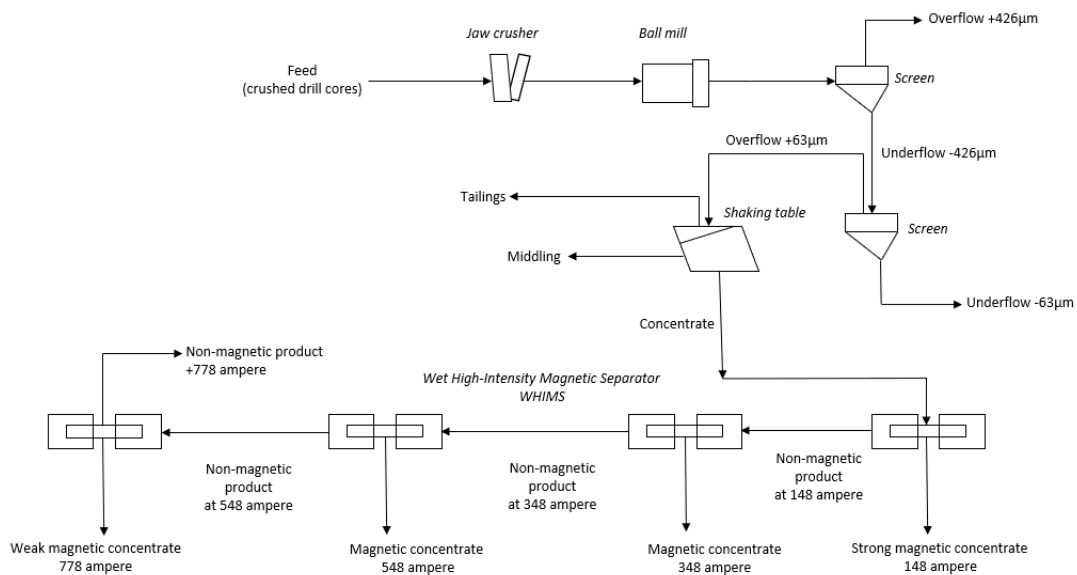


Figure 15. Flow sheet of the mineral processing.

4.3 SHAKING TABLE SEPARATIONS IGP, NTNU

Table 14. gives an overview of the products from shaking table separations, with the respective product sizes and running times. The separation yielded 3 products; concentrate, middling and tailings. Modal mineralogy and bulk chemical data can be found in Table 15 and Table 16, respectively.

Table 14. Overview of samples, with the respective running time, feed-, concentrate-, middling-, and tailings size from the shaking table analyses performed at IGP, NTNU.

The shaking table separations were run with an average feed flow rate of 2.87 kg/h, 200 L/h wash water and 270 L/h water for feed distribution.

Sample name	Running time (min:sec)	Feed (g)	Concentrate (g)	Middling (g)	Tailings (g)
-2,5V-1L	33:73 22:52*	1375.4	433.2	329.0 413.2*	15.0
-1,5V-1L	26:34	1404.9	760.7	478.1	17.1
0,5V-1L	30:40	1318.4	576.9	590.0	12.0
3,5V-1S	27:37	1254.7	569.0	546.1	21.2
5,0V-5N	24:58	1393.1	841.7	474.5	10.6
6,3V-1L	28:10	1317.3	590.4	613.3	13.4

* The concentrate of sample -2,5V-1L was run an additional time due to poor separation in the first run.

Table 15. Analyses of the modal mineralogy by XRD of the products from the gravity separation performed with a shaking table at the Mineral Processing Laboratory, IGP, NTNU. Each sample is separated into; concentrate, middling and tailings. Table 14. gives an overview of the respecting sample sizes. Analyses were performed at Titania and all values are normalized and given in wt%.

Sample name	Ilmenite	Hematite	Rutile	Magnetite	Pyrite	Orthopyroxene	Clinopyroxene	Plagioclase	Olivine	Biotite	Phlogopite	Quartz	calcite	Apatite	Spinel	Antigorite
-2.5V-1L Feed	26.77	2.16	0.14	2.58	0.01	17.23	2.67	44.01	2.40	0.58	0.67	0.17	0.10	0.06	0.15	0.31
-1.5V-1L Feed	31.38	2.14	0.15	2.23	0.06	18.37	2.31	39.34	1.98	0.73	0.51	0.39	0.07	0.08	0.08	0.20
0.5V-1L Feed	27.02	2.31	0.19	2.00	0.01	11.00	1.74	53.74	0.51	0.09	0.62	0.13	0.07	0.07	0.12	0.39
3.5V-1S Feed	35.23	3.29	0.26	2.99	0.06	13.89	1.53	37.36	1.92	0.40	0.63	0.12	0.05	0.02	0.17	2.07
5.0V-5N Feed	53.93	6.48	0.11	1.16	0.01	12.93	0.76	20.84	3.10	0.02	0.11	0.09	0.01	0.08	0.18	0.21
6.3V-1L Feed	33.11	3.65	0.10	0.82	0.02	14.82	1.58	44.28	0.55	0.41	0.37	0.07	0.07	0.09	0.07	0.00
-2.5V-1Lx1 Middling*	3.85	0.18	0.89	0.75	0.03	12.61	1.66	72.25	1.46	0.86	1.32	0.39	0.11	0.08	0.17	3.42
-2.5V-1Lx2 Middling*	12.30	1.01	0.22	1.67	0.00	22.84	2.78	53.56	3.41	0.75	0.45	0.27	0.06	0.07	0.15	0.47
-1.5V-1L Middling	8.54	0.60	0.26	1.12	0.02	19.82	2.31	62.95	2.19	0.83	0.65	0.21	0.07	0.10	0.17	0.18
0.5V-1L Middling	6.68	0.45	0.15	0.78	0.04	11.06	1.75	76.23	0.55	0.54	0.94	0.20	0.10	0.09	0.12	0.32
3.5V-1S Middling	6.87	0.16	0.85	1.30	0.04	13.37	1.76	64.99	1.87	0.95	1.43	0.49	0.14	0.06	0.13	5.58
5.0V-5N Middling	17.40	1.63	0.20	0.96	0.02	25.16	1.31	46.44	4.79	0.67	0.51	0.26	0.13	0.08	0.14	0.31
6.3V-1L Middling	6.09	0.59	0.10	0.15	0.01	14.72	1.57	73.38	0.55	0.63	0.67	0.18	0.10	0.10	0.08	1.09
-2.5V-1L Concentrate*	60.50	6.35	0.19	6.99	0.00	12.24	1.30	8.31	3.07	0.08	0.20	0.06	0.00	0.01	0.10	0.62
-1.5V-1L Concentrate	48.54	3.96	0.18	4.13	0.06	17.07	1.99	21.17	1.79	0.15	0.30	0.00	0.04	0.08	0.13	0.43
0.5V-1L Concentrate	49.46	4.64	0.20	2.90	0.14	11.76	1.68	28.18	0.55	0.21	0.08	0.01	0.01	0.05	0.07	0.06
3.5V-1S Concentrate	66.90	6.01	0.19	3.81	0.11	11.98	1.65	5.80	2.40	0.30	0.02	0.02	0.00	0.03	0.20	0.58
5.0V-5N Concentrate	76.46	10.39	0.16	1.58	0.04	4.73	0.08	3.23	2.20	0.12	0.20	0.00	0.00	0.04	0.15	0.63
6.3V-1L Concentrate	68.72	8.56	0.15	2.31	0.08	10.47	1.41	5.60	1.70	0.12	0.19	0.03	0.00	0.03	0.18	0.46
-2.5V-1L Tailings	13.83	1.43	0.46	1.61	0.03	28.93	3.90	35.45	5.46	1.24	2.27	0.74	0.13	0.07	0.21	4.25
-1.5V-1L Tailings	11.00	0.94	0.52	1.16	0.02	24.30	2.37	49.00	2.56	1.58	2.52	0.80	0.10	0.09	0.11	2.93
0.5V-1L Tailings	9.26	0.92	0.39	0.76	0.07	12.19	1.62	62.85	0.86	1.81	2.96	0.56	0.18	0.14	0.25	5.19
3.5V-1S Tailings	20.34	1.42	2.81	2.33	0.12	14.73	1.75	34.23	2.53	2.57	4.76	1.36	0.14	0.05	0.72	10.15
5.0V-5N Tailings	26.56	3.27	0.35	0.94	0.05	20.27	1.59	37.82	4.25	1.15	1.96	0.52	0.12	0.12	0.21	0.83
6.3V-1L Tailings	13.44	1.89	0.23	1.06	0.06	19.73	2.17	55.56	0.44	1.17	1.14	0.36	0.22	0.15	0.12	2.26

* The concentrate of sample -2.5V-1L was run an additional time due to poor separation in the first run.

Table 16. Bulk chemical analyses by XRF of the products from gravity separation, performed with a shaking table at the Mineral Processing Lab, IGP, NTNU. Each sample is separated into; concentrate, middling and tailings. Table 14. gives an overview of the respecting sample sizes. Analyses were performed at Titania and values are given in wt%.

Sample name	TiO ₂	P ₂ O ₅	S	Cr ₂ O ₃	Fe	SiO ₂	V ₂ O ₃	CaO	MgO	Al ₂ O ₃	MnO	K ₂ O	Na ₂ O	Zn	Ni	Cu	Co	Sr	Zr	Nb	Pb
-2.5V-1L Feed	16.13	0.226	0.204	0.030	17.62	32.82	0.079	4.10	7.89	10.87	0.164	0.73	1.93	0.0139	0.0318	0.0085	0.0134	0.0477	0.0181	0.0015	0.0021
-1.5V-1L Feed	18.19	0.162	0.373	0.040	19.37	30.50	0.092	3.73	7.87	9.84	0.179	0.54	1.68	0.0146	0.0489	0.0153	0.0146	0.0437	0.0170	0.0008	< 0.0001
0.5V-1L Feed	16.03	0.127	0.128	0.042	15.64	33.95	0.078	4.96	5.58	13.55	0.139	0.62	2.55	0.0108	0.0280	0.0074	0.0104	0.0605	0.0148	0.0015	0.0014
3.5V-1S Feed	19.30	0.162	0.304	0.038	19.68	28.55	0.086	3.38	8.30	9.20	0.179	0.53	1.46	0.0153	0.0446	0.0170	0.0131	0.0408	0.0173	0.0014	0.0034
5.0V-5N Feed	29.68	0.089	0.145	0.080	25.81	17.57	0.136	1.96	7.72	5.17	0.215	0.27	0.75	0.0176	0.0450	0.0089	0.0153	0.0221	0.0234	0.0019	0.0029
6.3V-1L Feed	30.02	0.087	0.140	0.084	26.14	17.88	0.143	1.97	7.65	5.25	0.217	0.27	0.77	0.0175	0.0463	0.0076	0.0175	0.0232	0.0237	0.0017	< 0.0001
-2.5V-1Lx1 Middling*	3.87	0.211	0.052	0.010	5.67	48.99	0.027	6.45	6.53	19.61	0.065	1.44	4.13	0.0058	0.0132	0.0032	0.0053	0.0800	0.0088	0.0004	0.0004
-2.5V-1Lx2 Middling*	8.44	0.304	0.139	0.016	11.70	42.60	0.045	5.28	9.64	13.62	0.134	0.72	2.47	0.0112	0.0251	0.0069	0.0101	0.0588	0.0139	0.0008	0.0005
-1.5V-1L Middling	5.82	0.189	0.151	0.014	8.43	46.11	0.034	5.95	8.26	16.81	0.099	0.91	3.17	0.0083	0.0242	0.0105	0.0074	0.0714	0.0114	0.0006	0.0005
0.5V-1L Middling	5.21	0.139	0.066	0.016	6.42	47.62	0.029	6.98	5.40	19.85	0.069	0.91	4.12	0.0059	0.0189	0.0049	0.0051	0.0852	0.0070	0.0004	0.0002
3.5V-1S Middling	5.09	0.184	0.106	0.015	7.98	45.90	0.031	5.69	9.40	16.78	0.081	0.88	2.96	0.0087	0.0263	0.0087	0.0066	0.0682	0.0120	0.0002	0.0006
5.0V-5N Middling	10.89	0.160	0.107	0.034	12.61	39.69	0.052	4.59	11.47	12.49	0.135	0.56	1.94	0.0136	0.0363	0.0092	0.0106	0.0495	0.0142	0.0008	0.0028
6.3V-1L Middling	4.78	0.170	0.052	0.016	5.90	48.58	0.024	7.04	5.96	19.90	0.069	0.87	4.04	0.0060	0.0168	0.0051	0.0049	0.0845	0.0074	0.0003	0.0001
-2.5V-1L Concentrate*	32.20	0.148	0.336	0.060	31.99	12.93	0.154	1.31	6.73	2.58	0.264	0.15	0.31	0.0229	0.0540	0.0113	0.0202	0.0113	0.0299	0.0016	< 0.0001
-1.5V-1L Concentrate	26.11	0.138	0.524	0.055	26.28	20.51	0.125	2.29	7.55	5.43	0.230	0.25	0.81	0.0182	0.0638	0.0184	0.0165	0.0244	0.0204	0.0007	< 0.0001
0.5V-1L Concentrate	27.32	0.105	0.195	0.067	25.36	20.00	0.130	2.83	5.60	7.05	0.214	0.26	1.21	0.0169	0.0388	0.0094	0.0147	0.0332	0.0227	0.0022	< 0.0001
3.5V-1S Concentrate	33.64	0.128	0.490	0.065	31.89	11.73	0.145	1.09	6.90	2.06	0.280	0.10	0.20	0.0223	0.0618	0.0217	0.0194	0.0076	0.0211	0.0018	0.0031
5.0V-5N Concentrate	40.72	0.049	0.157	0.111	33.98	5.41	0.184	0.43	5.82	1.12	0.265	0.06	0.07	0.0198	0.0509	0.0089	0.0180	0.0050	0.0287	0.0026	< 0.0001
6.3V-1L Concentrate	36.59	0.133	0.253	0.096	32.04	9.54	0.164	0.99	6.77	1.84	0.258	0.07	0.18	0.0206	0.0543	0.0131	0.0199	0.0066	0.0302	0.0022	< 0.0001
-2.5V-1L Tailings	9.28	0.479	0.251	0.022	12.45	39.16	0.056	3.61	13.28	11.10	0.136	2.58	1.37	0.0114	0.0279	0.0467	0.0143	0.0338	0.0131	0.0010	0.0017
-1.5V-1L Tailings	8.13	0.298	0.113	0.020	10.56	42.03	0.043	4.38	11.79	13.51	0.119	1.94	2.02	0.0090	0.0212	0.0257	0.0111	0.0480	0.0122	0.0009	0.0018
0.5V-1L Tailings	6.99	0.279	0.039	0.024	7.68	43.54	0.043	5.49	7.87	17.85	0.078	2.45	3.15	0.0063	0.0182	0.0067	0.0102	0.0653	0.0072	0.0009	0.0002
3.5V-1S Tailings	11.92	0.376	0.130	0.030	13.27	36.60	0.073	3.20	12.47	10.68	0.122	2.19	1.26	0.0122	0.0364	0.0180	0.0100	0.0331	0.0158	0.0009	0.0007
5.0V-5N Tailings	14.45	0.315	0.077	0.051	14.41	34.25	0.078	3.67	11.15	11.06	0.137	1.72	1.54	0.0134	0.0326	0.0093	0.0137	0.0376	0.0164	0.0009	0.0030
6.3V-1L Tailings	9.15	0.290	0.282	0.036	9.94	41.18	0.056	5.04	8.49	15.65	0.096	1.99	2.67	0.0082	0.0292	0.0454	0.0166	0.0591	0.0104	0.0006	0.0006

* The concentrate of sample -2.5V-1L was run an additional time due to poor separation in the first run.

4.4 SHAKING TABLE SEPARATIONS TITANIA

Table 17. gives an overview of the products from shaking table separations, with the respective product sizes and running times. The separation yielded 3 products; concentrate, middling and tailings. Modal mineralogy and bulk chemical data can be found in Table 18. and Table 19, respectively.

Table 17. Overview of samples, with the respective running time, feed-, concentrate-, middling-, and tailings size from the shaking table analyses performed at Titania. The shaking table separations were run with an average feed flow rate of 13.17 kg/h. Sample 1-6 were run with a water flow of 600 L/h, sample 7-8; 650 L/h and sample 13-14; 850 L/h.

Sample name	Sample number	Running time (min:sec)	Feed (g)	Concentrate (g)	Middling (g)	Tailings (g)
155149-1	1	05:35	733.6	181.2	471.2	24.3
155149-2	2	06:49	781.3	300.6	298.7	115.1
155149-3	3	07:03	684.5	240.6	381.7	24.9
155149-4	4	06:08	611.3	158.8	391.1	39.8
155149-5	5	08:40	905.0	372.8	458.0	36.0
155149-6	6	06:11	894.3	316.5	471.8	51.1
155149-7	7	05:40	837.3	171.0	553.9	70.1
155149-8	8	05:50	737.9	161.5	467.0	71.4
155149-9	9	06:12	900.7	155.1	618.9	77.0
155149-10	10	05:52	725.8	140.5	500.0	47.4
155149-11	11	05:30	758.8	132.5	513.5	58.3
155149-12	12	07:30	1046.2	243.9	663.3	92.0
155149-13	13	06:24	819.1	204.3	509.0	69.0
155149-14	14	08:06	1034.7	112.7	766.2	94.2

Table 18. Analyses of the modal mineralogy by XRD of the products from the gravity separation performed with a shaking table at Titania. Each sample is separated into; concentrate, middling and tailings. Table 17. gives an overview of the respecting sample sizes. Analyses were performed at Titania and all values are normalized and given in wt%.

Sample name	Ilmenite	Hematite	Rutile	Magnetite	Pyrite	Orthopyroxene	Clinopyroxene	Plagioclase	Olivine	Biotite	Phlogopite	Quartz	Calcite	Apatite	Spinel	Antigorite
155149-1 concentrate	86.13	8.88	0.08	0.25	0.07	1.60	0.04	1.55	0.94	0.03	0.07	0.00	0.00	0.04	0.00	0.30
155149-1 middling	26.41	2.14	0.17	0.17	0.03	21.25	2.58	43.60	1.38	0.78	0.60	0.19	0.09	0.10	0.12	0.41
155149-1 tailings	1.71	0.49	0.89	0.54	0.02	8.58	2.05	73.53	1.00	1.65	2.54	2.31	0.17	0.18	0.24	4.12
155149-2 concentrate	82.55	9.48	0.14	0.22	0.02	2.78	0.21	3.04	1.05	0.02	0.16	0.07	0.00	0.02	0.07	0.17
155149-2 middling	21.03	2.36	0.19	0.30	0.07	21.12	2.60	49.87	0.98	0.48	0.30	0.17	0.04	0.09	0.00	0.40
155149-2 tailings	0.21	0.04	1.79	0.32	0.06	5.10	0.90	83.21	0.01	1.06	2.31	0.62	0.09	0.10	0.20	3.98
155149-3 concentrate	85.50	8.46	0.09	0.24	0.00	1.64	0.06	1.69	1.33	0.04	0.33	0.03	0.00	0.03	0.04	0.53
155149-3 middling	7.87	0.43	1.00	0.46	0.02	21.87	3.04	58.58	1.33	0.59	0.82	0.39	0.16	0.06	0.16	3.22
155149-3 tailings	8.12	0.26	3.15	1.04	0.01	11.06	1.88	53.02	1.65	4.27	5.10	2.39	0.26	0.11	0.52	7.17
155149-4 concentrate	83.15	8.50	0.13	0.48	0.06	1.37	0.43	3.82	1.09	0.17	0.01	0.04	0.03	0.02	0.08	0.62
155149-4 middling	13.61	1.05	0.13	1.09	0.03	19.85	2.52	56.86	0.55	0.74	0.76	0.29	0.16	0.11	0.07	2.17
155149-4 tailings	3.21	0.12	3.56	0.90	0.04	8.35	2.45	62.89	0.08	2.67	3.57	2.06	0.48	0.14	0.58	8.91
155149-5 concentrate	85.84	9.33	0.14	0.09	0.03	1.42	0.00	1.82	0.64	0.02	0.17	0.04	0.00	0.01	0.04	0.42
155149-5 middling	7.76	0.66	1.06	1.31	0.06	31.94	2.92	51.34	0.62	0.45	1.07	0.13	0.15	0.08	0.11	0.35
155149-5 tailings	10.94	0.68	2.90	1.09	0.06	13.41	1.52	49.95	1.04	2.77	6.03	1.09	0.16	0.08	0.40	7.91
155149-6 concentrate	88.99	8.63	0.11	0.00	0.05	0.16	0.00	1.14	0.61	0.00	0.26	0.01	0.00	0.03	0.01	0.00
155149-6 middling	11.46	0.78	0.22	0.60	0.01	23.74	2.88	55.46	0.13	0.32	1.53	0.13	0.04	0.08	0.09	2.55
155149-6 tailings	5.91	0.53	2.59	1.64	0.09	9.02	1.40	57.62	1.62	2.33	5.59	1.19	0.09	0.10	0.62	9.67
155149-7 concentrate	87.90	10.85	0.17	0.00	0.05	0.02	0.00	0.77	0.01	0.02	0.18	0.00	0.00	0.02	0.01	0.00
155149-7 middling	21.44	2.22	0.24	0.11	0.05	11.12	2.93	58.92	0.00	0.57	0.72	0.30	0.10	0.05	0.22	1.02
155149-7 tailings	2.50	0.21	2.73	1.03	0.10	4.67	1.60	68.54	0.20	2.34	5.33	2.34	0.23	0.11	0.51	7.57
155149-8 concentrate	90.80	7.99	0.05	0.00	0.09	0.04	0.00	0.50	0.46	0.00	0.01	0.00	0.00	0.04	0.02	0.00
155149-8 middling	25.94	2.10	0.25	0.82	0.04	20.43	2.19	43.87	2.50	0.56	0.50	0.10	0.12	0.08	0.10	0.39
155149-8 tailings	12.04	0.83	2.28	0.88	0.04	11.82	1.29	56.94	2.04	1.71	3.20	1.01	0.21	0.08	0.12	5.52
155149-9 concentrate	90.60	7.68	0.17	0.02	0.09	0.04	0.00	0.65	0.62	0.01	0.08	0.00	0.00	0.00	0.00	0.05
155149-9 middling	20.06	1.37	0.25	0.89	0.05	17.34	2.42	53.08	1.24	0.57	0.50	0.29	0.07	0.08	0.16	1.65
155149-9 tailings	4.36	0.06	3.16	0.84	0.05	7.32	1.42	66.59	0.18	2.05	4.45	1.37	0.15	0.08	0.42	7.51
155149-10 concentrate	91.00	7.31	0.17	0.00	0.04	0.03	0.34	0.70	0.20	0.08	0.04	0.00	0.00	0.05	0.01	0.04
155149-10 middling	16.09	1.17	0.30	0.55	0.00	16.70	2.61	57.86	1.49	0.57	0.64	0.25	0.12	0.07	0.15	1.43
155149-10 tailings	2.13	0.15	2.73	1.30	0.06	6.68	1.64	68.24	0.45	2.23	4.17	0.89	0.30	0.09	0.49	8.44
155149-11 concentrate	89.31	7.94	0.14	0.00	0.05	0.01	0.01	1.25	0.81	0.01	0.23	0.00	0.00	0.00	0.00	0.23
155149-11 middling	20.83	1.38	0.18	0.55	0.03	17.02	2.30	55.09	0.83	0.58	0.30	0.10	0.10	0.05	0.05	0.61
155149-11 tailings	2.71	0.03	2.15	0.57	0.04	6.50	1.08	73.60	0.64	1.97	4.17	0.99	0.15	0.07	0.34	5.01
155149-12 concentrate	88.35	7.90	0.08	0.00	0.10	0.02	0.00	1.83	0.96	0.22	0.30	0.04	0.00	0.05	0.00	0.16
155149-12 middling	20.36	1.50	0.30	0.61	0.00	18.27	2.67	54.20	0.42	0.42	0.71	0.10	0.09	0.07	0.02	0.27
155149-12 tailings	0.85	0.00	1.93	0.90	0.10	5.11	1.16	76.81	0.59	1.59	4.05	0.68	0.19	0.07	0.18	5.81
155149-13 concentrate	88.93	9.34	0.01	0.02	0.04	0.04	0.03	0.98	0.36	0.01	0.01	0.03	0.00	0.00	0.03	0.17
155149-13 middling	9.32	0.54	0.17	0.54	0.03	18.78	2.22	65.94	0.00	0.48	0.98	0.17	0.21	0.02	0.14	0.47
155149-13 tailings	1.67	0.00	2.41	0.95	0.02	6.05	0.98	74.09	0.06	1.72	4.00	0.83	0.31	0.10	0.43	6.38
155149-14 concentrate	89.92	7.97	0.09	0.00	0.12	0.00	0.00	1.09	0.00	0.10	0.10	0.00	0.01	0.07	0.11	0.43
155149-14 middling	22.58	1.71	0.15	0.00	0.06	17.46	1.99	54.97	0.00	0.31	0.37	0.05	0.08	0.08	0.07	0.12
155149-14 tailings	1.70	0.09	1.57	0.36	0.06	6.35	1.11	78.22	0.16	1.21	3.16	0.70	0.15	0.07	0.31	4.77

4.5 WET HIGH-INTENSITY MAGNETIC SEPARATION

The products from WHIMS and their sample sizes are presented in Table 20. The WHIMS, which were done in 4 steps, see Figure 15, yielded 5 products; a strong magnetic concentrate separated at 148 ampere, 2 magnetic concentrates, separated at 348 and 548 ampere, a weak magnetic concentrate separated at 778 ampere, and non-magnetic material. The table shows that more than 50% of the feed gets separated at 348 and 548 ampere.

Table 20. Results from Wet-High-Intensity Magnetic Separation (WHIMS) with the respective sample size per field strengths; 148, 348, 548, 778 ampere.

Sample name	Feed (g)	Strong magnetic concentrate 148 ampere (g)	Magnetic concentrate 348 ampere (g)	Magnetic concentrate 548 ampere (g)	Weak magnetic concentrate 778 ampere (g)	Non-magnetic material (g)
-2,5V-1L	285.5	43.70	71.82	91.98	37.67	13.90
-1,5V-1L	288.2	41.51	73.77	84.08	20.74	43.88
0,5V-1L	283.2	32.70	89.09	60.54	23.14	59.76
3,5V-1S	294.3	41.37	101.7	97.04	20.03	15.25
5,0V-5N	274.8	27.37	78.55	98.18	49.30	9.33
6,3V-1L	280.5	25.35	95.28	104.48	32.30	12.19

XRD- and XRF-analyses of the products were performed at Titania, and is presented in Table 21. and 22., respectively. All products are analysed with a predefined mineral list and are normalized to 100%. Magnetic concentrate 348 ampere and 548 ampere have the highest content of ilmenite, whilst the non-magnetic material has the lowest. Orthopyroxene and olivine is distributed randomly, with no apparent trend, which might be due to week magnetic properties or poor mineral liberation. A 100% of the magnetite is separated at 148 ampere, as expected due to a high magnetic susceptibility.

Table 21. Analyses of the modal mineralogy by XRD of the products from magnetic separation. Table 20. gives an overview of the respecting sample sizes. All values are normalized and given in wt%.

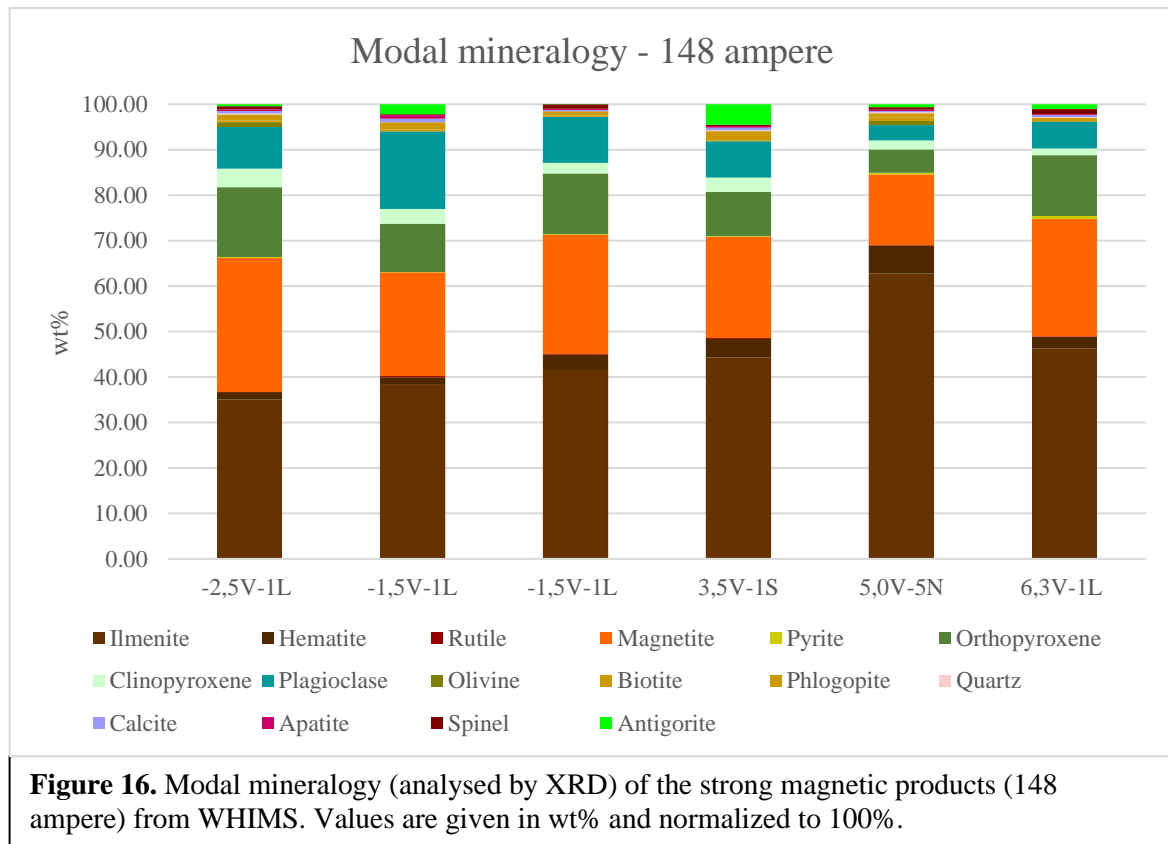
Sample name	Ilmenite	Hematite	Rutile	Magnetite	Pyrite	Orthopyroxene	Clinopyroxene	Plagioclase	Olivine	Biotite	Phlogopite	Quartz	Calcite	Apatite	Spinel	Antigorite
-2,5V-1L 148 ampere	35.09	1.63	0.01	29.52	0.17	15.33	4.11	9.12	1.08	0.39	1.33	0.22	0.54	0.35	0.72	0.40
-2,5V-1L 348 ampere	76.97	2.74	0.21	0.05	0.10	11.07	1.85	5.59	0.42	0.54	0.08	0.22	0.00	0.17	0.00	0.00
-2,5V-1L 548 ampere	65.67	3.30	0.35	0.00	0.17	19.70	0.22	8.45	1.01	0.08	0.66	0.18	0.00	0.20	0.01	0.00
-2,5V-1L 778 ampere	66.59	2.38	0.12	0.00	0.10	18.48	0.65	8.17	2.10	0.09	0.63	0.51	0.00	0.18	0.00	0.00
-1,5V-1L 148 ampere	38.47	1.48	0.25	22.86	0.06	10.59	3.25	17.03	0.11	0.37	1.56	0.01	0.76	0.81	0.23	2.16
-1,5V-1L 348 ampere	65.57	3.58	0.32	0.00	0.22	11.61	4.09	12.83	0.44	0.38	0.13	0.03	0.26	0.29	0.21	0.06
-1,5V-1L 548 ampere	69.83	3.51	0.16	0.00	0.16	9.99	0.00	14.82	0.83	0.05	0.26	0.16	0.01	0.11	0.10	0.00
-1,5V-1L 778 ampere	50.93	1.95	0.15	0.00	0.26	23.97	2.51	17.32	0.99	0.41	0.17	0.48	0.10	0.19	0.15	0.44
-1,5V-1L Non-magnetic	3.16	0.13	0.03	0.00	0.09	10.94	1.22	80.04	0.34	0.98	0.27	0.45	0.02	0.07	0.16	2.10
0,5V-1L 148 ampere	41.52	3.41	0.15	26.19	0.14	13.40	2.29	10.14	0.00	0.31	0.90	0.00	0.29	0.26	1.00	0.00
0,5V-1L 348 ampere	54.30	2.41	0.29	0.00	0.14	16.96	2.84	20.16	0.31	0.59	0.54	0.15	0.19	0.16	0.04	0.91
0,5V-1L 548 ampere	68.45	2.87	0.26	0.00	0.30	11.59	0.04	15.62	0.01	0.05	0.00	0.23	0.00	0.26	0.03	0.28
0,5V-1L 778 ampere	50.14	2.89	0.23	0.00	0.28	20.02	2.04	22.72	0.21	0.14	0.20	0.44	0.12	0.26	0.26	0.05
0,5V-1L Non-magnetic	2.63	0.03	0.12	0.00	0.07	11.09	2.85	80.14	0.00	0.73	0.68	0.59	0.06	0.15	0.13	0.75
3,5V-1S 148 ampere	44.29	4.09	0.22	22.24	0.18	9.73	3.14	7.93	0.27	0.95	1.10	0.20	0.53	0.36	0.28	4.52
3,5V-1S 348 ampere	73.59	3.56	0.24	0.00	0.26	9.49	0.48	8.93	0.03	0.45	0.86	0.24	0.08	0.25	0.00	1.54
3,5V-1S 548 ampere	65.33	2.74	0.19	0.00	0.19	14.12	1.43	12.05	0.11	1.02	1.37	0.53	0.26	0.31	0.17	0.19
3,5V-1S 778 ampere	65.28	4.03	0.13	0.00	0.30	16.83	1.31	9.07	1.44	0.71	0.43	0.22	0.00	0.15	0.10	0.00
3,5V-1S Non-magnetic	12.65	1.45	0.03	0.00	0.08	39.29	4.51	38.49	0.56	1.06	0.42	0.37	0.23	0.23	0.02	0.63
5,0V-5N 148 ampere	62.78	6.10	0.16	15.55	0.31	5.18	1.93	3.43	0.90	0.73	0.98	0.18	0.32	0.25	0.57	0.64
5,0V-5N 348 ampere	79.68	6.04	0.04	0.00	0.59	4.77	0.02	5.96	0.00	0.76	1.26	0.36	0.15	0.30	0.02	0.05
5,0V-5N 548 ampere	73.65	5.52	0.05	0.00	0.32	5.20	0.03	7.46	0.00	0.94	0.02	0.59	0.12	0.38	0.00	5.72
5,0V-5N 778 ampere	76.15	4.82	0.02	0.00	0.37	8.91	0.00	7.81	0.00	0.31	0.66	0.68	0.00	0.26	0.00	0.00
6,3V-1L 148 ampere	46.27	2.53	0.16	25.81	0.67	13.39	1.49	5.87	0.00	0.00	0.78	0.20	0.41	0.20	1.14	1.08
6,3V-1L 348 ampere	74.80	6.52	0.17	0.00	0.50	10.86	1.01	3.39	1.46	0.51	0.54	0.08	0.01	0.11	0.05	0.00
6,3V-1L 548 ampere	62.58	4.06	0.20	0.00	0.42	22.57	1.90	4.92	0.99	0.63	0.61	0.06	0.00	0.16	0.48	0.43
6,3V-1L 778 ampere	62.13	5.17	0.29	0.00	0.11	17.18	2.02	9.48	0.81	1.01	0.72	0.11	0.10	0.22	0.17	0.49

Table 22. Bulk chemical analyses by XRF of the products from magnetic separation. Table 20. gives an overview of the respecting sample sizes. Values are given in wt%.

Sample name	TiO ₂	P ₂ O ₅	S	Cr ₂ O ₃	Fe	SiO ₂	V ₂ O ₃	CaO	MgO	Al ₂ O ₃	MnO	K ₂ O	Na ₂ O
-2,5V-1L 148 ampere	17.42	0.053	2.405	0.222	44.88	9.52	0.315	0.76	5.87	2.37	0.158	0.08	0.12
-2,5V-1L 348 ampere	39.44	0.044	0.059	0.025	32.03	9.06	0.113	0.70	6.38	1.30	0.309	0.10	0.14
-2,5V-1L 548 ampere	37.00	0.052	0.050	0.024	30.61	11.78	0.102	0.88	7.63	1.56	0.304	0.12	0.14
-2,5V-1L 778 ampere	35.71	0.060	0.055	0.024	29.93	13.20	0.104	1.03	7.85	1.78	0.300	0.15	0.17
-1,5V-1L 148 ampere	17.96	0.052	5.001	0.225	41.81	10.83	0.278	0.94	6.13	2.69	0.159	0.10	0.22
-1,5V-1L 348 ampere	37.07	0.036	0.132	0.029	30.40	11.75	0.115	0.89	7.44	1.81	0.298	0.10	0.19
-1,5V-1L 548 ampere	33.48	0.045	0.076	0.026	28.23	15.79	0.100	1.15	9.03	2.36	0.287	0.15	0.24
-1,5V-1L 778 ampere	29.90	0.056	0.080	0.025	26.13	19.68	0.090	1.48	10.23	3.09	0.276	0.21	0.33
-1,5V-1L Non-magnetic	3.74	0.537	0.106	0.007	5.62	49.43	0.018	7.44	6.48	19.29	0.077	0.74	3.90
0,5V-1L 148 ampere	20.21	0.040	1.337	0.330	43.04	9.59	0.312	0.96	5.34	2.91	0.167	0.07	0.23
0,5V-1L 348 ampere	39.31	0.031	0.096	0.041	31.17	9.34	0.123	0.98	6.12	2.13	0.288	0.08	0.23
0,5V-1L 548 ampere	37.80	0.029	0.086	0.040	30.19	11.07	0.117	1.13	6.69	2.43	0.282	0.11	0.29
0,5V-1L 778 ampere	33.41	0.041	0.100	0.036	27.60	15.76	0.108	1.58	7.93	3.40	0.267	0.17	0.41
0,5V-1L Non-magnetic	3.42	0.363	0.086	0.008	4.13	50.27	0.014	8.17	3.95	21.91	0.051	0.72	4.77
3,5V-1S 148 ampere	22.04	0.052	3.020	0.250	43.13	8.01	0.298	0.64	5.20	2.00	0.186	0.08	0.12
3,5V-1S 348 ampere	39.97	0.049	0.126	0.039	32.78	9.53	0.130	0.63	5.82	1.38	0.315	0.06	0.11
3,5V-1S 548 ampere	36.11	0.064	0.117	0.034	30.51	12.37	0.127	0.92	7.42	1.77	0.301	0.10	0.16
3,5V-1S 778 ampere	35.20	0.069	0.137	0.032	29.87	13.55	0.112	1.00	8.05	1.93	0.296	0.11	0.17
3,5V-1S Non-magnetic	8.13	1.229	1.556	0.014	12.59	40.47	0.036	5.83	13.98	9.04	0.158	0.34	1.15
5,0V-5N 148 ampere	32.06	0.037	1.261	0.382	41.46	3.67	0.273	0.32	4.72	1.53	0.206	0.04	0.06
5,0V-5N 348 ampere	44.79	0.027	0.064	0.084	34.94	2.83	0.179	0.25	4.96	0.64	0.278	0.04	0.04
5,0V-5N 548 ampere	43.37	0.033	0.053	0.078	33.92	4.36	0.155	0.33	5.83	0.84	0.276	0.06	0.06
5,0V-5N 778 ampere	40.53	0.038	0.056	0.074	32.36	7.35	0.153	0.44	7.13	1.12	0.269	0.07	0.08
6,3V-1L 148 ampere	22.72	0.041	3.223	0.442	44.39	5.98	0.330	0.63	4.54	2.31	0.159	0.06	0.12
6,3V-1L 348 ampere	41.63	0.036	0.061	0.064	33.05	6.26	0.143	0.57	6.03	1.24	0.276	0.05	0.11
6,3V-1L 548 ampere	39.27	0.038	0.046	0.060	31.70	8.86	0.141	0.71	7.06	1.47	0.272	0.07	0.14
6,3V-1L 778 ampere	35.88	0.047	0.055	0.057	29.85	12.66	0.126	0.90	8.76	1.73	0.264	0.08	0.16

4.5.1 STRONG MAGNETIC CONCENTRATE 148 AMPERE

Figure 16. shows the modal mineralogy of the strong magnetic concentrate - 148 ampere (analyses from XRD). The main constituents in the strong magnetic concentrate are ilmenite: 35-63 wt%; magnetite: 15-29%; plagioclase: 3-17%; orthopyroxene: 5-15%; hematite: 1-6% and clinopyroxene: 1-3%.



4.5.2 MAGNETIC CONCENTRATE 348 AMPERE

Figure 17. shows the modal mineralogy of the magnetic concentrate - 348 ampere (analyses from XRD). The main constituents are ilmenite: 54-80 wt%; plagioclase: 3-20%; orthopyroxene: 4-17%; hematite: 2-6% and clinopyroxene: 0-4%.

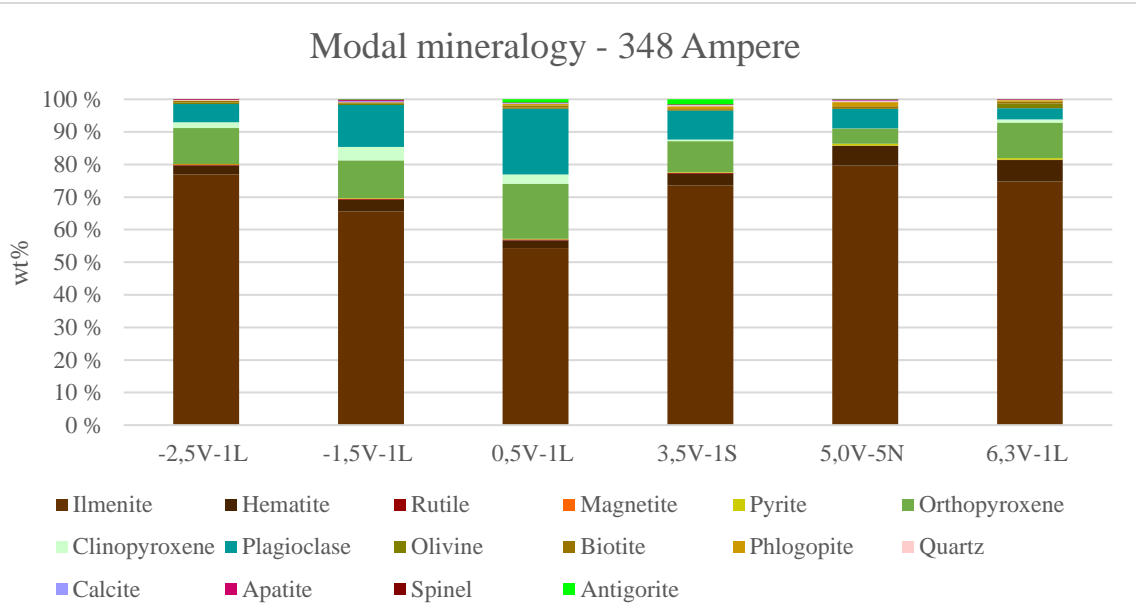


Figure 17. Modal mineralogy (analysed by XRD) of the magnetic products (348 ampere) from WHIMS. Values are given in wt% and normalized to 100%.

4.5.3 MAGNETIC CONCENTRATE 548 AMPERE

Figure 18. shows the modal mineralogy of the magnetic concentrate - 548 ampere (analyses from XRD). The main constituents are ilmenite: 62-73 wt%; orthopyroxene: 5-22%; plagioclase: 5-15%; hematite: 2-6% and clinopyroxene: 0-2%.

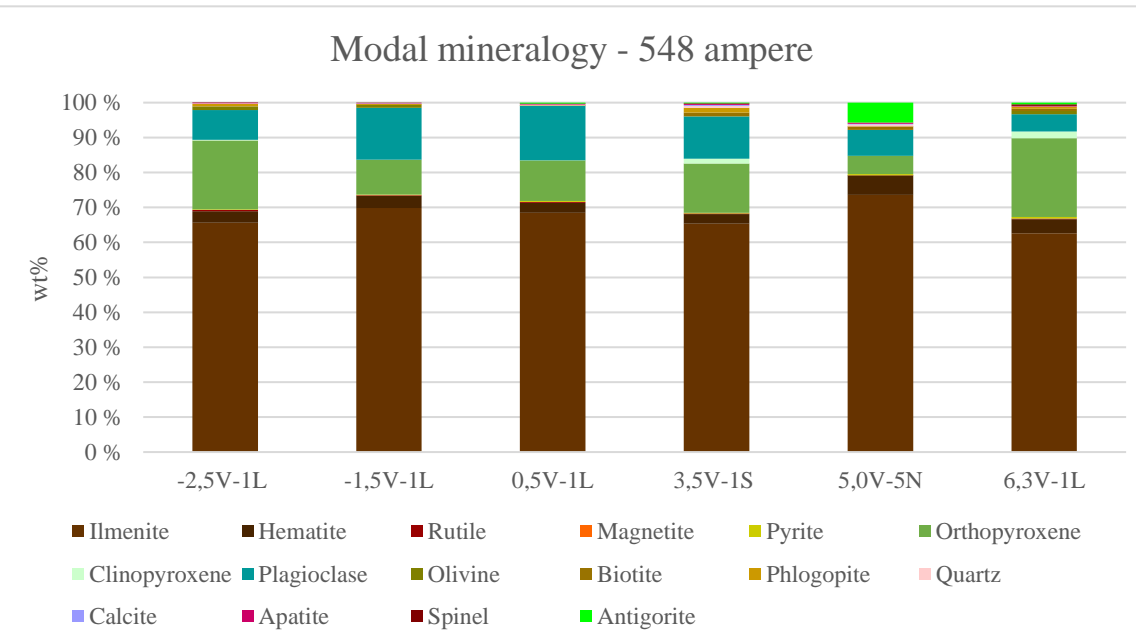


Figure 18. Modal mineralogy (analysed by XRD) of the magnetic products (548 ampere) from WHIMS. Values are given in wt% and normalized to 100%.

4.5.4 WEAK MAGNETIC CONCENTRATE 778 AMPERE

Figure 19. shows the modal mineralogy of the weak magnetic concentrate - 778 ampere (analyses from XRD). The main constituents are ilmenite: 50-76 wt%; orthopyroxene: 9-24%; plagioclase: 8-23%; hematite: 2-5%; olivine: 0-2%; clinopyroxene: 0-2% and biotite: 0-1%. Of the 4 magnetic concentrates this has the highest content of plagioclase. This can be explained to no magnetic properties and it is therefore reasonable to expect that the plagioclase in this fraction will have a higher degree of liberation, compared to the stronger magnetic concentrates.

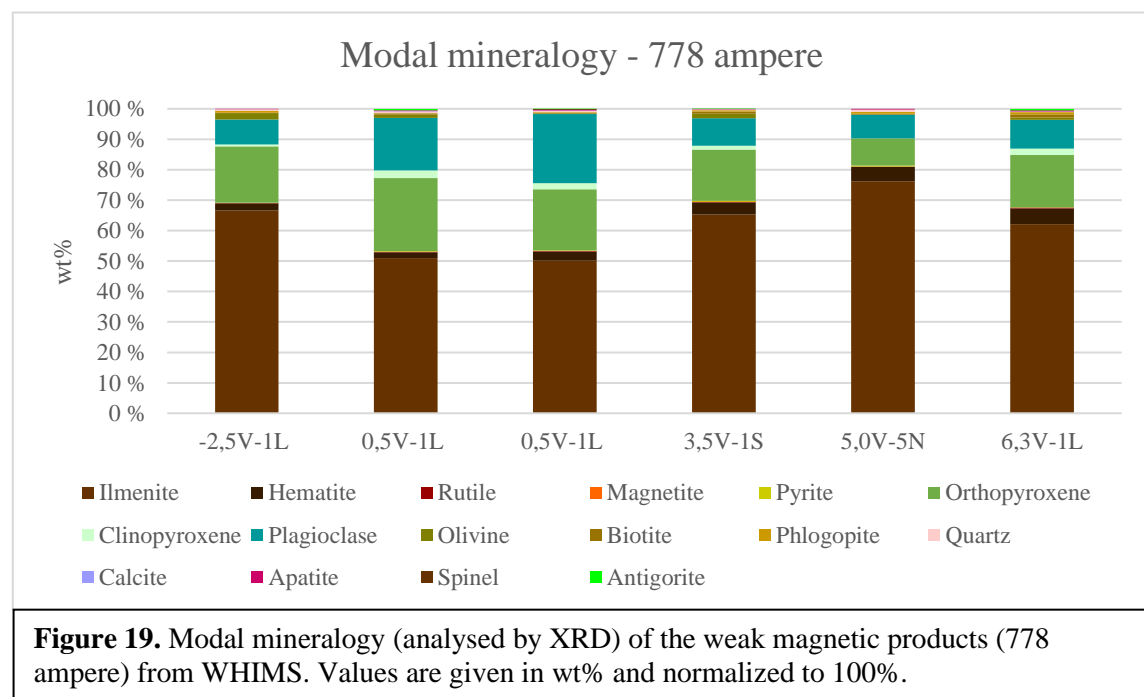
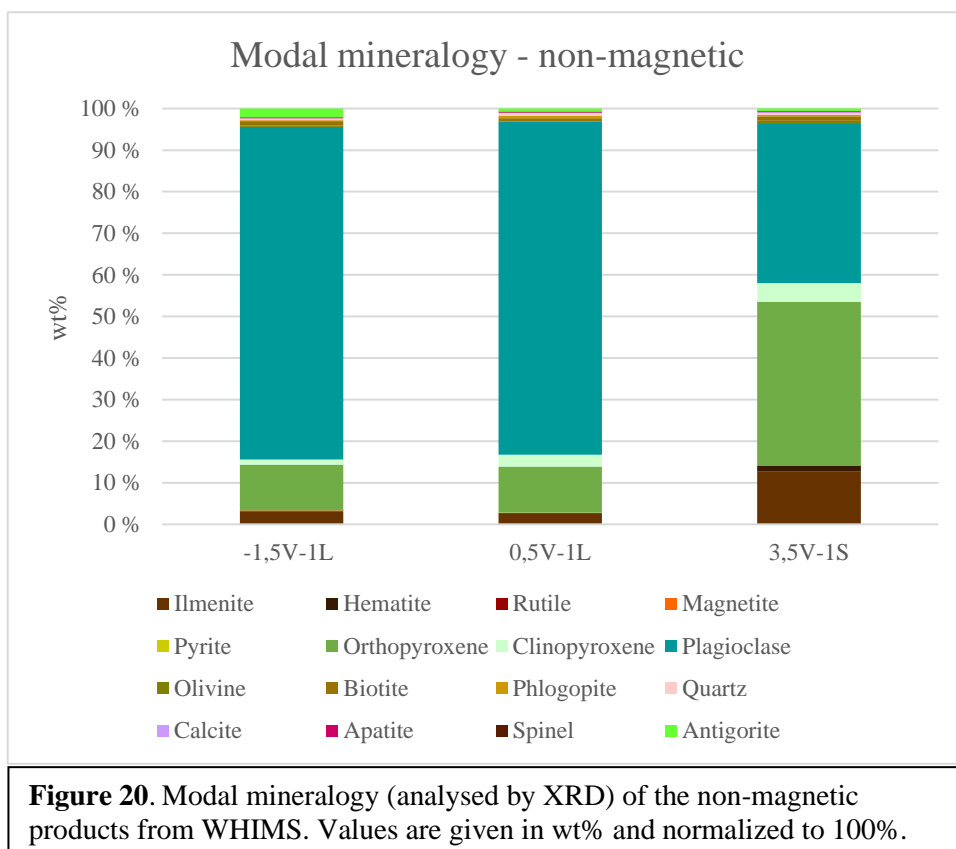


Figure 19. Modal mineralogy (analysed by XRD) of the weak magnetic products (778 ampere) from WHIMS. Values are given in wt% and normalized to 100%.

4.5.5 NON-MAGNETIC MATERIAL

Figure 20. shows the modal mineralogy of the non-magnetic material (analyses from XRD). The main constituents are plagioclase: 39-80 wt%; orthopyroxene: 11-39%; ilmenite: 2-12%; clinopyroxene: 1-5%; hematite 0-2%; antigorite: 0-2% and biotite: 0-1%. As expected this product is dominated by non or weak magnetic minerals such as plagioclase and orthopyroxene. Ilmenite constitutes no more than 2-15 wt% and due to magnetic properties it can be expected that a lot of the ilmenite either appears as locked particles or composite grains.



5 DISCUSSION

5.1 MINERALOGICAL VARIATIONS

It is important to emphasize that analysed samples does not represent the drill core as a whole. Previous studies, for example (Kullerud, 2007), shows compositional variations towards depth in the Skogestad area.

Olivine is only present in some of the drill cores and the spatial distribution show no obvious pattern. The chemical analyses of the olivines shows limited variations among the main elements; MgO, FeO, SiO₂ and MnO, indicating that the olivines analysed, were crystallized at similar conditions. The chemical data is retrieved from 5 olivines from two thin sections. Few analyses will in general give a larger uncertainty and it is therefore reasonable to expect that there might be larger variations than detected in this masters' project.

Clinopyroxene are present in all thin sections. Often occurring as partly altered orthopyroxene, typically along the rim. Indicating that the mineral has crystallized from a residual melt at a late stage. The minerals analysed by EPMA show little to no chemical variation among the main constituents; CaO, MgO, FeO Al₂O₃ and SiO₂.

Orthopyroxene is in addition to plagioclase and ilmenite the most predominant mineral in the ore. It occurs typically with two crystal habits; coarse grained, subhedral, prismatic crystals and medium to fine grained, sub- to euhedral, tabular crystals. The minerals analysed by EPMA shows little to no chemical variation among the main constituents; MgO, FeO, Al₂O₃ and SiO₂. A distinctive feature for the orthopyroxene in the ore are the iron-oxide exsolution lamellas.

Some orthopyroxenes occurs without the lamellas, typically with lower interference colours, usually first order greys and whites. This might indicate that these are of two different generations. Both types were analysed with EPMA, Table 23. gives the chemical analyses of the grains in Figure 22. and 23. however the results show that even though they are visually different, they are relatively equal chemically.

Table 23. Comparison of the average chemical composition (wt% oxides) of the two different types of orthopyroxenes, retrieved from EPMA-data.

Sample name	MgO	FeO	Al ₂ O ₃	CaO	MnO	TiO ₂	SiO ₂
3.5V-1S	27.17	14.86	1.99	1.07	0.28	0.19	54.16
3.0V-4N	26.80	14.76	1.96	1.12	0.26	0.17	53.85

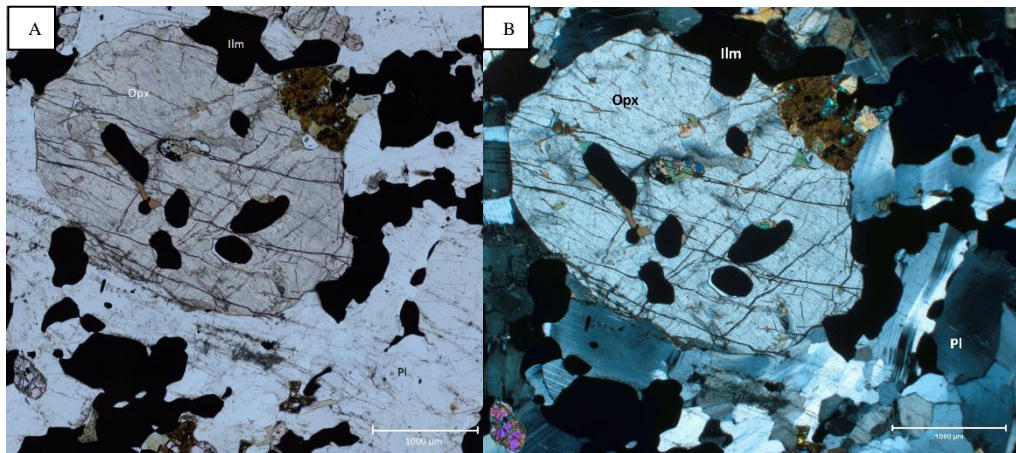


Figure 21. A) Coarse-grained orthopyroxene, with inclusions of ilmenite and biotite in PPL (thin section 3.5V-1S). B) Picture A) in XPL. Abbreviations: Opx – orthopyroxene, ilm – ilmenite, Pl – plagioclase.

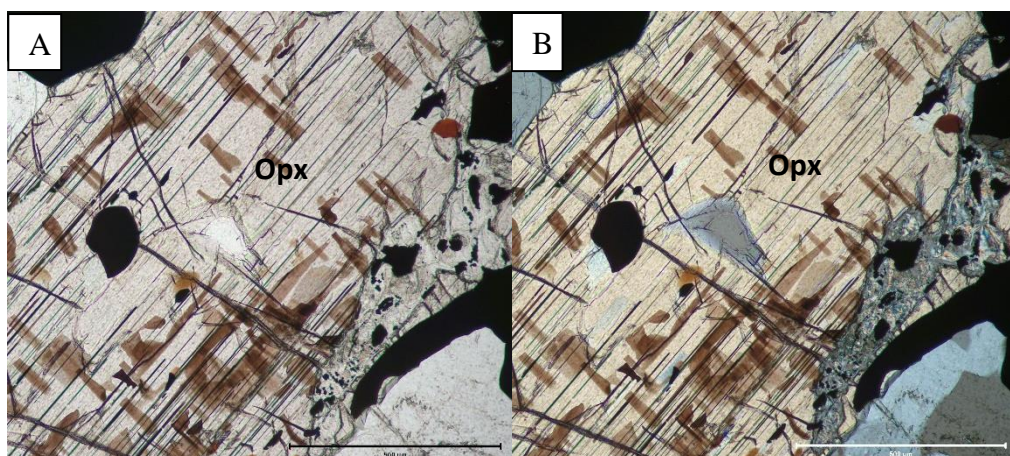


Figure 22. A) Coarse-grained orthopyroxene, with brown iron-oxide exsolution lamellas and inclusions of ilmenite in PPL (thin section 3.0V-4N). B) Picture A) in XPL. Abbreviation: Opx – orthopyroxene.

5.2 SHAKING TABLE SEPARATIONS

Shaking table separations performed at IPG, NTNU were done on crushed and ground drill cores and were operated with the exact same settings; degree of inclination, length of stroke and waterflow. Experienced differences can be attributed to mineralogical and textural variations between the samples. The shaking table separations performed at Titania were done on drill cuttings with the intention to investigate how large the mineralogical and chemical variations are within one blast. This specific blast is located within the main ore and not the Skogestad area, as the samples separated at IPG. Settings; waterflow and inclination, were changed during the separations, which leads to a certain degree of uncertainty. The experienced variations may therefore be attributed to the change of settings.

The initial ilmenite content in the feed varies for both shaking table separations. Complete data can be found in Section 4.4, Table 18. The ilmenite content in the drill cuttings samples varies with a difference of 8 wt%. The crushed drill core samples have a higher difference, of 32.1 wt% which is reasonable since they are not from the same blast but from different parts of the Skogestad area. The orthopyroxene and clinopyroxene content are quite comparable, but the olivine content are slightly higher in the drill core samples.

Table 24. Shaking table feeds with the respective ilmenite, orthopyroxene, clinopyroxene and olivine content (wt%), modal mineralogy analysed by XRD.

Titania					IGP, NTNU				
Sample name	Ilmenite	Orthopyroxene	Clinopyroxene	Olivine	Sample name	Ilmenite	Orthopyroxene	Clinopyroxene	Olivine
155149-1	38.615	15.343	2.029	1.09	-2.5V-1L	26.77	17.23	2.67	2.4
155149-2	40.045	12.879	0.997	0.322	-1.5V-1L	31.38	18.37	2.31	1.98
155149-3	37.575	14.767	1.449	1.613	0.5V-1L	27.02	11	1.74	0.51
155149-4	26.578	14.187	2.225	0.357	3.5V-1S	35.23	13.89	1.53	1.92
155149-5	39.255	19.284	1.877	0.799	5.0V-5N	53.93	12.93	0.76	3.1
155149-6	38.074	15.482	1.907	0.292	6.3V-1L	33.11	14.82	1.58	0.55
155149-7	33.537	8.596	1.372	0.426					
155149-8	39.69	15.688	1.821	1.753					
155149-9	29.169	13.267	1.504	0.451					
155149-10	29.02	12.698	2.037	1.135					
155149-11	31.209	12.476	1.646	0.44					
155149-12	32.645	13.688	2.306	0.462					
155149-13	26.535	13.08	2.321	0.168					
155149-14	26.68	15.089	1.822	0.016					

The ilmenite content in the concentrate are noticeably different between the two samples. The samples done at Titania has an average content of 87.8 wt%, whilst the drill core samples ranges from 48-76

wt% ilmenite, see Table 25. the content of clinopyroxene, orthopyroxene and olivine is also noticeably higher.

The apparent differences between the two separations can be a consequence of many factors; There are differences between drill cuttings and crushed drill cores. There will naturally be a difference in grain shapes, particle size distribution and grain size, if the material is not screened to a certain size fraction. The shaking table separations were done on two different tables, with different settings and size. If the goal was to optimize the method for gravity separation, recovery should be calculated for each concentrate.

Table 25. Shaking table concentrates with the respective ilmenite, orthopyroxene, clinopyroxene and olivine content (wt%), modal mineralogy analysed by XRD.

Titania					IGP, NTNU				
Sample name	Ilmenite	Orthopyroxene	Clinopyroxene	Olivine	Sample name	Ilmenite	Orthopyroxene	Clinopyroxene	Olivine
155149-1	86.134	1.598	0.042	0.94	-2.5V-1L	60.5	12.24	1.3	3.07
155149-2	82.554	2.78	0.21	1.048	-1.5V-1L	48.54	17.07	1.99	1.79
155149-3	85.5	1.641	0.059	1.327	0.5V-1L	49.46	11.76	1.68	0.55
155149-4	83.149	1.369	0.43	1.094	3.5V-1S	66.9	11.98	1.65	2.4
155149-5	85.841	1.417	0.002	0.64	5.0V-5N	76.46	4.73	0.08	2.2
155149-6	88.99	0.157	0	0.613	6.3V-1L	68.72	10.47	1.41	1.7
155149-7	87.901	0.018	0	0.008					
155149-8	90.795	0.038	0	0.459					
155149-9	90.598	0.044	0	0.618					
155149-10	90.995	0.029	0.34	0.201					
155149-11	89.305	0.008	0.008	0.814					
155149-12	88.353	0.015	0.003	0.963					
155149-13	88.934	0.04	0.026	0.361					
155149-14	89.924	0.003	0	0.002					

The particle size ranges between 425 µm and 63 µm in the crushed drill cores and between 212 µm and 63 µm in the drill cuttings. The higher content of orthopyroxene, clinopyroxene and olivine in the crushed drill core concentrate can be a consequence of a larger size range. A larger size range will probably have a higher content composite grains and may therefore be explained by poor mineral liberation.

5.1 MAGNETIC PROPERTIES VERSUS LIBERATION

Titania is interested to get a better understanding of why larger portions of orthopyroxene, olivine and clinopyroxene, than desired, tends to end up in the ilmenite concentrate. This is most likely due to magnetic properties and/or poor liberation.

By studying element maps from SEM it is apparent that in sample 3,5V-IS - 148 ampere the olivine generally occurs as middling together with magnetite, orthopyroxene, sulphides and ilmenite, supported by association data, however there are coarser liberated grains.

Approximately 23% of the grains are liberated, 44% as middling and 33% as locked. Sample - 2,5V-IL - 348 ampere has a larger portion of liberated grains, compared to 3,5V-IS - 148 ampere and grains are generally smaller, both liberated and middling. As middling, the olivine is typically together with orthopyroxene, ilmenite and plagioclase. Liberation data shows that 35% of the olivine is liberated, 50% is middling and 15% locked.

The olivine in sample -1,5V-IL - 548 ampere and in sample -2,5V-IL - 778 ampere occurs relatively similar to sample -2,5V-IL - 348 ampere. Liberation data for sample -1,5V-IL - 548 ampere shows that 41% of the olivine is liberated, 47% is middling and 5% is locked. In sample -2,5V-IL - 778 ampere 48 % of the olivine is liberated, 37% is middling and 15% is locked. As for in sample -1,5V-IL - non magnetic the olivine occurs either as small liberated grains or grains locked in plagioclase. Liberation data shows that 31% of the olivine is liberated, 44% is middling and 25% is locked.

The liberation data shows that the olivine liberation increases with the decreasing magnetic flux density. The largest liberated olivine grains gets separated out at 148 ampere indicating that the olivine grains do have some magnetic properties. It is important to emphasise that the liberation is apparent, the grains are analysed by the cut surface, which is random, and may not represent the correct mineral liberation. Another factor is that olivine is often associated with magnetite in the strong magnetic concentrate (148 ampere), a consequence of poor liberation. The analyses were done on separation products from different drill cores, there is therefore a certain degree of uncertainty regarding the discussed results.

If the analyses had been done consequent on products from only one core, it would be possible to get a clearer picture of how the olivine behaves, and at which magnetic flux density the separation would be most optimal. However, the optimal settings for one core/ore

type, is not necessary the optimal settings for other cores/ore types, due to mineralogical and textural variations.

In sample 3,5V-IS - 148 clinopyroxene occurs mainly as composite grains, often in association with several minerals, such as ilmenite, orthopyroxene, olivine, magnetite and plagioclase. The Fe-content is low, 7 wt% in average. Liberation data shows that 15% occurs as liberated, 59% as middling and 26% as locked particles. In sample -2.5V-1L – 348 22% of the grains are liberated, 46% as middling and 32% as locked particles. Clinopyroxene is to a greater extent associated with ilmenite, but also orthopyroxene and plagioclase. The Fe-content is still low (7 wt%). Sample -1.5V-1L – 548 ampere show the same Fe-content as the previous discussed samples. The liberation is higher at 26% with 37% being middling and being 37% locked particles. Associated with orthopyroxene, ilmenite and plagioclase. Sample -2,5V-1L – 778 ampere can be compared to the two previous samples. The clinopyroxene in the non-magnetic product, sample -1.5V-1L – non-magnetic can also be compared to the three previous samples.

The liberation data shows that the degree of liberation increases after the first separation but stays at a constant, approximately 26% for the rest of the separations. The Fe-content also stays at 7 wt%.

In sample 3,5V-IS - 148 ampere orthopyroxene make up approximately 8 wt%, where 18% are liberated grains, 64% middling and 18% locked. It is generally associated with magnetite, ilmenite and clinopyroxene. -2.5V-1L - 348 ampere has a larger portion of liberated grains compared to sample 3.5V-1S – 148. 38% of the grains are liberated, whilst 54% are middling and 7% are locked. Orthopyroxene makes up approximately 10 wt% of the sample, and is mainly associated with ilmenite, plagioclase, clinopyroxene and olivine. In sample -1.5V-1L – 548 ampere 48% of the orthopyroxene grains are liberated, 47% are middling and 5% are locked. It makes up 19 wt% of the sample and are mainly associated with ilmenite, clinopyroxene, olivine, plagioclase and sulphides. Sample -2,5V-1L – 778 ampere is made up of 16 wt% orthopyroxene, and is the sample with the highest degree of liberation; 50% liberated, 45% middling, 5% locked. Commonly associated with ilmenite, clinopyroxene, plagioclase and sulphides. In sample -1.5V-1L – non-magnetic orthopyroxene constitutes 17 wt% of the sample. The liberation is relatively high; 47% with 44% middling and 9% locking and generally associated with plagioclase and clinopyroxene.

The liberation data shows that the degree of liberation increases with decreasing magnetic flux density. The degree of liberation is lowest in the strong magnetic product (148 ampere), and highest in the weak magnetic product (778 ampere). The content of orthopyroxene in the strong magnetic and magnetic products can to a certain degree be explained due to a high number of composite grains (middling) of either orthopyroxene and magnetite or orthopyroxene and ilmenite. However there are also liberated grains, which might indicate that some of the orthopyroxene has magnetic properties. The average Fe-content in orthopyroxene is lowest in sample 3,5V-IS - 148 ampere (15.3 wt%), which is the strong magnetic product, whilst the magnetic concentrates (348 and 548 ampere) and the weak magnetic concentrate has the highest content of approximately 17 wt%.

For complete; bulk data, liberation data, locking data and association data see Appendix D. SEM element maps can be found in Appendix E.

6 CONCLUSION

The olivine and pyroxene in the analysed samples show only minor chemical variations. The analysed orthopyroxene has a noticeably higher MgO content compared to FeO and CaO and corresponds chemically to more of an enstatite than a ferrosilite. The MgO content in olivine is also high compared to FeO and show clear negative correlation. The olivine corresponds chemically to more of an forsterite than a fayalite. The clinopyroxene is high in CaO and MgO and low in FeO and chemically corresponds to an augite.

The drill cores chosen for mineral processing show noticeable mineralogical variations and is therefore expected to behave somewhat different in the processing. Liberation data, retrieved from SEM-analyses from WHIMS, for orthopyroxene shows that the degree of liberation increases with decreasing magnetic flux density. The degree of liberation is lowest in the strong magnetic product (148 ampere), and highest in the weak magnetic product (778 ampere). The content of orthopyroxene in the strong magnetic and magnetic products can to a certain degree be explained due to a high number of composite grains (middling) of either orthopyroxene and magnetite or orthopyroxene and ilmenite. However there are also liberated grains, which might indicate that some of the orthopyroxene has magnetic properties.

Olivine show a higher degree of liberation than orthopyroxene in the strong magnetic concentrate (148 ampere), especially coarser grains appears as liberated grains. This may indicate that olivine has stronger magnetic properties compared to orthopyroxene.

Results show rather small chemical variations among the olivine and the pyroxenes. Liberation and association data shows that olivine and pyroxene occurs as liberated or as composite grains, often associated with magnetite or ilmenite in stronger magnetic concentrates. It has therefore been suggested that the reason why olivine and pyroxene may end up in the concentrate is a combination of mineral liberation and magnetic properties.

7 FURTHER WORK

Further work should include; analyses of a larger quantity of olivines and pyroxenes from different parts of the Skogestad area, to further investigate chemical variations. SEM-analyses of the different streams at Titania would give a better understanding for what kind of olivine and pyroxene minerals that actually do end up in the concentrate. Separation with a Frantz magnetic separator to further investigate the magnetic properties of olivine and pyroxene.

REFERENCES

- Charlier, B., Duchesne, J.-C. & Vander Auwera, J. (2006) Magma chamber processes in the Tellnes ilmenite deposit (Rogaland Anorthosite Province, SW Norway) and the formation of Fe-Ti ores in massif-type anorthosites *Chemical Geology*, Vol. 3, pp. 264-290.
- Diot, H., Bolle, O., Lambert, J.-M., Launeau, P. & Duchesne, J.-C. (2003) The Tellnes ilmenite deposit (Rogaland, South Norway): magnetic and petrofabric evidence for emplacement of a Ti-enriched noritic crystal mush in a fracture zone, *Journal of Structural Geology*, Vol. 25, pp. 481-501.
- Duchesne, J.-C. (2001) *The Rogaland Intrusive Massifs - an excursion guide*. (Report no.: 2001.029). Trondheim, Norway: Geological Survey of Norway (NGU). Available at: <https://www.ngu.no/en/publikasjon/rogaland-intrusive-massifs-excursion-guide> (Accessed: 19.01.2020).
- Duchesne, J. C. (1999) Fe-Ti deposits in Rogaland anorthosites (South Norway): geochemical characteristics and problems of interpretation, *Mineralium Deposita*, vol. 34(2), pp. 182-194.
- Dybdahl, I. (1960) Ilmenite deposits of the Egersund anorthosite complex, *Mines in south and central Norway, Internat. Geol. Cong.*, 21st, Copenhagen. pp. 48-53.
- Gierth, E. & Krause, H. (1973) Die Ilmenitlagerstätte Tellnes (Süd-Norwegen), *Norsk geologisk tidsskrift*, Vol. 53, pp. 359-402.
- Kofstad, P. K. & Pedersen, B. (2019) *Titan in Store norske leksikon*
Available at: <https://snl.no/titan> (Accessed: 19.07.2020).
- Krause, H. & Pedall, G. (1980) *Fe-Ti Mineralizations in the Åna-Sira Anorthosite, Southern Norway*. (Bulletin 307 Report no.: 1547). Espoo, Finland: Geological Survey of Finland.
- Krause, H., Gierth, E. & Schott, W. (1985) Ti-Fe Deposits in the South Rogaland Igneous Complex, with Special Reference to the Åna-Sira Anorthosite Massif, *Norges geologiske undersøkelse Bulletin 402*, pp. 25-37.
- KRONOS (n.d.) *Hauge i Dalane, Norway*. Available at: <https://kronostio2.com/en/manufacturing-facilities/hauge-norway>.
- Kullerud, K. (2003) Geochemistry and mineralogy of the Tellnes ilmenite ore body, *Ilmenite deposits and their geological environment*, pp. 70.
- Kullerud, K. (2005) *Cr₂O₃ og MgO-innhold i ilmenitt fra Tellnesmalmen - oppfølging av tidligere arbeider*. (Unpublished report for Titania AS).
- Kullerud, K. (2007) *Compositional variations of the Tellnes ore in the Skogestad area*. (Unpublished report for Titania AS).
- Kullerud, K. (2008) *Kjemiske variasjoner i malmen i Skogestadområdet*. (Unpublished report for Titania AS).
- Maijer, C. & Padget, P. (ed.) (1987) *The geology of southernmost Norway: an excursion guide*. Norway, Trondheim: Norges geologiske undersøkelse (Geological Survey of Norway).
- Malvik, T. (2014) History and growth of modern process mineralogy, *Mineralproduksjon*, vol. 5.
- NGU (2015a) *Titan*. Available at: <https://www.ngu.no/fagomrade/titan#> (Accessed: 31.01.2020).
- NGU (2015b) *Transcript from Database Norwegian Ores*. Available at: <http://geo.ngu.no/kart/mineralressurser/> (Accessed: 09.04.2020).
- NGU (2017) *Transcript from Database Norwegian Ores*. Available at: <http://geo.ngu.no/kart/mineralressurser/> (Accessed: 10.04.2020).
- Schiellerup, H., Korneliussen, A., Heldal, T., Marker, M., Bjerksgård, T. & Nilsson, L.-P. (2003) Mineral resources in the Rogaland Anorthosite Province, South Norway: origins, history and recent developments *Ilmenite deposits and their geological environment*, pp. 121-122.

- Schärer, U., Wilmart, E. & Duchesne, J. C. (1996) The short duration and anorogenic character of anorthosite magmatism: U-Pb dating of the Rogaland complex, Norway, *Earth and Planetary Science Letters*, 139, pp. 335-350.
- Strekeisen, A. (n.d.) *Norite*. Available at: <http://www.alexstrekeisen.it/english/pluto/norite.php> (Accessed: 12.07.2020).
- Whitney, D. L. & Evans, B. W. (2010) Abbreviations for names of rock-forming minerals, *American Mineralogist*, Vol. 95, pp. 185-187.
- Wilmart, E., Demaiffe, D. & Duchesne, J. C. (1989) Chemical Constraints on the Genesis of the Tellnes Ilmenite Deposit, Southwest Norway *Economic Geology*, Vol. 84, pp. 1047-1056.
- Zeino-Mahmalat, R. & Krause, H. (1976) Plagioklase im Anorthosit-Komplex von Åna-Sira, SW-Norwegen. Petrologische und chemische Untersuchungen., *Norsk geologisk tidsskrift*, Vol. 56, pp. 51-94.

APPENDIX A – DRILL CORE SECTIONS

Table A 1

A complete overview of available drill core sections, including drill hole collar coordinates and XRF-data provided by Titania. Values are given in wt%.

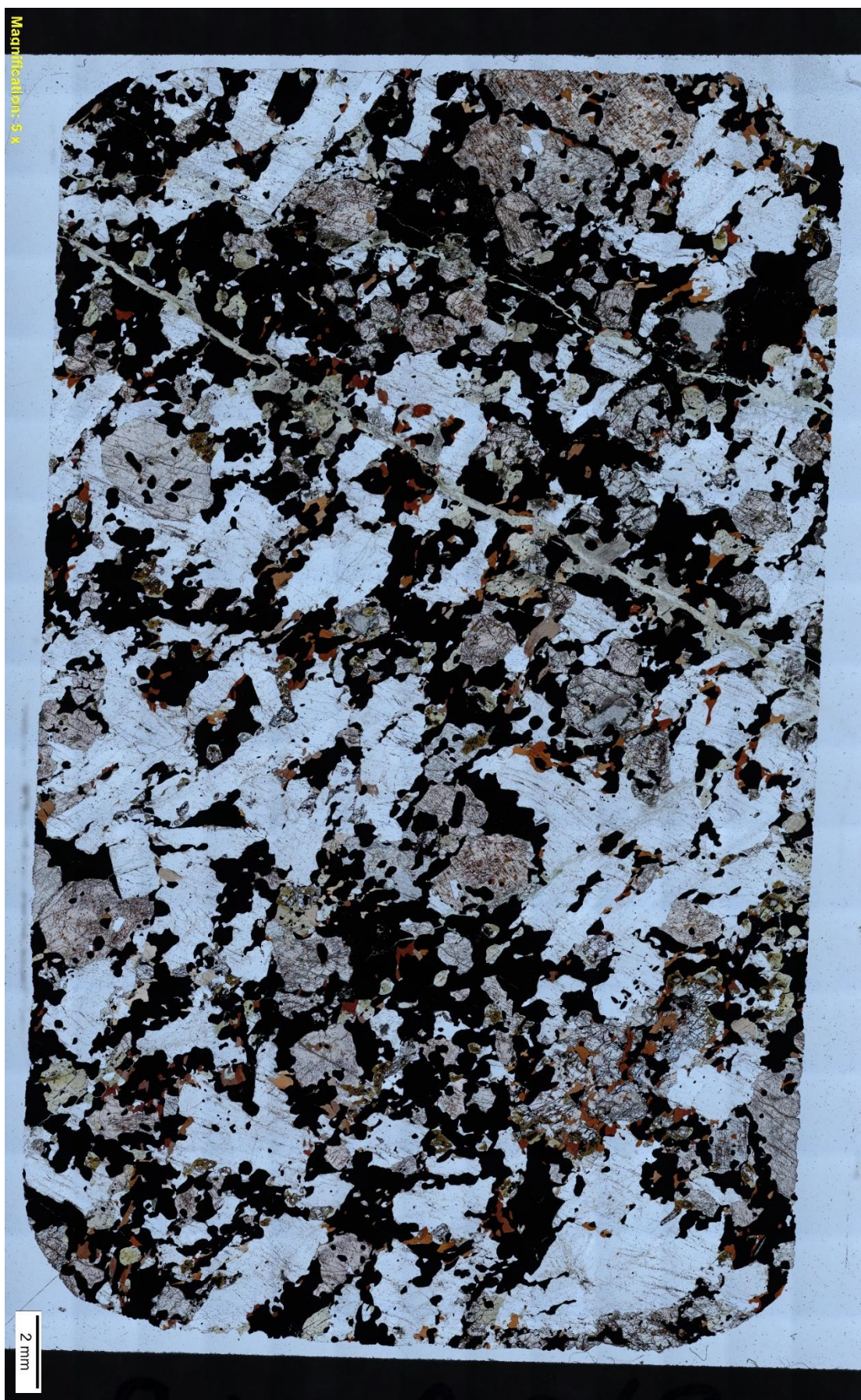
Table A 2

A complete overview of available drill core sections, including drill hole collar coordinates and XRD-data provided by Titania. Values are given in wt% and normalized to 100%.

APPENDIX B – THIN SECTION SCANS

Scan B 1	Thin section scan of drill core 3.5V-1S, PPL
Scan B 2	Thin section scan of drill core 3.5V-1S, XPL
Scan B 3	Thin section scan of drill core 3.5V-1S, transmitted lightning
Scan B 4	Thin section scan of drill core 3.0V-4N, PPL
Scan B 5	Thin section scan of drill core 3.0V-4N, XPL
Scan B 6	Thin section scan of drill core 3.0V-4N, transmitted lightning

Scan B 1



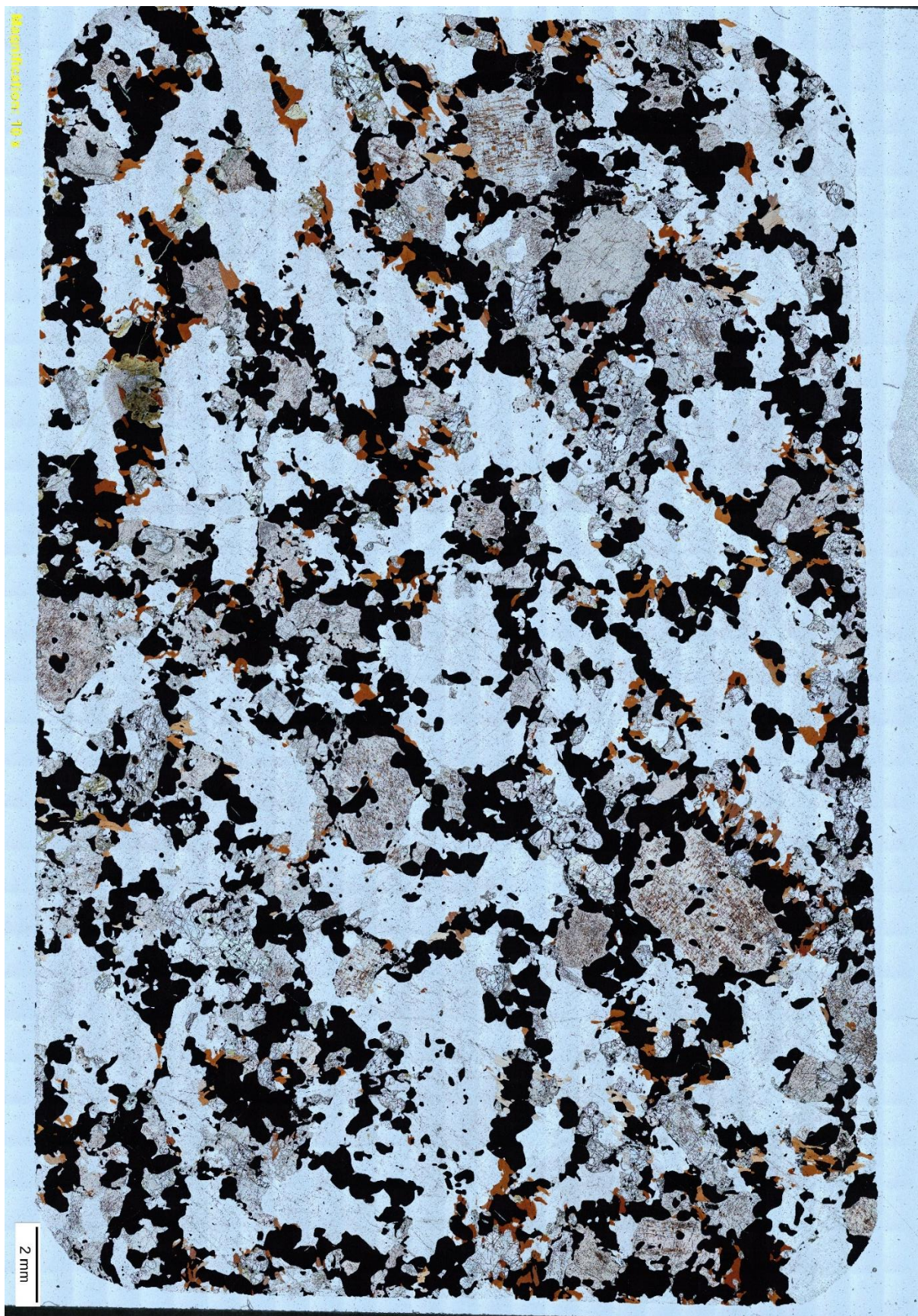
Scan B 2



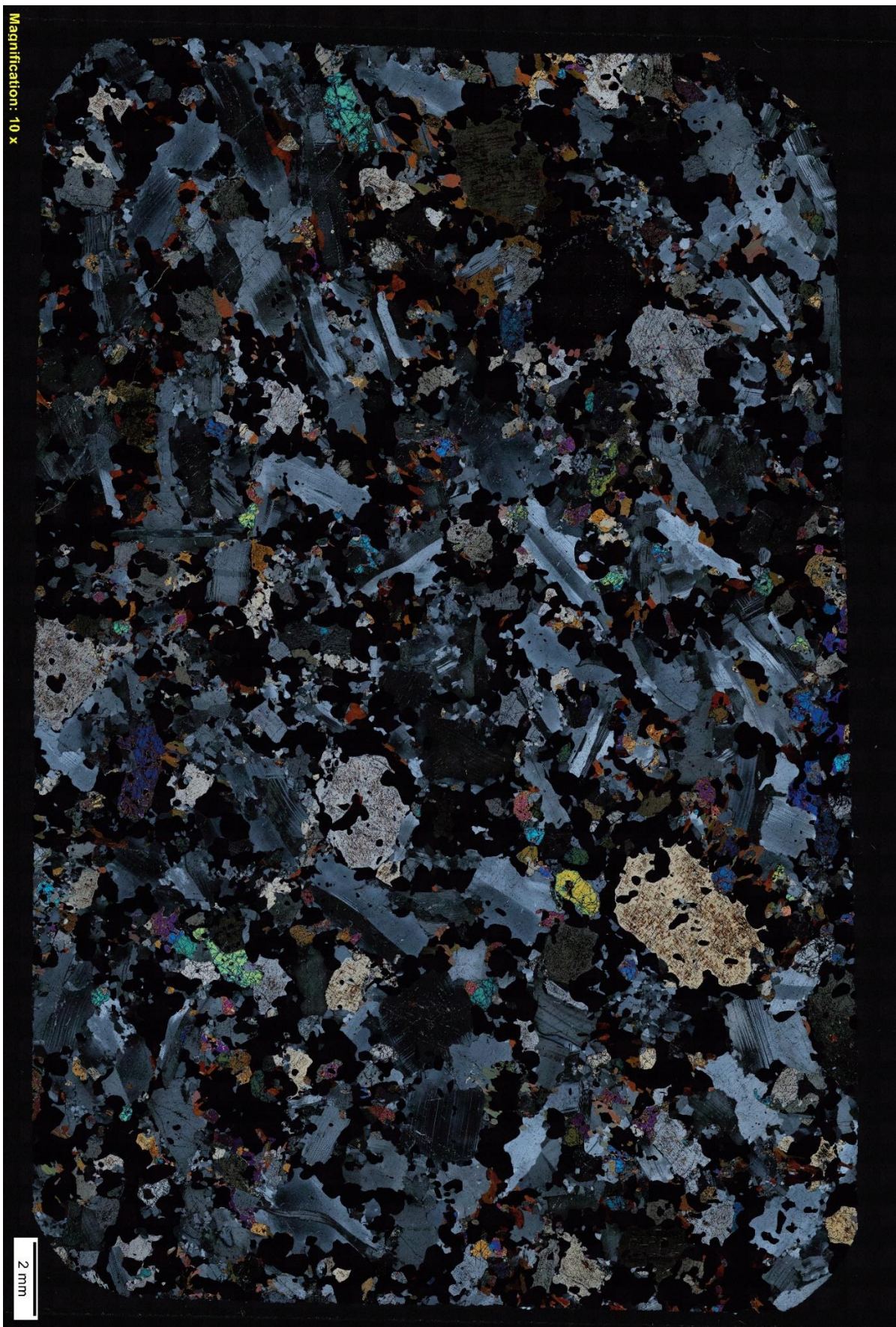
Scan B 3



Scan B 4



Scan B 5



Scan B 6



APPENDIX C – EPMA-ANALYSES

Table C 1	ORTHOPYROXENE	Chemical composition (wt% oxides) of analysed orthopyroxene retrieved from EPMA-data .
Table C 2	CLINOPYROXENE	Chemical composition (wt% oxides) of analysed clinopyroxene retrieved from EPMA-data
Table C 3	OLIVINE	Chemical composition (wt% oxides) of analysed olivine retrieved from EPMA-data
Table C 4	BIOTITE	Chemical composition (wt% oxides) of analysed biotite retrieved from EPMA-data
Table C 5	PLAGIOCLASE	Chemical composition (wt% oxides) of analysed plagioclase retrieved from EPMA-data
Table C 6	ILMENITE	Chemical composition (wt% oxides) of analysed ilmenite retrieved from EPMA-data
Table C 7	LAMELLAS	Chemical composition (wt% oxides) of analysed lamellas in orthopyroxene retrieved from EPMA-data
Table C 8	SULPHIDES	Chemical composition (wt% oxides) of analysed sulphides retrieved from EPMA-data

Table C 1

ORTHOPYROXENE																		
Point	Sample – point name	Na ₂ O	MgO	Al ₂ O ₃	SiO ₂	CaO	K ₂ O	Cr ₂ O ₃	V ₂ O ₃	FeO	TiO ₂	MnO	NiO	ZrO ₂	ZnO	Ce ₂ O ₃	CoO	Total
7	30V-4N-1-pxp1	0.0121	27.01	1.8246	53.53	0.6718	0.0058	0.0055	0.0172	15.59	0.1945	0.2776	0	0	0.0476	0	0.0378	99.2245
8	30V-4N-1-pxp2	0.0083	27.2	1.8603	53.46	0.6549	0.0068	0.0048	0.0425	15.15	0.1919	0.3038	0.0124	0	0.016	0.0427	0.0429	98.9973
9	30V-4N-1-pxp3	0.0228	27.19	1.7432	53.79	0.4749	0	0.0079	0.0019	15.53	0.164	0.2894	0.04	0.0233	0.0197	0.0099	0.053	99.36
10	30V-4N-1-pxp4	0.0123	27.2	1.888	53.93	0.5958	0	0	0.0345	15.14	0.1706	0.2858	0.0465	0.0028	0.0388	0	0.0325	99.3776
11	30V-4N-1-pxp5	0.0332	26.79	1.8756	53.73	0.6183	0.011	0.0008	0	15.53	0.1725	0.2751	0.023	0.0192	0.0769	0.0078	0.0294	99.1928
12	30V-4N-1-pxp6	0.0368	26.99	1.91	53.87	0.5692	0.0005	0.0071	0	15.5	0.1548	0.2402	0.0158	0	0.0221	0	0.0223	99.3388
13	30V-4N-1-pxp7	0.0135	26.82	1.8471	53.99	0.6012	0.0168	0.0353	0.0122	15.75	0.2099	0.2877	0.0115	0	0.0702	0.0122	0.0059	99.6835
19	30V-4N-2-pxp1	0.0093	27.15	1.879	53.84	0.6756	0.0068	0.0403	0.0071	15.03	0.2025	0.2755	0.0137	0	0.0257	0.0308	0.0325	99.2188
20	30V-4N-2-pxp2	0.0489	27.09	1.8636	53.84	0.6844	0	0.0213	0.0345	15.19	0.193	0.2828	0.0209	0	0.0322	0	0.0274	99.329
21	30V-4N-2-pxp3	0.0256	26.79	1.91	53.75	0.6278	0	0.0379	0.0071	15.08	0.1543	0.276	0.0055	0	0.0131	0.0316	0.0256	98.7345
22	30V-4N-2-pxp4	0.0061	26.83	1.855	53.94	0.657	0	0	0.0182	15.1	0.1523	0.2778	0.0111	0	0.0035	0	0.0682	98.9192
23	30V-4N-2-pxp5	0.025	26.92	1.92	53.8	0.673	0.01	0.0063	0.0405	15.25	0.1379	0.2578	0.0333	0	0.0316	0.0083	0.0135	99.1272
24	30V-4N-2-pxp6	0.0229	26.94	1.9	53.84	0.6086	0	0.0016	0.0122	15.41	0.1552	0.2875	0.0149	0.0055	0.0662	0.0641	0.0332	99.3619
25	30V-4N-2-pxp7	0.4919	26.92	1.8713	53.7	0.6777	0.047	0.0087	0.0264	15.13	0.1778	0.2822	0.0068	0.0014	0.0513	0.0341	0.0446	99.4712
26	30V-4N-2-pxp8	0.0332	26.97	1.8845	53.84	0.6316	0.0058	0.0158	0.0274	15.13	0.1401	0.2911	0.0132	0	0.0226	0.0031	0.0287	99.0371
27	30V-4N-2-pxp9	0.1357	25.32	2.2	53.73	3.93	0.0029	0.0112	0.0132	13.67	0.2492	0.2289	0	0.0164	0.0281	0	0.046	99.5816
28	30V-4N-2-pxp10	0.0271	26.77	1.8483	53.88	0.718	0.0003	0.03	0	15.33	0.1766	0.2516	0.0068	0	0.0066	0	0.0581	99.1034
29	30V-4N-2-pxp11	0.0513	27.08	1.8447	53.96	0.6439	0	0	0.0112	14.92	0.1879	0.2966	0.009	0	0.0382	0	0.0378	99.0806
30	30V-4N-2-pxp12	0.0074	27.71	1.97	54.3	0.6387	0.0108	0.0198	0.0082	14.21	0.1573	0.2321	0.0423	0	0.0676	0.0251	0.0295	99.4288
31	30V-4N-2-pxp13	0.011	27.57	1.95	54.2	0.6575	0.0058	0.0261	0.0204	14.59	0.1794	0.2681	0.0162	0	0.0334	0	0.0223	99.5502
32	30V-4N-2-pxp14	0.012	27.1	1.92	54.14	0.6753	0.0084	0.0024	0.0081	15.03	0.1573	0.2964	0.0261	0.0151	0.0436	0	0.0203	99.455
33	30V-4N-2-pxp15	0.0223	26.8	1.91	54	0.6091	0	0.0039	0.0051	15.46	0.1878	0.2723	0.0265	0.0014	0.0716	0	0.0063	99.3763
34	30V-4N-2-pxp16	0	27.32	1.93	54.24	0.6551	0	0.0103	0.0051	14.93	0.21	0.2947	0.0402	0	0.0592	0	0.064	99.7586
35	30V-4N-2-pxp17	0.7278	15.69	2.89	52.71	20.46	0	0.0371	0.0136	6.42	0.57	0.1293	0.0158	0	0.0287	0	0.0276	99.7199
36	30V-4N-2-pxp18	0.0307	26.81	1.8361	53.96	0.6841	0.0024	0.0118	0.006	15.29	0.1873	0.3286	0.0115	0	0.0346	0	0.0851	99.2782
37	30V-4N-2-pxp19	0.023	26.78	1.94	54.03	0.6086	0.0029	0.0237	0.0172	15.01	0.1501	0.2636	0.0329	0	0.0657	0.0134	0.016	98.9771
38	30V-4N-2-pxp20	0.0916	26.83	1.8515	54.03	0.6061	0.0066	0.0063	0.0204	15	0.1799	0.2785	0.0244	0	0.0544	0.0208	0.0342	99.0347
39	30V-4N-2-pxp21	0.041	27.53	1.8873	54.27	0.6818	0.01	0	0	14.32	0.1944	0.2394	0	0	0.0717	0.0278	0.0548	99.3282
53	30V-4N-3-pxp1	0.0516	26.02	2.14	53.54	3.11	0.0076	0.0294	0.0101	14.2	0.2264	0.2377	0.0325	0.0041	0.0382	0	0.0679	99.7155
54	30V-4N-3-pxp2	0.0171	27.14	1.91	53.97	0.6506	0	0.0198	0.0294	14.93	0.1736	0.2778	0.0179	0	0.0723	0	0.0185	99.227
55	30V-4N-3-pxp3	0.0172	26.97	1.873	54.02	0.5943	0.0016	0.015	0.0335	14.95	0.1606	0.2509	0.0103	0.022	0	0	0.0257	98.9441
56	30V-4N-3-pxp4	0.0454	27.18	1.99	53.86	0.611	0.0113	0.0087	0.0071	15.03	0.1225	0.2727	0.0051	0	0.0083	0.0202	0.0253	99.1976
57	30V-4N-3-pxp5	0.0433	26.7	1.8658	53.85	0.6581	0.0008	0.0166	0	14.71	0.1605	0.2636	0	0	0.0484	0.0002	0.0502	98.3675
66	30V-4N-4-incl3	0	2.87	0.0719	0.0164	0	0.0045	0.0422	0.3002	43.34	48.78	0.3442	0.0072	0	0.0291	0	0.0984	95.9041
67	30V-4N-4-pxp1	0.0118	27.58	1.95	54.2	0.6126	0.0008	0.0214	0.0112	14.29	0.2023	0.2822	0.03	0	0.0055	0	0.0556	99.2534
68	30V-4N-4-pxp2	0.0319	26.5	1.95	53.79	1.1698	0.0047	0.0221	0.0316	14.88	0.1923	0.2573	0.0235	0	0.0131	0	0.0391	98.9054
69	30V-4N-4-pxp3	0.0205	26.95	1.96	54.05	0.7525	0.0037	0	0	15.09	0.2125	0.2937	0.0333	0	0.0837	0	0.0223	99.4722

70	30V-4N-4-opx4	0.0106	27.09	1.93	53.96	0.7479	0	0	0.0122	14.93	0.1789	0.2756	0.0226	0.0164	0.0645	0.0012	0.045	99.2849
71	30V-4N-4-opx5	0.0135	27.16	1.95	54.06	0.6041	0.0026	0.0103	0.0243	14.92	0.1756	0.2783	0.0337	0	0.0794	0.0161	0.0462	99.3741
72	30V-4N-4-opx6	0	27.27	1.8653	54.06	0.7029	0	0.0331	0.009	14.88	0.2134	0.2722	0.0141	0.0013	0.0143	0.0155	0.0299	99.381
73	30V-4N-4-opx7	0.0098	27.06	1.8757	54.14	0.6116	0	0.0039	0.009	15.06	0.1818	0.277	0.0145	0.0247	0.018	0	0.0361	99.3221
74	30V-4N-4-opx8	0.0311	26.81	1.9	53.85	0.6416	0	0.0024	0.0416	15.42	0.1803	0.2781	0.0337	0	0.0035	0.0013	0.0253	99.2189
75	30V-4N-4-opx9	0.011	27.11	1.8588	54	0.7679	0	0.0024	0.0071	14.87	0.1843	0.3176	0.0107	0.0123	0.0423	0	0.048	99.2424
76	30V-4N-4-opx10	0.0138	26.92	1.96	53.97	0.7431	0	0.0071	0.0142	15.22	0.185	0.2843	0.0017	0.0219	0.0329	0	0.0462	99.4202
77	30V-4N-4-opx11	0.0097	26.73	1.93	53.84	0.7563	0	0.011	0.0315	15.17	0.2365	0.2953	0.0217	0.0028	0.0423	0.0533	0.0627	99.1931
78	30V-4N-4-opx12	0.0242	26.95	1.8588	53.86	0.7573	0	0	0.0244	15.28	0.2157	0.2883	0.0308	0	0.0269	0.0097	0.0366	99.3627
79	30V-4N-4-opx13	0.0189	27.18	1.8509	54.02	0.6175	0.0095	0.0071	0.0234	15.12	0.1856	0.2947	0.0004	0	0.0215	0	0.0502	99.3997
80	30V-4N-4-opx14	0.025	26.69	1.91	53.9	0.8889	0.0039	0	0.0274	15.46	0.1849	0.2738	0.0141	0.0096	0	0	0.05	99.4376
81	30V-4N-4-opx15	0.017	26.97	1.92	53.95	0.7117	0	0.0063	0.0275	15.08	0.1647	0.2697	0.0274	0	0	0.0353	0.0556	99.2352
82	30V-4N-4-opx16	0.0501	26.59	2.06	53.91	1.2871	0.0013	0.0127	0.0101	14.89	0.2137	0.2763	0.059	0	0	0.0031	0.0342	99.3976
83	30V-4N-4-opx17	0.0188	26.81	2.01	53.83	0.8226	0	0.0111	0.0244	15.17	0.2193	0.2778	0.0299	0	0.0859	0.0778	0.037	99.4246
136	30V-4N-7-opx1	0.0255	27.05	1.89	54.2	0.6732	0	0	0.0223	15.14	0.1631	0.2737	0.0423	0	0.0359	0.072	0.0345	99.6225
137	30V-4N-7-opx2	0.0219	27.26	2.07	54.37	0.8119	0	0.0056	0.0337	14.6	0.1306	0.2912	0	0.0151	0.0239	0	0.0588	99.6927
138	30V-4N-7-opx3	0.0271	26.81	1.92	54.38	1.0799	0	0.0095	0.0193	14.96	0.1873	0.2604	0.0026	0	0.0401	0	0.0109	99.7071
139	30V-4N-7-opx4	0	27.18	1.95	54.23	0.7116	0	0.0071	0.0182	15.36	0.1764	0.2918	0.0086	0	0.0035	0	0.0616	99.9988
140	30V-4N-7-opx5	0.0228	27.1	1.97	54.17	0.6257	0	0.0079	0.0133	15.3	0.1616	0.2795	0.0188	0	0.0245	0	0.0329	99.727
141	30V-4N-7-opx6	0.0136	27.2	1.94	54.37	0.7298	0	0	0.0397	15.18	0.1525	0.3032	0.006	0	0.0197	0	0.0332	99.9877
142	30V-4N-7-opx7	0.0395	27.3	1.8165	54.38	0.8052	0	0	0.0264	14.93	0.2088	0.3105	0.0308	0.0014	0.0287	0	0.0434	99.9212
143	30V-4N-7-opx8	0.0245	27.58	1.96	54.36	0.6916	0.001	0.0048	0.0286	14.67	0.1837	0.3021	0.0128	0.0068	0.0724	0.0149	0.0409	99.9541
144	30V-4N-7-opx9	0.0053	27.18	1.9	54.21	0.5792	0	0.0332	0.0315	15.15	0.2112	0.2857	0.0141	0.0055	0.0162	0.1186	0.0366	99.7771
145	30V-4N-7-opx10	0.0327	27.05	1.733	54.16	0.7226	0.0064	0.0103	0.0011	15.28	0.1901	0.2758	0.0192	0	0	0.0524	0.0324	99.566
146	30V-4N-7-opx11	0.0235	27.68	1.96	54.2	0.6326	0	0.0237	0.003	14.71	0.163	0.2793	0.018	0	0.0263	0	0.0185	99.7379
147	30V-4N-7-opx12	0.0194	27.54	1.89	54.28	0.6206	0	0.0253	0	14.95	0.1815	0.2798	0.0218	0	0.0557	0	0.0291	99.8932
148	30V-4N-7-opx13	0.0507	26.77	1.8026	54.26	1.2104	0	0	0.0193	14.93	0.1713	0.29	0.0026	0.0123	0.0228	0.0049	0.0342	99.5811
149	30V-4N-7-opx14	0.0506	27.22	1.92	54.17	0.6993	0.0168	0.0142	0	15.09	0.1512	0.2666	0.0175	0.0041	0.0491	0.0472	0.0147	99.7313
150	30V-4N-7-opx15	0.1277	27.05	1.91	54.05	0.6467	0.0403	0.0079	0.0133	15.31	0.1495	0.2678	0.0325	0	0.009	0	0.0451	99.6598
151	30V-4N-7-opx16	0.0222	27.1	1.89	54.21	0.6411	0	0.0213	0	15.07	0.1815	0.2808	0.0026	0.0097	0.0186	0.0128	0.041	99.5016
152	30V-4N-7-opx17	0.1818	24.82	2.19	54.27	5.08	0	0	0.0112	13.89	0.2209	0.2538	0.0261	0	0	0.062	0.0195	101.0253
153	30V-4N-7-opx18	0.1962	24.4	2.28	53.77	5.61	0.0052	0.0248	0.0258	13.22	0.2898	0.2273	0.0197	0.0055	0.0414	0	0.0317	100.1474
154	30V-4N-7-opx19	0.0357	26.76	1.93	53.93	0.6973	0	0.015	0.0111	15.56	0.1782	0.3149	0.0132	0.0178	0.055	0	0.0451	99.5633
155	30V-4N-7-opx18	0.1245	25.38	2.09	53.96	3.95	0	0.0263	0.0061	14.09	0.2235	0.2588	0.0081	0.0137	0	0	0.0299	100.1609
176	30V-4N-9-opx1	0.024	26.77	1.8784	54.2	0.6701	0	0.0087	0	15.26	0.1686	0.2726	0.0213	0.0083	0.0412	0	0.0097	99.3329
177	30V-4N-9-opx2	0.028	27.1	1.8342	54	0.6332	0.0058	0	0	15.49	0.1841	0.2791	0.0081	0.0137	0.0226	0	0.0206	99.6194
178	30V-4N-9-opx3	1.0503	15.49	3.09	52.7	21.58	0.0033	0.0255	0.0452	6.11	0.5577	0.1174	0.009	0.0106	0.0489	0.0556	0.0373	100.9308
179	30V-4N-9-opx4	0.0143	26.72	1.8802	54.16	1.0174	0	0	0.0142	15.35	0.1569	0.29	0.009	0	0.0197	0	0.0282	99.6599
180	30V-4N-9-opx5	0.0188	27.32	1.91	54.15	0.6346	0	0.0103	0.003	14.79	0.1765	0.2472	0.0295	0.0206	0.0406	0.0093	0.0249	99.3853
181	30V-4N-9-opx6	0.0145	27.17	1.97	54.14	0.6943	0.0032	0.0048	0.0253	15.04	0.1684	0.2769	0.0021	0	0	0.0793	0.0294	99.6182
182	30V-4N-9-opx7	0.0193	27.65	1.95	54.39	0.6447	0	0	0	14.17	0.1595	0.2328	0.0351	0.0221	0	0.0243	0.027	99.3248
183	30V-4N-9-opx8	0.0866	26.63	1.94	53.83	0.6339	0.0022	0.0024	0.0021	15.62	0.1908	0.2776	0.0137	0.0192	0.0567	0	0.0441	99.3493
184	30V-4N-9-opx9	0.026	26.82	1.91	53.87	0.6859	0	0.0039	0.0305	15.12	0.1776	0.3053	0.0337	0.0178	0.0984	0	0.0383	99.1374

185	30V-4N-9-opx10	0.0132	26.82	1.8675	54.03	0.6755	0.0018	0.0276	0	15.45	0.1773	0.2995	0.0337	0	0.003	0	0.0383	99.4374
204	35V-1S-1-opx1	0.0603	27.06	2.06	53.9	0.584	0	0	0.0214	15.36	0.1844	0.279	0.036	0.0288	0.0079	0	0.0405	99.6223
205	35V-1S-1-opx2	0.0075	27.18	2.01	53.97	0.7274	0	0.0419	0.0092	15.43	0.1878	0.2933	0.0141	0.0206	0.0628	0.0654	0.0139	100.0339
206	35V-1S-1-opx3	0.0193	27.16	1.98	54.19	0.6037	0	0.0222	0	15.07	0.1801	0.2486	0.0107	0.0261	0.0048	0	0.0469	99.5624
207	35V-1S-1-opx4	0.0262	27.07	2.03	54.17	0.5767	0	0.0214	0.0306	15.16	0.188	0.2841	0.036	0	0	0.0307	0.0317	99.6554
208	35V-1S-1-opx5	0.0116	27.08	1.98	54.16	0.6203	0	0.0317	0.0418	15.17	0.1659	0.2545	0.0172	0.0055	0.0282	0	0.0478	99.6145
209	35V-1S-1-opx6	0.0336	26.85	2.04	54.36	1.44	0	0.0167	0.0275	14.48	0.1889	0.2996	0.0236	0.0262	0.0337	0	0.0119	99.8317
210	35V-1S-1-opx7	0.031	27.18	1.93	54.33	0.8254	0.0047	0	0.003	14.77	0.1743	0.258	0.0167	0	0.0414	0.0365	0.0304	99.6314
211	35V-1S-1-opx8	0.027	27.07	1.95	54.21	0.6854	0.0013	0.0158	0.0214	15.32	0.169	0.2744	0.0137	0	0.0545	0	0.0427	99.8552
212	35V-1S-1-opx9	0.0356	26.9	1.8351	54.15	1.2156	0	0.0087	0.0153	14.92	0.1651	0.2528	0.0532	0.0537	0.0006	0	0.0504	99.6561
213	35V-1S-1-opx10	0	27.27	1.8324	54.31	0.557	0.0051	0	0.0122	15.2	0.1687	0.3034	0.0163	0	0.1031	0.0879	0.022	99.8881
214	35V-1S-1-opx11	0.0132	27.1	1.98	54.18	0.5703	0.002	0	0.0133	15.33	0.1494	0.2476	0.0296	0	0	0.0272	0.0321	99.6747
254	35V-1S-4-opx1	0.0143	27.15	1.9	54.18	0.5768	0	0	0.0193	14.99	0.1407	0.2715	0.0162	0	0.0526	0	0.0325	99.3439
255	35V-1S-4-opx2	0.0579	26.89	1.97	54.08	1.74	0.0066	0.0246	0.0183	14.43	0.1899	0.2788	0.0316	0.0068	0.0526	0	0.0063	99.7834
256	35V-1S-4-opx3	0.0236	27.42	1.9	54.13	0.6435	0.0047	0	0.0101	14.84	0.199	0.2798	0.0222	0.0247	0.0066	0.0262	0.0451	99.5755
257	35V-1S-4-opx4	0.127	27.5	1.8711	54.14	0.6809	0	0.0324	0.0172	15.18	0.1873	0.2774	0	0	0.0143	0	0.0556	100.0832
258	35V-1S-4-opx5	0.0157	27.77	1.98	54.21	0.6567	0	0.0134	0.0142	14.89	0.1709	0.2423	0.0316	0.0206	0.0059	0.0279	0.0927	100.1419
259	35V-1S-4-opx6	0.0806	27.09	1.99	54.04	1.2808	0.0067	0.0142	0.0204	14.82	0.1907	0.286	0.0222	0	0.0215	0.0342	0.0367	99.934
260	35V-1S-4-opx7	0.0232	27.32	2	54.24	0.7154	0	0.0048	0.0041	15.03	0.1845	0.3214	0.0146	0	0.0228	0.007	0.0253	99.9131
261	35V-1S-4-opx8	0.0414	26.85	2.08	54.11	1.46	0.0006	0.0071	0.0193	14.85	0.21	0.2636	0.0111	0.0357	0.0101	0.029	0.0119	99.9898
262	35V-1S-4-opx9	0.0162	27.55	2	54.34	0.5724	0	0.0143	0.0214	14.93	0.1643	0.2881	0.0381	0	0.0322	0.0541	0.0063	100.0274
263	35V-1S-4-opx10	0.1105	26.5	2.11	53.98	1.64	0.0182	0.0159	0	14.85	0.1927	0.2757	0.0163	0.0041	0.0699	0	0.0329	99.8162
264	35V-1S-4-opx11	0.7695	15.27	3.38	52.09	21.76	0.0099	0.0355	0.0369	6.23	0.6541	0.1452	0.0445	0.0066	0.0234	0.0179	0.028	100.5015
265	35V-1S-4-opx12	0.0721	26.78	2.04	54.34	1.76	0.0045	0	0.0316	14.67	0.2334	0.2935	0	0	0.0233	0.0395	0.0405	100.3284
266	35V-1S-4-opx13	0.1983	24.58	2.14	54.22	5.7	0.0064	0.0128	0.0319	12.71	0.2148	0.2301	0.0099	0.0027	0.0371	0	0.0228	100.1168
272	35V-1S-6-opx1	0.0064	27.87	1.98	54.46	0.6065	0.0049	0.0278	0	14.18	0.1457	0.2804	0.018	0.0248	0.1018	0	0.03	99.7363
273	35V-1S-6-opx2	0.0313	27.71	1.99	54.39	0.6428	0.0102	0.0214	0	14.56	0.182	0.2515	0.027	0	0.0101	0.0315	0.0363	99.8941
274	35V-1S-6-opx3	0.0192	27.27	1.97	54.35	0.6288	0.0129	0.0055	0.0264	14.68	0.1345	0.2621	0.0141	0	0	0.0682	0.068	99.5097
275	35V-1S-6-opx4	0.0142	27.77	1.91	54.57	0.5149	0.0082	0.0253	0	14.7	0.1526	0.262	0.0124	0.0124	0.0125	0.0097	0.062	100.0362
276	35V-1S-6-opx5	0.0107	27.54	1.98	54.37	0.6768	0.0075	0.0198	0.0213	14.4	0.1494	0.2725	0.0098	0	0.003	0	0	99.4608
277	35V-1S-6-opx6	0.026	27.46	1.8719	54.47	0.6598	0.0058	0.0245	0.0092	14.67	0.1743	0.2939	0.0269	0	0.0513	0	0.0021	99.7457
278	35V-1S-6b-opx1	0.0336	27.35	1.97	54.23	0.6486	0.0153	0.0276	0	15.15	0.1922	0.3047	0.0419	0	0.0173	0	0.0274	100.0086
279	35V-1S-6b-opx2	0.0124	26.97	1.98	54.17	0.6432	0	0.0142	0	15.59	0.1911	0.2704	0.0205	0.0466	0.0309	0.0894	0.0647	100.0934
280	35V-1S-6b-opx3	0.0142	26.58	2.07	54.04	0.7275	0	0	0	15.23	0.1892	0.2606	0.0269	0.0151	0.0471	0.0103	0.0089	99.2198
281	35V-1S-6b-opx4	0.0874	25.96	2.13	54	2.73	0	0.0048	0.0194	14.62	0.2179	0.254	0.0265	0.0273	0.0381	0	0.0564	100.1718
282	35V-1S-6b-opx5	0.0424	26.91	2.02	54.04	1.2802	0.0006	0.0142	0.0234	14.75	0.1844	0.2753	0.0277	0.0206	0.0467	0	0.0358	99.6713
283	35V-1S-6b-opx6	0.0234	27.08	2.02	54.19	0.6516	0.0065	0.0316	0.0131	15.2	0.1636	0.2936	0.0167	0	0.0532	0	0.0404	99.7837
284	35V-1S-6b-opx7	0.5928	18.92	2.99	52.91	15.03	0.0126	0.022	0.0375	8.39	0.5151	0.1452	0.0222	0	0.0006	0	0.0143	99.6023
285	35V-1S-6c-opx1	0.0261	27.07	1.98	54.09	0.7028	0.0101	0.0284	0.0204	15.41	0.1723	0.2819	0.021	0	0	0	0.0434	99.8564
286	35V-1S-6c-opx2	0.0773	26.65	2.14	54.07	1.66	0.0081	0.0198	0.0142	14.82	0.2267	0.2475	0.0107	0.0233	0.034	0.0478	0.0302	100.0796
287	35V-1S-6c-opx3	0.0142	27.31	1.93	54.4	0.6251	0.0059	0.0039	0.0112	15.18	0.1841	0.2951	0.0064	0.0014	0.0114	0	0.0337	100.0124
288	35V-1S-6c-opx4	0.0198	27.31	2.01	54.22	0.7254	0.0043	0.0308	0	14.88	0.1914	0.2945	0.0068	0	0.025	0.0242	0.0008	99.743
289	35V-1S-6c-opx5	0.0562	26.91	2.01	53.93	1.46	0	0	0.0213	14.79	0.1518	0.2728	0.0119	0.011	0.0542	0.0152	0.0412	99.7356

290	35V-1S-6d-opx1	0.0288	27.46	1.8478	54.34	0.5513	0	0.019	0	15.07	0.1667	0.2669	0.0304	0.0096	0	0.0037	0.0464	99.8406
291	35V-1S-6d-opx2	0.0271	27.42	1.6946	54.56	0.5628	0.0007	0.0173	0	15.01	0.1471	0.2768	0.0436	0	0	0	0.0523	99.8123
292	35V-1S-6d-opx3	0.0265	27.32	2	54.12	0.6555	0	0	0.0131	15.16	0.1774	0.2649	0.0188	0.0137	0.0298	0.0626	0.0358	99.8981
293	35V-1S-6d-opx4	0.0579	26.8	2.05	54.1	1.69	0	0	0	14.68	0.2017	0.2426	0.0316	0	0.0096	0.0375	0.016	99.9169
294	35V-1S-6d-opx5	0.0395	27.13	2.01	53.91	0.6768	0.0115	0.0458	0.0172	15.25	0.2046	0.3146	0.0115	0.0219	0.0388	0.0204	0.0375	99.7401
295	35V-1S-6d-opx6	0.0157	27.46	1.99	54.11	0.7197	0.0011	0.0253	0.0021	14.83	0.1815	0.2792	0.0193	0.0179	0.0107	0	0.0637	99.7262
296	35V-1S-6d-opx7	0.0298	27.87	1.89	54	0.666	0	0.0253	0.0172	14.83	0.1496	0.2557	0.0197	0.0289	0.0055	0.0423	0.0472	99.8772

Table C 2

CLINOPYROXENE

Point	Sample – point name	Na ₂ O	MgO	Al ₂ O ₃	SiO ₂	CaO	K ₂ O	Cr ₂ O ₃	V ₂ O ₃	FeO	TiO ₂	MnO	NiO	ZrO ₂	ZnO	Ce ₂ O ₃	CoO	Total
14	30V-4N-1-cpx1	0.7753	14.5	3.53	51.52	21.46	0.0038	0.0057	0.0597	6.73	0.8146	0.1525	0.0047	0.0224	0.0011	0.0613	0.0178	99.6589
15	30V-4N-1-cpx2	0.7846	14.5	3.46	51.61	21.93	0.0053	0.0189	0.0273	6.38	0.7589	0.1493	0	0.0395	0.0035	0.0119	0.0347	99.7139
16	30V-4N-1-cpx3	0.7495	14.91	3.46	51.32	20.85	0.0104	0.0041	0.0858	7.15	0.7474	0.1604	0.0154	0	0.0589	0	0.0414	99.5633
17	30V-4N-1-cpx4	0.7623	14.52	3.48	51.22	21.69	0.0081	0.0337	0.0504	6.57	0.7492	0.1341	0.0141	0.0092	0.0394	0	0.0174	99.2979
18	30V-4N-1-cpx5	0.7818	14.51	3.45	51.56	21.66	0	0	0.0482	6.44	0.7545	0.1431	0.0222	0	0	0.0239	0.0271	99.4208
186	30V-4N-9-cpx1	0.7919	14.51	3.65	51.64	21.54	0.0008	0.037	0.0473	6.83	0.8277	0.1319	0.0158	0.0079	0.0291	0	0	100.0594
187	30V-4N-9-cpx2	0.7491	14.46	3.63	51.76	21.89	0.002	0.0337	0.0378	6.45	0.79	0.167	0.0081	0	0.0162	0	0.0132	100.0071
188	30V-4N-9-cpx3	0.7828	14.55	3.46	52.16	22.03	0.0046	0.0321	0.0632	6.21	0.6919	0.1423	0.0128	0	0.0173	0.0231	0.0319	100.212
189	30V-4N-9-cpx4	0.7494	14.75	3.49	51.76	21.85	0.0017	0.0231	0.0443	6.1	0.7361	0.1181	0.0278	0.0172	0.0346	0	0.0296	99.7319
190	30V-4N-9-cpx5	0.7573	14.82	3.43	51.89	21.95	0.0058	0.0255	0.0231	6.3	0.6575	0.1513	0	0.0092	0.0311	0.045	0	100.0958
191	30V-4N-9-cpx6	0.7765	14.6	3.44	51.79	21.87	0	0.0173	0.0295	6.44	0.6897	0.1637	0.0132	0.0475	0.009	0	0.0064	99.8928
192	30V-4N-9-cpx7	0.697	15.81	3.35	51.75	20.29	0.0046	0.0123	0.0304	6.73	0.6646	0.1461	0	0	0.0018	0.0078	0.0127	99.5073
193	30V-4N-9-cpx8	0.6882	15.5	3.37	51.36	20.11	0.0008	0.0181	0.0303	7.79	0.8288	0.1235	0	0.0251	0.0418	0	0.0081	99.8947
194	30V-4N-9-cpx9	0.8087	14.75	3.53	52.05	21.63	0.0041	0.0338	0.0422	6.37	0.6995	0.1267	0.0026	0.0265	0	0.0092	0	100.0833
195	30V-4N-9-cpx10	0.7371	14.66	3.44	51.81	21.82	0	0	0.0462	6.52	0.7556	0.1299	0.003	0.0066	0.0227	0	0.0509	100.002
196	30V-4N-9-cpx11	0.782	14.63	3.47	52.15	21.92	0	0.0025	0.0474	6.32	0.6831	0.1339	0.0132	0.0132	0.0143	0	0.0115	100.1911
197	30V-4N-9-cpx12	0.7341	15.02	3.46	51.91	21.13	0.0009	0.0156	0.0262	6.85	0.7372	0.1383	0.0051	0.0185	0.0346	0	0.014	100.0945
215	35V-1S-1-cpx1	0.7675	14.67	3.52	51.93	21.91	0.0018	0.0421	0.0369	6.68	0.7381	0.1419	0.0073	0.0106	0.0066	0	0.0255	100.4883
216	35V-1S-1-cpx2	0.7583	14.71	3.5	52.09	22.11	0	0.0273	0.0634	6.05	0.7326	0.1161	0.0283	0.0172	0.0059	0	0.054	100.2631
217	35V-1S-1-cpx3	0.7719	14.73	3.36	51.82	22.07	0.0084	0.0264	0.0433	6.34	0.6867	0.1245	0	0	0	0.0221	0.0148	100.0181
218	35V-1S-1-cpx4	0.7939	14.79	3.14	52.21	21.89	0	0.0347	0.0211	6.21	0.6709	0.1382	0.0145	0.0146	0	0	0	99.9279
219	35V-1S-1-cpx5	0.8076	14.58	3.38	51.8	21.96	0	0.0446	0.0391	6.26	0.7978	0.133	0	0.0145	0	0	0.0148	99.8314
220	35V-1S-1-cpx6	0.7607	14.71	3.48	52.06	22.34	0.0097	0.0182	0.0096	5.94	0.6473	0.1335	0	0.0265	0	0.0278	0.0021	100.1654
221	35V-1S-1-cpx7	0.7483	14.66	3.32	51.95	21.49	0	0.0247	0.0748	6.8	0.7493	0.1757	0.0021	0	0	0	0.0204	100.0153
222	35V-1S-1-cpx8	0.7226	14.67	3.33	52.16	21.92	0	0.0487	0.0369	6.32	0.6961	0.147	0.009	0.0265	0.0048	0	0.0021	100.0937
223	35V-1S-1-cpx9	0.7501	14.6	3.56	51.82	21.95	0	0.038	0.0464	6.52	0.7177	0.1419	0.0329	0	0.0311	0	0	100.2081
224	35V-1S-1-cpx10	0.8516	14.51	3.67	51.53	21.86	0.0103	0.0124	0.0273	6.54	0.7758	0.1396	0.0424	0.0053	0.0322	0	0.0076	100.0145

225	35V-1S-1-cpx11	0.7048	15.59	3.49	51.68	19.96	0	0.0099	0.0494	7.42	0.77	0.1608	0	0	0	0	0.0382	99.8731
226	35V-1S-1-cpx12	0.7678	14.71	3.54	51.96	22.06	0.0009	0.0562	0.0127	6.16	0.7046	0.1261	0.0081	0.0344	0.0473	0	0.0255	100.2136

Table C 3

OLIVINE

Point	Sample – point name	Na ₂ O	MgO	Al ₂ O ₃	SiO ₂	CaO	K ₂ O	Cr ₂ O ₃	V ₂ O ₃	FeO	TiO ₂	MnO	NiO	ZrO ₂	ZnO	Ce ₂ O ₃	CoO	Total
90	30V-4N-5-ol1	190.21	52.67	0.008	39.79	0	0	0	0	18.91	0.0021	0.208	0.081	0.0225	0.0101	0	0.0306	301.9423
91	30V-4N-5-ol2	0	40.95	0.0007	38.86	0.0006	0	0	0.012	19.06	0.0158	0.2021	0.0996	0.0203	0.0375	0	0.0519	99.3105
92	30V-4N-5-ol3	0.0044	40.84	0.0088	38.68	0	0.0042	0.0208	0.0021	19.27	0	0.2002	0.1012	0	0.0238	0	0.0594	99.2149
93	30V-4N-5-ol4	0.0116	40.85	0.0156	38.95	0.0087	0	0	0.0129	19.27	0	0.1992	0.0493	0	0.0273	0.0027	0.0393	99.4366
94	30V-4N-5-ol5	0.0068	40.82	0.0154	38.83	0	0.0018	0	0	18.9	0.0038	0.1832	0.0557	0	0.0286	0.0493	0.0209	98.9155
95	30V-4N-5-ol6	0	41.04	0.0081	38.88	0	0	0.0077	0.001	18.77	0	0.1932	0.0608	0	0.0054	0	0.0769	99.0431
96	30V-4N-5-ol7	0	40.74	0.0069	38.9	0	0	0	0	19.16	0	0.1982	0.0936	0	0.0065	0	0.0673	99.1725
97	30V-4N-5-ol8	0.012	40.49	0.0054	38.83	0	0	0.0225	0	19	0.0027	0.2108	0.0808	0	0.0321	0	0.0661	98.7524
98	30V-4N-5-ol9	0.0176	40.84	0.0063	39	0	0.0031	0.0047	0.004	19.47	0	0.2275	0.0757	0	0.0303	0.0193	0.0426	99.7411
99	30V-4N-5-ol10	0.0476	40.84	0.0139	38.8	0	0	0.0031	0	19.1	0	0.2259	0.0698	0	0.003	0.1015	0.0703	99.2751
100	30V-4N-5-ol11	0.1114	41.98	0.0133	39.12	0	0	0	0	18.06	0	0.1759	0.0873	0.0352	0.0434	0.0489	0.0323	99.7077
101	30V-4N-5-ol12	0	40.61	0.0063	38.85	0	0.0013	0.0147	0.007	18.95	0	0.2095	0.069	0.0122	0.0137	0.0448	0.0519	98.8404
114	30V-4N-6-ol1	0	40.96	0.0143	38.8	0.0049	0.005	0.0023	0	18.78	0.0152	0.2108	0.0712	0	0	0	0.0595	98.9232
115	30V-4N-6-ol2	0	41.04	0.0067	38.88	0	0.0086	0	0	18.64	0.0052	0.1864	0.0712	0	0.0536	0	0.0721	98.9638
116	30V-4N-6-ol3	0.0083	40.82	0.0139	38.72	0	0.0068	0	0	18.97	0	0.1802	0.0979	0	0.0255	0	0.0536	98.8962
117	30V-4N-6-ol4	0	40.85	0.0121	38.81	0	0.0068	0.0109	0.008	19	0.0334	0.205	0.0694	0	0.0338	0.0369	0.0733	99.1496
118	30V-4N-6-ol5	0	40.8	0.0156	38.75	0	0.0003	0	0	18.95	0.0741	0.2	0.0618	0.0109	0	0	0.0678	98.9305
119	30V-4N-6-ol6	0.0221	40.94	0.021	38.77	0	0	0	0	19.05	0.0421	0.1852	0.0839	0	0	0.0119	0.0742	99.2004
120	30V-4N-6-ol7	0.0594	40.91	0.004	38.81	0	0.0068	0	0	18.46	0.048	0.1908	0.0827	0	0.0013	0	0.0403	98.6133
121	30V-4N-6-ol8	0.0096	40.43	0.0146	38.47	0	0.0018	0	0.03	19.56	0.0141	0.2047	0.0932	0	0.0059	0.0288	0.0448	98.9075
122	30V-4N-6-ol9	0.0057	40.28	0.0152	38.61	0.0049	0.0104	0.017	0	19.31	0.0131	0.2049	0.0779	0.0311	0	0.0035	0.0791	98.6628
123	30V-4N-6-ol10	0	40.86	0.0079	38.88	0	0.0039	0.0395	0.0099	19.15	0.0045	0.2232	0.0571	0.0176	0	0.0905	0.0888	99.4329
124	30V-4N-6-ol11	0.0082	41.07	0.0088	38.85	0	0.0065	0.0039	0	18.81	0	0.208	0.0806	0.0244	0	0.0387	0.0541	99.1632
125	30V-4N-6-ol12	0	41.03	0.0001	38.77	0	0	0	0.0059	19.06	0.0073	0.2112	0.0865	0.0257	0	0	0.0793	99.276
126	30V-4N-6-ol13	0.0618	40.97	0.0072	38.65	0	0.0005	0	0	18.94	0.0048	0.2079	0.0877	0	0.0678	0.0459	0.0793	99.1229
127	30V-4N-6-ol14	0.024	40.96	0.0214	38.73	0	0.0057	0	0	19.18	0.0027	0.2359	0.0536	0	0	0.0071	0.0524	99.2728

128	30V-4N-6-ol15	0.0021	41.05	0.0071	38.84	0	0	0.0365	0	18.97	0.009	0.1825	0.0848	0.0054	0.0434	0.0272	0.0579	99.3159		
129	30V-4N-6-ol16	0	40.98	0.0041	38.78	0	0.0003	0.0085	0.007	18.54	0	0.189	0.0822	0.0176	0.0207	0.0837	0.0537	98.7668		
156	30V-4N-8-ol1	0	41.04	0.0086	38.98	0	0	0.0124	0.0021	19.31	0	0.204	0.1006	0	0.0316	0.0042	0.0788	99.7723		
157	30V-4N-8-ol2	0	40.73	0.0141	38.87	0	0	0.0062	0.0291	19.64	0.0159	0.2282	0.1014	0	0.1106	0	0.0691	99.8146		
158	30V-4N-8-ol3	0.0152	40.62	0.0091	38.99	0	0	0	0.008	19.66	0	0.1957	0.1005	0.0298	0	0.0233	0.0365	99.6881		
159	30V-4N-8-ol4	0.0092	41.03	0.0174	38.91	0	0.0009	0	0	19.64	0	0.2029	0.0452	0.0217	0	0.0428	0.075	99.9951		
160	30V-4N-8-ol5	0.0152	41.05	0.0127	38.92	0.0001	0	0	0	19.79	0.0135	0.2133	0.0737	0	0.0392	0	0.0742	100.2019		
161	30V-4N-8-ol6	0.0235	40.71	0.01	38.86	0	0	0.0046	0	19.93	0.0197	0.2156	0.098	0	0	0.017	0.0583	99.9467		
162	30V-4N-8-ol7	0.0054	40.78	0.0052	38.8	0	0.0008	0	0	19.51	0.0244	0.1846	0.0614	0.0149	0.0161	0.0008	0.0783	99.4819		
163	30V-4N-8-ol8	0	39.97	0.0171	38.46	0	0	0.0077	0	20.26	0	0.208	0.0872	0.0014	0.0137	0	0.0716	99.0967		
164	30V-4N-8-ol9	0.0156	39.78	0.0019	38.65	0.0017	0.0024	0.0046	0.024	20.32	0.0103	0.2174	0.0826	0.0094	0.0131	0	0.044	99.177		
165	30V-4N-8-ol10	0	40.15	0.0111	38.73	0.0057	0	0	0.008	20.1	0.0124	0.2335	0.0753	0	0.0124	0	0.0603	99.3987		
166	30V-4N-8-ol11	0.0188	40.69	0.0016	38.71	0	0	0	0.0238	20.13	0.0027	0.2258	0.0937	0.0094	0.013	0	0.082	100.0008		
167	30V-4N-8-ol12	0	41.22	0.0058	39.06	0.004	0.0039	0.0085	0.0169	19.39	0	0.2055	0.0932	0.0379	0.0309	0	0.075	100.1516		
168	30V-4N-8-ol13	0.0222	40.68	0.0206	38.88	0	0	0.0092	0.0289	19.61	0	0.2256	0.0876	0.0136	0.0297	0.0097	0.0669	99.684		
169	30V-4N-8-ol14	0.0177	41.09	0.0131	39.01	0	0	0.0101	0	19.17	0.0035	0.2063	0.0693	0	0	0.0831	0.0753	99.7484		
170	30V-4N-8-ol15	0.0125	39.88	0.0169	39.42	0.0172	0	0	0.0089	18.26	0.0196	0.2059	0.0859	0	0	0.0174	0.0782	98.0225		
171	30V-4N-8-ol16	0	40.16	0.0074	38.83	0	0	0	0.001	20.03	0	0.2509	0.0937	0.0149	0.0242	0.0089	0.0367	99.4577		
227	35V-1S-2-ol1	0	41.42	0.0018	39.24	0.0002	0.003	0.0093	0	18.61	0.0014	0.2169	0.0989	0	0.0364	0.0841	0.0529	99.7749		
228	35V-1S-2-ol2	0.0139	41.27	0.0108	39.13	0	0	0	0.0051	18.4	0	0.1827	0.0636	0	0.0013	0.0015	0.0361	99.115		
229	35V-1S-2-ol3	0.0205	41.05	0.0159	38.62	0.0007	0	0.0256	0	19.31	0.0031	0.2195	0.0835	0	0.0244	0.0228	0.0637	99.4597		
230	35V-1S-2-ol4	0.0191	41.06	0.0108	38.95	0	0	0.0194	0.007	19.08	0	0.2023	0.0575	0	0.0297	0.0052	0.0536	99.4946		
231	35V-1S-2-ol5	0	40.69	0.0188	39.06	0	0	0	0	19.3	0.0314	0.216	0.0907	0.0163	0	0	0.0494	99.4726		
232	35V-1S-2-ol6	0	40.98	0.001	38.94	0.0042	0	0.017	0	19.44	0	0.2072	0.0877	0.0176	0.0262	0.0012	0.0594	99.7815		
233	35V-1S-2-ol7	0	41.72	0.02	38.9	0.0008	0	0.0053	0.0178	18.99	0.0219	0.2004	0.0735	0	0.013	0	0.0368	99.9995		
234	35V-1S-2-ol8	0	41.33	0.004	39.11	0	0	0	0.003	18.66	0.0076	0.2283	0.0946	0	0.0321	0	0.0641	99.5337		
235	35V-1S-2-ol9	0.0028	42	0.017	39.02	0.0016	0.0069	0	0.0051	17.89	0.0073	0.1861	0.0947	0	0.0048	0	0.0633	99.2996		
236	35V-1S-3-ol1	0	41.68	0.0157	39.25	0	0	0.0218	0	18.33	0	0.1716	0.0759	0	0	0	0.0403	99.5853		
237	35V-1S-3-ol2	0.0166	41.19	0.0138	39.19	0	0	0	0.0091	19.22	0.0197	0.2162	0.0972	0.0203	0.0096	0.022	0.0705	100.095		
238	35V-1S-3-ol3	0.0054	41.36	0.0046	39.15	0	0	0.0124	0	18.46	0	0.2069	0.0925	0	0.0238	0	0.0734	99.389		

239	35V-1S-3-ol4	0	41.03	0	39.07	0	0	0	0	19.18	0.0135	0.2305	0.0996	0	0.0327	0.0394	0.0302	99.7259
240	35V-1S-3-ol5	0.0206	41.1	0.0052	39.05	0	0	0	0.004	19.1	0.0017	0.2089	0.0886	0	0.041	0	0.0577	99.6777
241	35V-1S-3-ol6	0.0128	40.77	0.0093	39.06	0	0.0066	0	0.004	19.76	0.0076	0.2182	0.0817	0.0136	0.0381	0.0285	0.0624	100.0728
242	35V-1S-3-ol7	0.0231	41.1	0.012	39.18	0.0099	0	0	0.0131	19.1	0.0031	0.1825	0.0694	0	0	0.0245	0.0607	99.7783
243	35V-1S-3-ol8	0.2521	42.04	0.0013	39.38	0	0.0411	0.0117	0	17.87	0.0253	0.1916	0.0874	0	0	0.0423	0.0621	100.0049
244	35V-1S-3-ol9	0.0147	42.08	0.0152	39.28	0.0034	0	0.0109	0.0051	17.97	0	0.1899	0.0703	0	0.0387	0.0417	0.0553	99.7752
245	35V-1S-3-ol10	0	43.5	0.0078	39.56	0	0	0	0	16.89	0.0098	0.1953	0.0961	0	0	0	0.0677	100.3267
246	35V-1S-3-ol11	0.0111	41.8	0.0081	39.32	0.0045	0	0.0039	0	18.07	0.0003	0.1605	0.0473	0	0	0.0301	0.0465	99.5023
247	35V-1S-3-ol12	0	42.19	0.0132	39.47	0	0	0.0086	0.01	18.08	0	0.2148	0.0827	0	0.0125	0	0.0545	100.1363

Table C 4
BIOTITE

Point	Sample – point name	Na ₂ O	MgO	F	Al ₂ O ₃	SiO ₂	CaO	Cr ₂ O ₃	K ₂ O	FeO	TiO ₂	MnO	Cl	H	Total
1	35v1s-4-bt1	2.41	11.81	0.1145	12.73	40.49	11.67	0.0449	1.63	10.55	5.41	0.0873	0.043	4	100.9897
2	35v1s-4-bt2	2.38	12.06	0.0998	12.81	40.84	11.61	0.0792	1.66	10.85	5.33	0.0761	0.017	4	101.8121
3	35v1s-4-bt3	2.29	12.36	0.0875	13.02	40.81	11.63	0.0466	1.74	10.66	5.25	0.0542	0.0225	4	101.9708
4	35v1s-4-bt4	0.2025	16.15	0.2741	14.77	37.09	0	0.0655	9.87	8.85	8.96	0.0263	0.0185	4	100.2769
5	35v1s-4-bt5	0.199	16.46	0.2173	14.83	36.99	0.0044	0.0755	9.89	8.54	9.14	0.0234	0.0209	4	100.3905
6	35v1s-4-bt6	0.1616	16.37	0.1432	14.76	37.13	0.0084	0.0459	9.85	8.92	9.11	0.0278	0.0169	4	100.5438
7	35v1s-4-bt7	0.2103	15.89	0.2344	14.81	36.9	0	0.0499	9.88	9.25	8.96	0	0.0177	4	100.2023
8	35v1s-4-bt8	0.1714	15.98	0.3094	14.77	37.3	0.0108	0.0549	9.85	9.05	9.03	0.0244	0.014	4	100.5649
9	35v1s-4-bt9	2.3	12.06	0.0534	12.88	40.08	11.7	0.0638	1.74	10.74	5.24	0.0732	0.0233	4	100.9537
10	35v1s-4-bt10	2.3	12.38	0.2141	12.81	40.27	11.6	0.0425	1.75	10.73	5.17	0.084	0.0223	4	101.3729
11	35v1s-4-bt11	2.27	12.35	0.0518	12.85	39.18	11.57	0.0875	1.7	10.53	5.24	0.0346	0.0248	4	99.8887
12	35v1s-4-bt12	2.48	11.67	0.119	12.64	39.82	11.6	0.0726	1.62	11.51	5.55	0.0741	0.0228	4	101.1785
13	35v1s-4-bt13	2.51	11.61	0.1454	12.7	40.1	11.68	0.0759	1.59	11.55	5.57	0.0708	0.0215	4	101.6236
14	35v1s-4-bt14	2.47	11.66	0.1593	12.66	40.19	11.68	0.0859	1.57	11.27	5.58	0.0669	0.0236	4	101.4157
15	30v4n-7-bt1	0.1263	15.57	0.284	14.73	36.69	0.0284	0.0385	9.84	9.41	9.36	0	0.0184	4	100.0956
16	30v4n-7-bt2	0.1376	15.6	0.241	14.83	36.37	0.0135	0.0246	10	9.55	9.29	0.0146	0.012	4	100.0833
17	30v4n-7-bt3	0.1901	14.62	0.2146	14.74	36.07	0.026	0.0416	9.69	10.73	9.37	0.0156	0.008	4	99.7159
18	30v4n-7-bt4	0.2737	15.78	0.2087	14.7	36.86	0.0052	0.0739	9.89	8.85	9.31	0	0.0522	4	100.0037
19	30v4n-7-bt5	0.2873	15.83	0.2342	14.71	36.77	0.007	0.0377	9.89	9.17	9.36	0.0117	0.042	4	100.3499

Table C 5
PLAGIOCLASE

Point	Sample – point name	Na ₂ O	MgO	Al ₂ O ₃	SiO ₂	CaO	TiO ₂	SrO	BaO	FeO	K ₂ O	MnO	Total
1	35v1s-1-plag1	6.04	0	26.79	57.52	9.1	0.0614	0.1482	0	0.0647	0.482	0	100.2063
2	35v1s-1-plag2	6.29	0.0049	26.31	58.37	8.56	0.0388	0.1609	0.0075	0.0675	0.5067	0.0059	100.3222
3	35v1s-1-plag3	6.22	0	26.54	58.03	8.81	0.0304	0.1953	0.0117	0.0765	0.5384	0	100.4523
4	35v1s-1-plag4	5.7	0.0062	27.31	56.76	9.85	0.0645	0.1429	0	0.074	0.4276	0.0034	100.3386
5	35v1s-1-plag5	5.6	0.0318	27.62	56.48	9.93	0.0407	0.1433	0.0041	0.0895	0.4212	0	100.3606
6	35v1s-1-plag6	6.25	0.0042	26.22	58.21	8.57	0.0154	0.162	0.0028	0.0645	0.4426	0.02	99.9615
7	35v1s-1-plag7	6.24	0	26.45	58.04	8.69	0.0312	0.1441	0	0.0663	0.4923	0.0127	100.1666
8	35v1s-1-plag8	6.26	0	26.39	58.2	8.66	0.0589	0.1668	0.012	0.1067	0.4798	0.0064	100.3406
9	35v1s-1-plag9	5.67	0	27.29	56.69	9.67	0.0733	0.1565	0	0.0888	0.4568	0	100.0954
10	35v1s-1-plag10	6.09	0.0182	26.65	57.27	9.06	0.0547	0.1606	0	0.1241	0.4817	0	99.9093
11	35v1s-1-plag11	6.53	0.0024	26.06	57.76	8.43	0.0388	0.1654	0.0189	0.0694	0.4383	0.0049	99.5181
12	35v1s-4-plag1	6.4	0.0083	25.97	58.08	8.37	0.0286	0.1676	0.0321	0.0756	0.5602	0	99.6924
13	35v1s-4-plag2	6.03	0.013	26.66	57.4	8.96	0.0264	0.1503	0.0283	0.0513	0.5127	0.0073	99.8393
14	35v1s-4-plag3	6.25	0.0533	26.28	57.88	8.62	0.0034	0.1509	0.001	0.1101	0.5085	0.0078	99.865
15	35v1s-4-plag4	6.29	0.1463	26.32	57.29	8.69	0.0202	0.1643	0	0.1915	0.4501	0.0054	99.5678
16	35v1s-4-plag5	6.23	0.2569	26.2	57.51	8.49	0.0143	0.1287	0	0.2555	0.4788	0	99.5642
17	35v1s-4-plag6	6.46	0	26.15	57.97	8.44	0.017	0.1381	0.0116	0.1032	0.5269	0.0019	99.8187
18	35v1s-4-plag7	6.46	0	26.02	58.09	8.3	0.0493	0.1751	0.0119	0.0799	0.5522	0	99.7384
19	35v1s-4-plag8	6.61	0	25.78	58.7	8.04	0.0168	0.164	0.026	0.0836	0.6244	0	100.0448
20	35v1s-4-plag9	6.07	0	26.44	56.72	9.06	0.0438	0.1401	0	0.1134	0.5051	0.0274	99.1198
21	35v1s-4-plag10	6.56	0	26.11	58.54	8.27	0.0186	0.1857	0.0185	0.075	0.5764	0.0029	100.3571
22	35v1s-4-plag11	6.38	0	26.42	58.13	8.65	0.0279	0.1729	0.01	0.09	0.473	0	100.3538
23	30v4n-9-plag1	6.77	0.0026	25.33	59.41	7.49	0.021	0.1484	0	0.1315	0.7905	0.0044	100.0984
24	30v4n-9-plag2	6.59	0.0042	25.33	59.15	7.62	0.0146	0.1491	0.011	0.1504	0.8557	0.0083	99.8833
25	30v4n-9-plag3	6.56	0	25.36	58.8	7.69	0.0077	0.1382	0	0.1418	0.9812	0	99.6789
26	30v4n-9-plag4	6.33	0.7881	25.1	56.52	7.6	0.0317	0.1825	0.0026	1.2185	0.5779	0	98.3513
27	30v4n-9-plag5	5.98	0.0127	26.75	56.58	9.12	0.0245	0.1365	0	0.0879	0.5512	0	99.2428
28	30v4n-9-plag6	5.96	0	26.6	56.82	9.08	0.0476	0.1998	0	0.1069	0.5044	0	99.3187
29	30v4n-9-plag7	5.85	0.0127	26.89	56.55	9.38	0.0952	0.1731	0.0167	0.0954	0.4715	0.0097	99.5443
30	30v4n-9-plag8	6.24	0.001	26.27	57.56	8.51	0.0366	0.1523	0.0114	0.1218	0.607	0	99.5101
31	30v4n-9-plag9	5.97	0.014	26.67	56.83	9.2	0.0869	0.1799	0.0361	0.0926	0.4929	0.0352	99.6076
32	30v4n-9-plag10	5.72	0.0148	27.14	56.61	9.51	0.0645	0.1325	0	0.0747	0.5374	0	99.8039
33	30v4n-9-plag11	6.35	0.0036	25.91	58.55	8.16	0.0323	0.1864	0.0191	0.0886	0.6252	0	99.9252
34	30v4n-9-plag12	6.35	0.0229	26.23	57.98	8.49	0.0574	0.1745	0.0294	0.0979	0.5582	0	99.9903
35	30v4n-9-plag13	6.52	0.0018	25.84	58.31	8.12	0.0277	0.1519	0	0.1	0.729	0.0171	99.8175
36	30v4n-9-plag14	5.96	0	26.48	57.41	8.95	0.0477	0.1752	0.0252	0.0851	0.5821	0.0083	99.7236
37	30v4n-9-plag15	5.85	0.0213	26.6	57.07	9.21	0.0477	0.1581	0	0.0823	0.5819	0	99.6213
38	30v4n-9-plag16	6.17	0.0148	26.39	57.34	8.8	0.0327	0.1556	0	0.0886	0.5344	0	99.5261
39	30v4n-9-plag17	6.05	0.015	26.4	57.48	8.72	0.0399	0.1695	0	0.0821	0.6049	0	99.5614
40	30v4n-9-plag18	6.07	0	26.47	57.66	8.78	0.0393	0.1339	0.0014	0.0982	0.6751	0.0078	99.9357
41	30v4n-9-plag19	6.26	0	25.89	58.56	8.2	0.0152	0.1499	0.0002	0.0987	0.7375	0.0059	99.9174

Table C 6

ILMENITE												
Point	Sample – point name	MgO	Al ₂ O ₃	TiO ₂	V ₂ O ₃	Cr ₂ O ₃	FeO	As ₂ O ₅	MnO	NiO	ZnO	Total
9	3-ilm1	2.03	0.0385	47.36	0.3443	0.0457	48.68	0	0.3057	0.0191	0.0478	98.8711
10	3-ilm2	1.98	0.0443	48.1	0.2806	0.0255	47.94	0.0979	0.3351	0.0257	0.0006	98.8297
11	3-ilm3	2.01	0.0061	48.59	0.2862	0.0437	47.69	0.1306	0.3293	0.0341	0	99.12
12	2-ilm1	3	0.0552	47.79	0.3231	0.0349	48.06	0.025	0.3142	0	0.0636	99.666
13	2-ilm2	2.97	0.0672	47.71	0.3454	0.0386	47.61	0.075	0.3083	0	0.0169	99.1414
14	2-ilm3	3.02	0.0333	48.2	0.3104	0.0525	47.65	0.0039	0.3526	0.0115	0.0517	99.6859
15	2-ilm4	3.05	0.0495	48.68	0.3495	0.0197	47	0.2077	0.3296	0.0081	0.0614	99.7555
16	2-ilm5	2.96	0.0632	47.78	0.3507	0.0576	47.33	0	0.3176	0.0092	0.0805	98.9488
17	7-ilm6	3.06	0.0332	48.16	0.3264	0.0467	46.97	0.1385	0.3218	0.0269	0.0849	99.1684
18	7-ilm7	3.12	0.0449	48.64	0.338	0.0343	46.97	0	0.2958	0	0.031	99.474
19	7-ilm8	2.99	0.0388	48.04	0.3764	0.0255	47.12	0.0154	0.3062	0.0614	0.1103	99.084
23	7-ilm9	3.22	0.017	49.17	0.3348	0.0351	46.47	0.0077	0.3432	0.0062	0.0648	99.6688
24	7-ilm10	3.2	0.032	48.72	0.2973	0.0051	47.07	0.0307	0.3136	0	0.0697	99.7384
27	9-ilm1	3.11	0.0357	49.25	0.3209	0.0168	46.64	0.0443	0.3584	0	0.0103	99.7864
28	9-ilm2	3.1	0.0265	49.53	0.2944	0.0264	46.38	0.231	0.3331	0	0.0071	99.9285
29	9-ilm3	3.16	0	48.84	0.2652	0.0212	46.77	0.0058	0.3706	0	0.0038	99.4366
30	9-ilm4	3.11	0.0479	48.65	0.2939	0.0358	46.96	0	0.3091	0	0	99.4067
31	9-ilm5	3.14	0.0289	49.42	0.3157	0.0667	46.15	0.0771	0.3409	0.0184	0.0201	99.5778
32	9-ilm6	3.13	0.0495	50.16	0.2692	0.0081	45.65	0.1927	0.3375	0	0.0495	99.8465

Table C 7

LAMELLAS

Point	Sample – point name	Na ₂ O	MgO	Al ₂ O ₃	SiO ₂	CaO	K ₂ O	Cr ₂ O ₃	V ₂ O ₃	FeO	TiO ₂	MnO	NiO	ZrO ₂	ZnO	Ce ₂ O ₃	CoO	Total
40	30V-4N-2-lam1	0.0618	12.26	0.9302	28.92	2.55	0.0041	0.0508	0.1507	29.97	24.34	0.3099	0.0322	0.0112	0.0607	0	0.0615	99.7131
41	30V-4N-2-lam2	0	21.04	1.4249	37.23	0.3499	0	0.2109	0.2116	37.3	0.4179	0.2244	0.0505	0.0039	0.0115	0	0.0763	98.5518
42	30V-4N-2-lam3	0	22.8	1.454	45.86	0.4667	0.0015	0.0311	0.0656	20.24	7.49	0.3108	0.011	0.012	0.0348	0	0.0615	98.839
43	30V-4N-2-lam4	0.0164	27.12	1.8556	53.33	0.6837	0	0.0158	0.0051	15.14	0.1961	0.2509	0.0381	0.0083	0.055	0.033	0.0459	98.7939
84	30V-4N-4-lam1	0.0106	27.29	1.96	54.09	0.5646	0.1206	0	0.0324	14.81	0.2546	0.2977	0.021	0	0.0776	0	0.0393	99.5684
85	30V-4N-4-lam2	0.0186	27.08	1.9	54	0.7241	0.0037	0.0048	0	15.2	0.2075	0.283	0.0304	0	0.0035	0	0.0358	99.4914
86	30V-4N-4-lam3	0.01	25.36	1.776	52.61	0.5181	0	0.0102	0.0141	16.25	0.3835	0.2973	0.0154	0.0151	0.0131	0	0.0529	97.3257
87	30V-4N-4-lam4	0.0652	17.19	1.6687	25.19	0.0926	0.0029	0.4008	0.4399	51.66	0.4974	0.1104	0.0829	0.0228	0	0	0.1026	97.5262
88	30V-4N-4-lam5	0.0162	26.13	1.6726	50.93	0.5291	0.0044	0.0335	0.0693	17.86	0.4424	0.2765	0.0383	0.03	0.0386	0	0.08	98.1509
89	30V-4N-4-lam6	0.0203	26.97	1.8392	54.11	0.7093	0	0	0	15.12	0.208	0.2692	0.0342	0.0055	0	0	0.0434	99.3291

Table C 8
SULPHIDES

Point	Sample – point name	Se	As	Fe	Mn	Co	Cu	Zn	S	Ni	Total
1	30V-4N-9-sulfide1	0.1409	0.3039	45.77	0	0.9493	0.0035	0	53.88	0.0211	101.0687
2	30V-4N-9-sulfide2	0.232	0.275	44.93	0	1.76	0.0082	0	53.94	0.0583	101.2035
3	30V-4N-9-sulfide3	0.0456	0.1341	29.91	0	0.0134	34.54	0.0317	34.72	0.0294	99.4242
4	30V-4N-9-sulfide4	0.129	0.2242	30.21	0	0.0274	34.76	0.027	34.65	0.0514	100.079
5	30V-4N-9-sulfide5	0.2144	0.2755	44.22	0.0019	2.43	0.0219	0	53.81	0.0361	101.0098
6	30V-4N-9-sulfide6	0.0786	0.1093	29.82	0	0.0347	35.01	0.0181	34.87	0.0509	99.9916
7	30V-4N-9-sulfide7	0.1805	0.1556	29.49	0.0005	0.8926	0.0396	0	33.2	36.09	100.0488
8	30V-4N-9-sulfide8	0.2469	0.522	64.67	0.0029	0.0348	0	0	0	0.0575	65.5341
9	30V-4N-9-sulfide9	0.3221	0.5318	63.95	0	0.0432	0	0	0	0.0525	64.8996
10	30V-4N-9-sulfide10	0.4723	0.6357	64.74	0.0071	0.023	0	0.0057	0	0.066	65.9498
11	30V-4N-9-sulfide11	0.1467	0.2667	45.73	0	1.04	0.0048	0.0033	53.82	0.0176	101.0291
12	30V-4N-9-sulfide12	0.1686	0.1512	29.99	0.0056	0	34.75	0.0251	34.68	0.0108	99.7813
13	30V-4N-9-sulfide13	0.0787	0.1028	30.15	0.0073	0.0081	34.62	0.0448	34.41	0.0202	99.4419
14	30V-4N-9-sulfide14	0.1969	0.2585	45.53	0	1.22	0.0038	0	53.84	0.0203	101.0695
15	30V-4N-9-sulfide15	0.1431	0.2242	30.3	0	0.0034	34.6	0.0347	34.9	0.0171	100.2225
16	30V-4N-9-sulfide16	0.1175	0.1361	30.33	0	0.0181	34.64	0.0206	34.39	0.0224	99.6747
17	30V-4N-9-sulfide17	0.1446	0.173	58.8	0	0.0396	0.2786	0	39.6	1.01	100.0458
18	30V-4N-9-sulfide18	0.1513	0.2018	59.06	0.0053	0.0441	0.303	0	39.54	0.9802	100.2857
19	30V-4N-9-sulfide19	0.1045	0.1065	30.1	0.0071	0.0255	34.6	0.0344	34.72	0.039	99.737
20	30V-4N-9-sulfide20	0.1169	0.1431	28.34	0	1.57	0.1849	0	32.92	36.63	99.9049
21	30V-4N-9-sulfide21	0.1559	0.1782	58.74	0	0.0353	0.2355	0	39.44	1.15	99.9349
22	30V-4N-9-sulfide22	0.106	0.1495	30.1	0.0013	0	34.2	0.0207	34.76	0.0639	99.4014

APPENDIX D – SEM ANALYSES

- Bulk data
- Liberation data
- Mineral association data
- Locking data

Due to large amounts of data Appendix D is given in a OneDrive map
use link below:

<https://1drv.ms/u/s!AmgC6nPn5vhpy1-q5LOIR1fBk4Eq?e=jbTmOT>

(Appendix D is only available in the digital version of the thesis)

APPENDIX E – SEM ELEMENT MAPS

E 1 -2,5V-1L – 348 ampere

E 2 -2,5V-1L – 778 ampere

E 3 -1,5V-1L – 548 ampere

E 4 -1,5V-1L – non-magnetic material

E 5 0,5V-1L – 348 ampere

E 6 0,5V-1L – 548 ampere

E 7 3,5V-1S – 148 ampere

E 8 3,5V-1S – 548 ampere

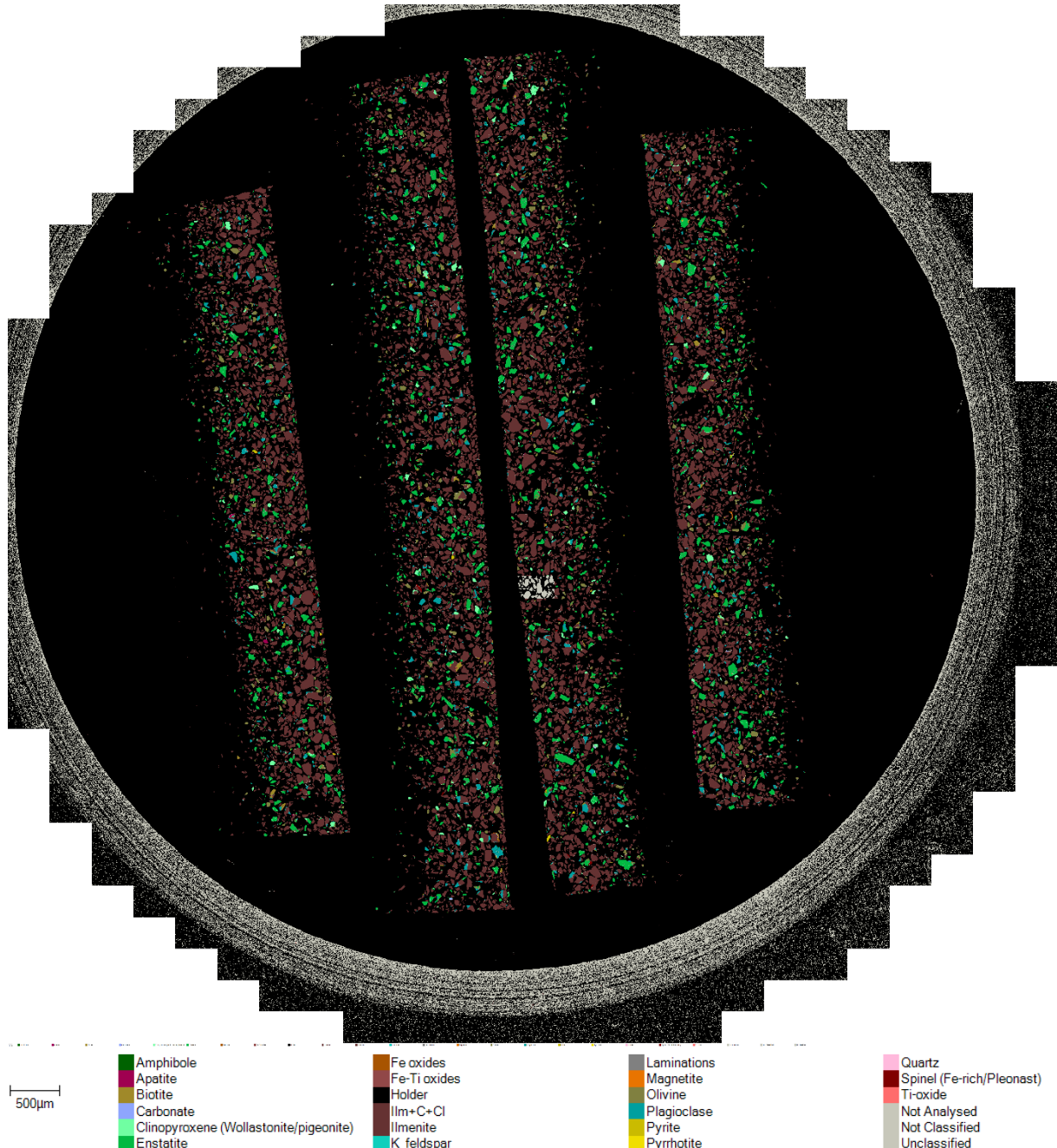
E 9 5,0V-5N – 348 ampere

E 10 5,0V-5N – 548 ampere

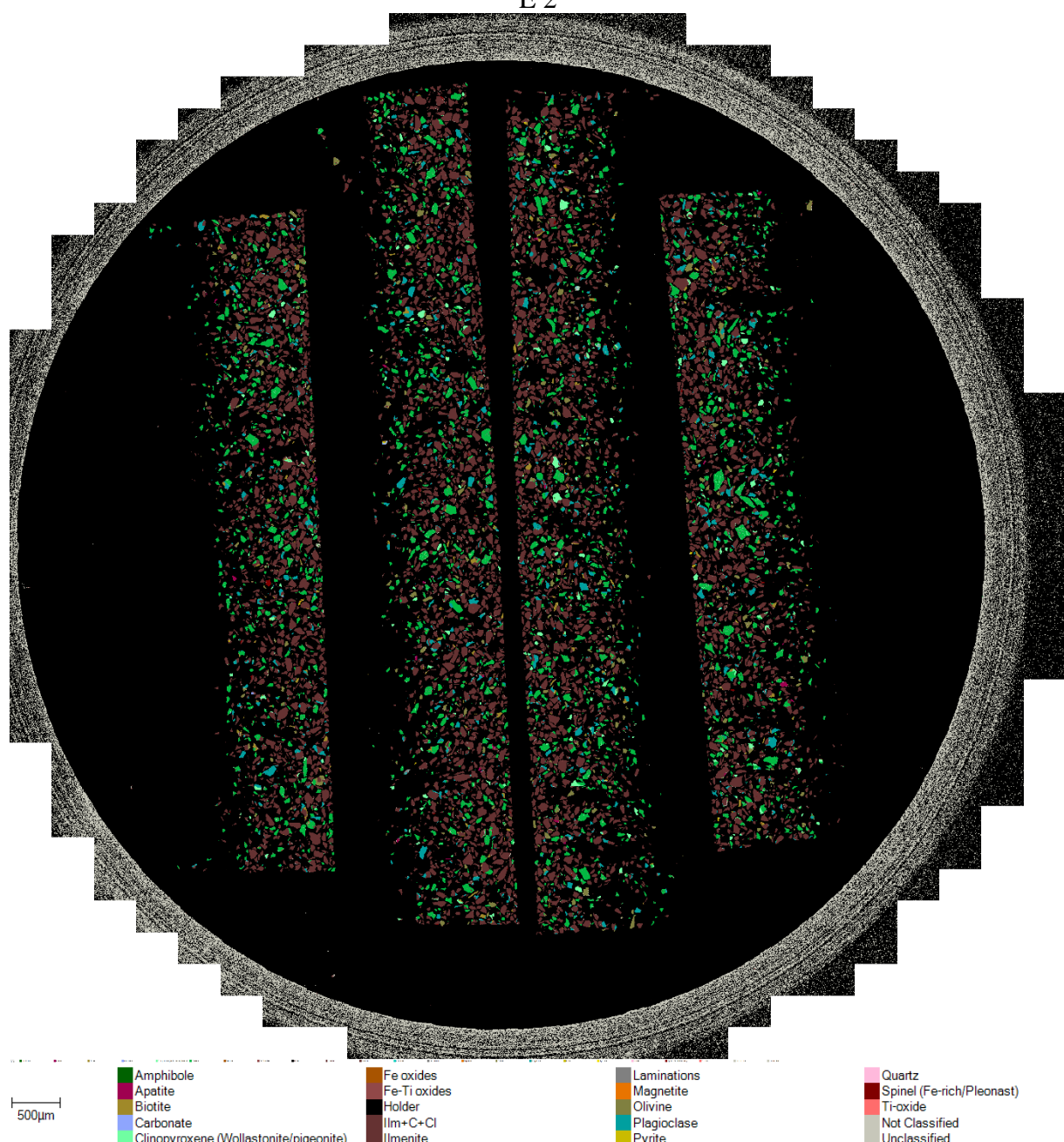
E 11 6,3V-1L – 348 ampere

E 12 6,3V-1L – 548 ampere

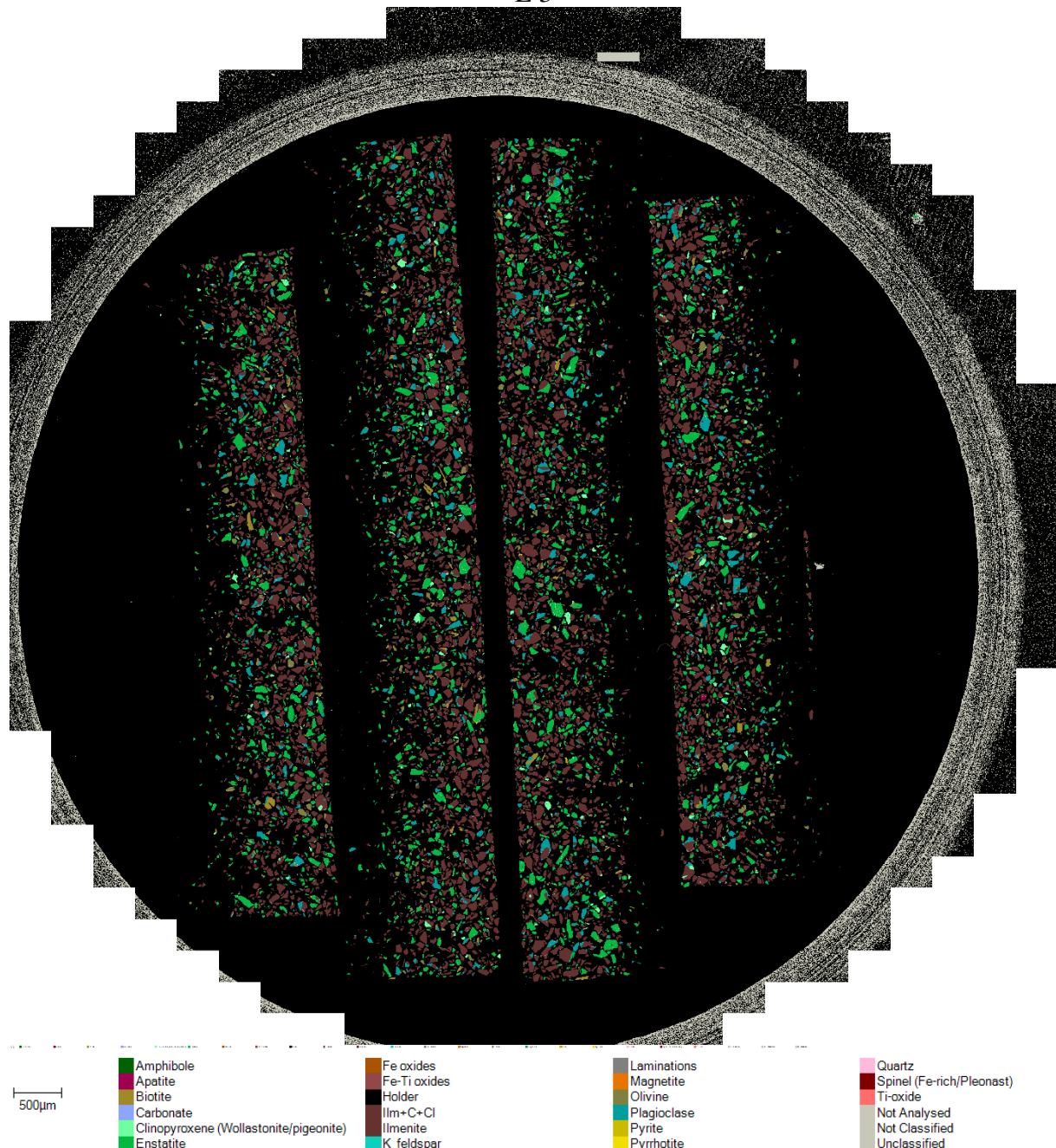
E 1



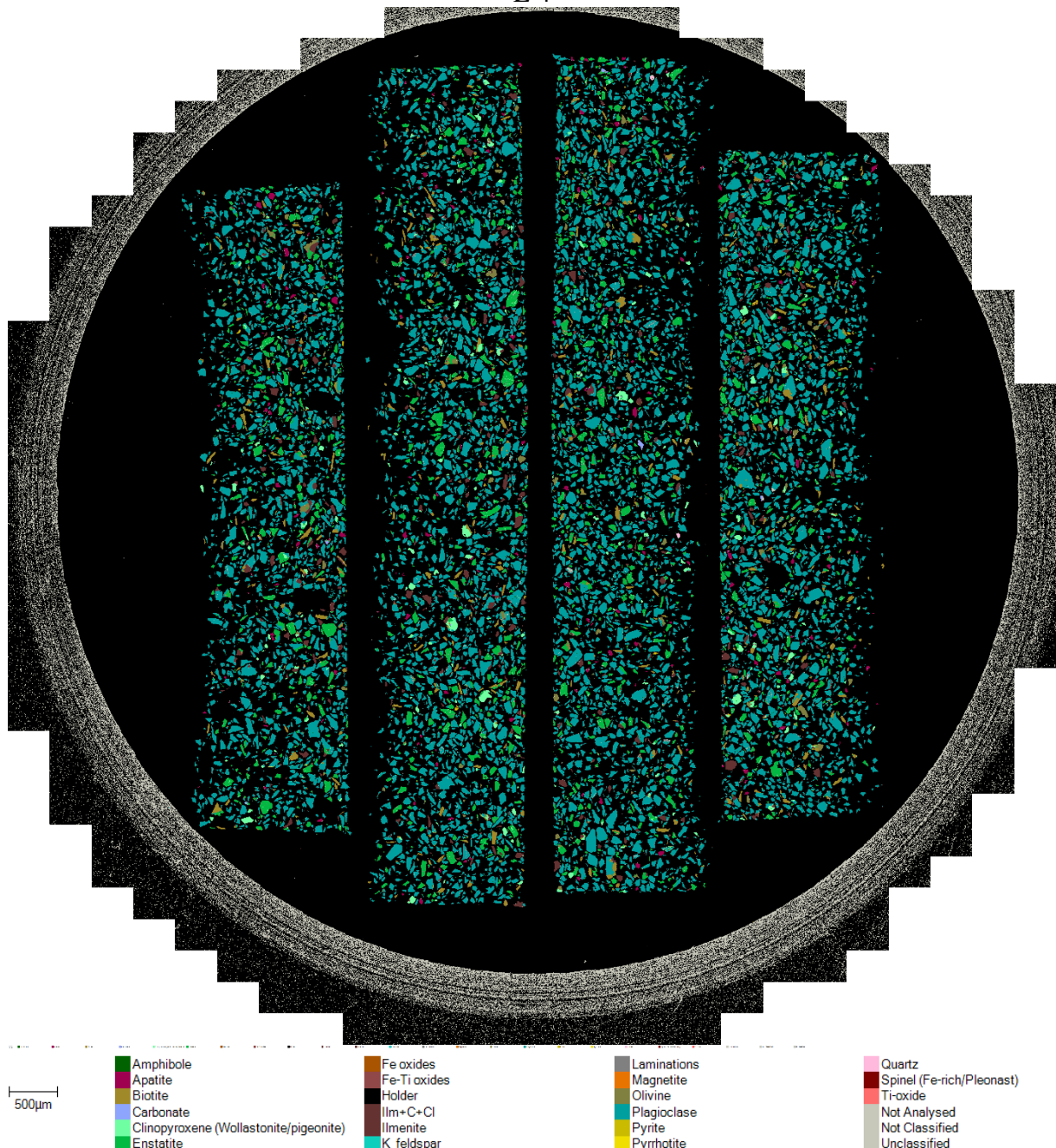
E 2



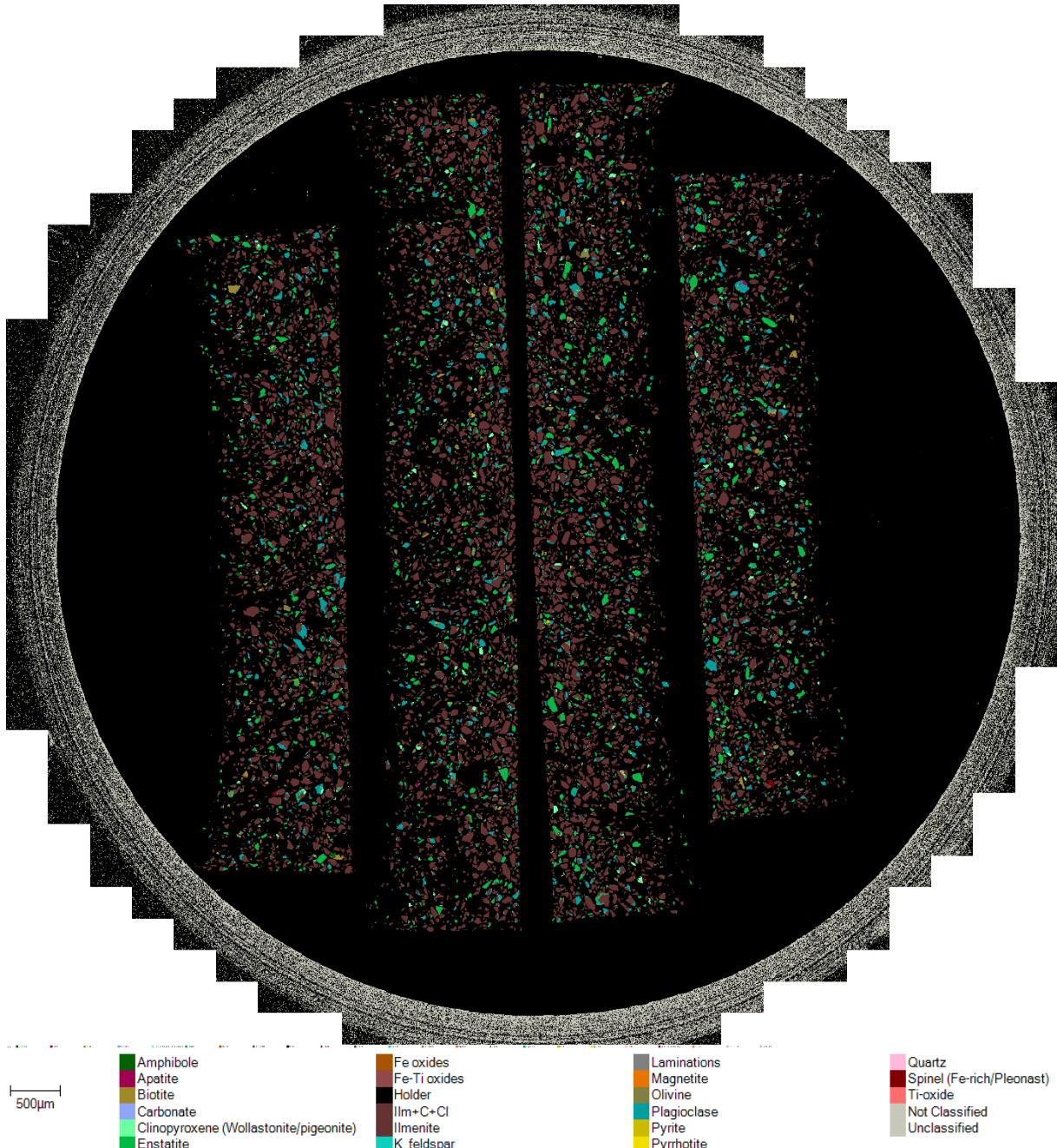
E 3



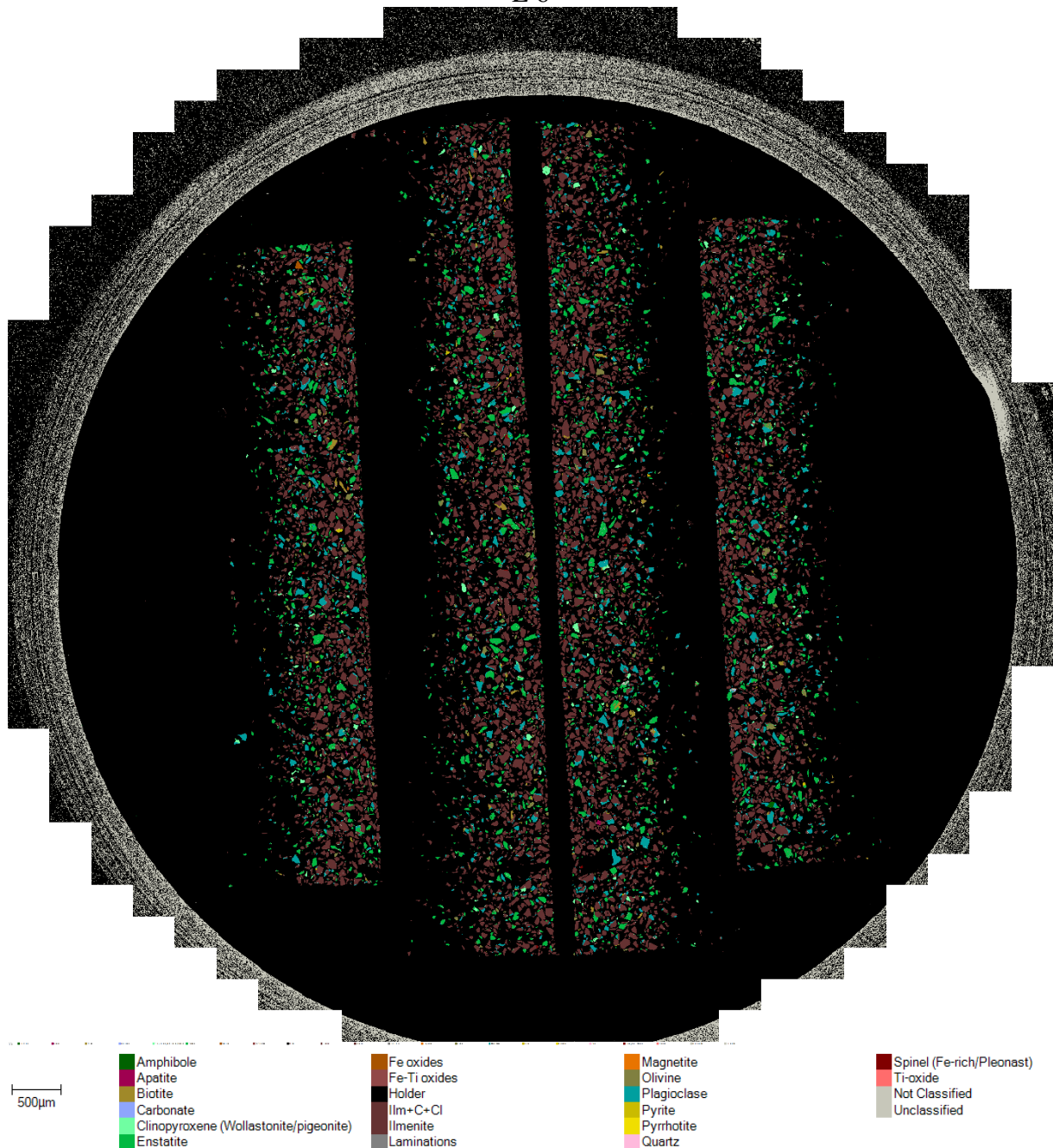
E 4



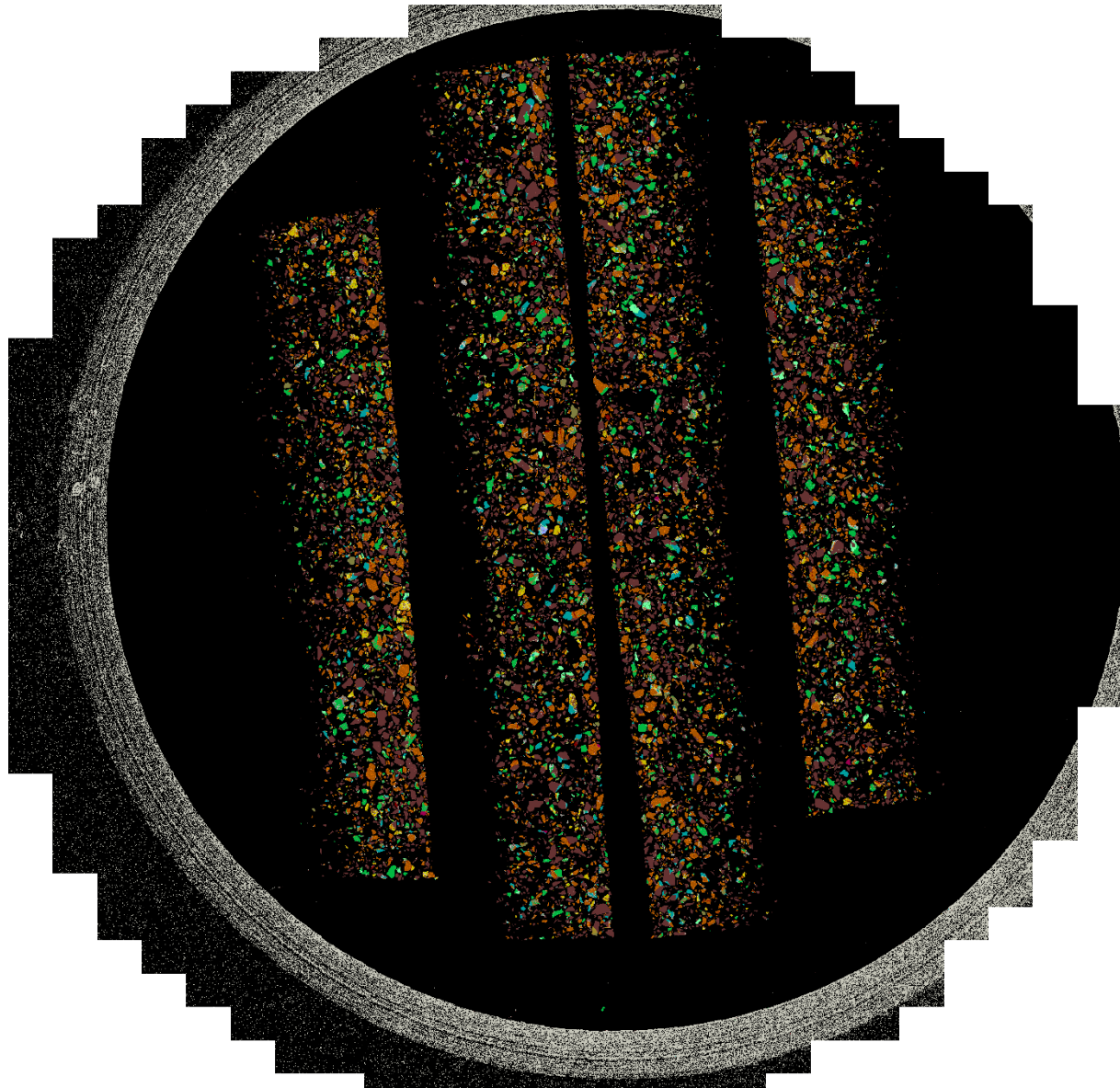
E 5



E 6



E 7



500µm

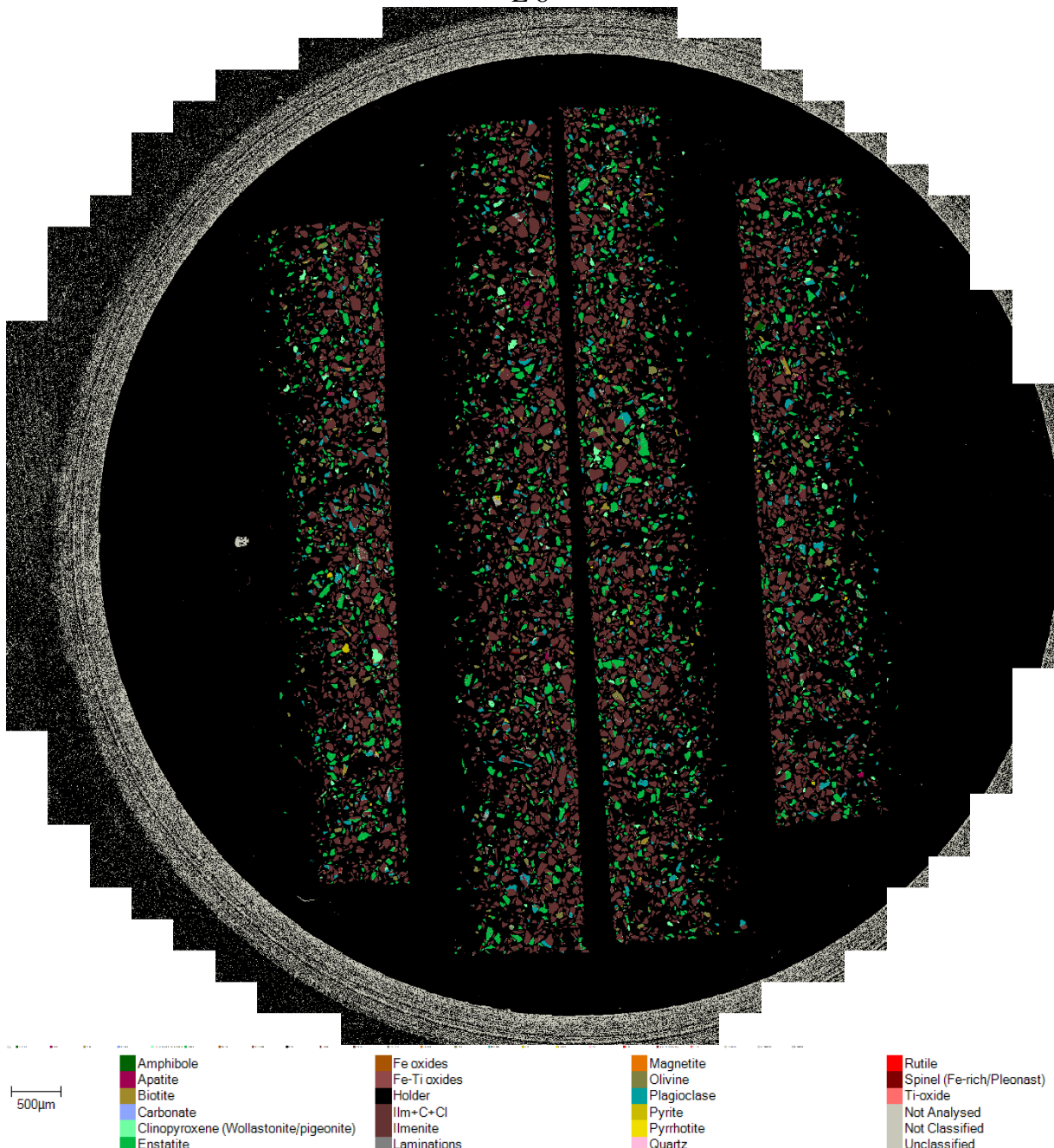
Amphibole
Apatite
Biotite
Carbonate
Clinopyroxene (Wollastonite/pigeonite)
Enstatite

Fe oxides
Fe-Ti oxides
Holder
Ilm+C+Cl
Ilmenite
K feldspar

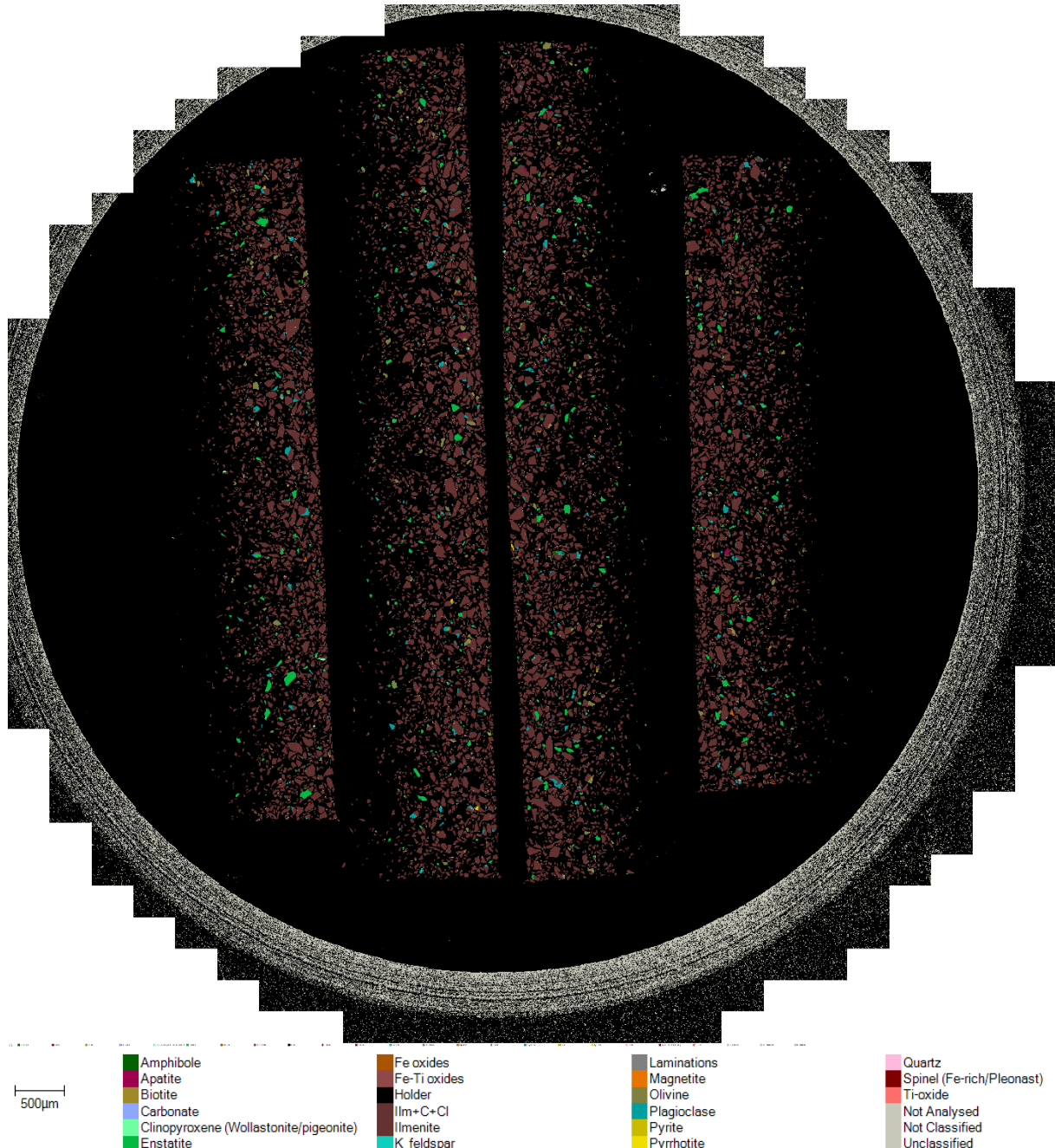
Laminations
Magnetite
Olivine
Plagioclase
Pyrite
Pyrhotite

Quartz
Spinel (Fe-rich/Pleonast)
Ti-oxide
Not Classified
Unclassified

E 8



E 9

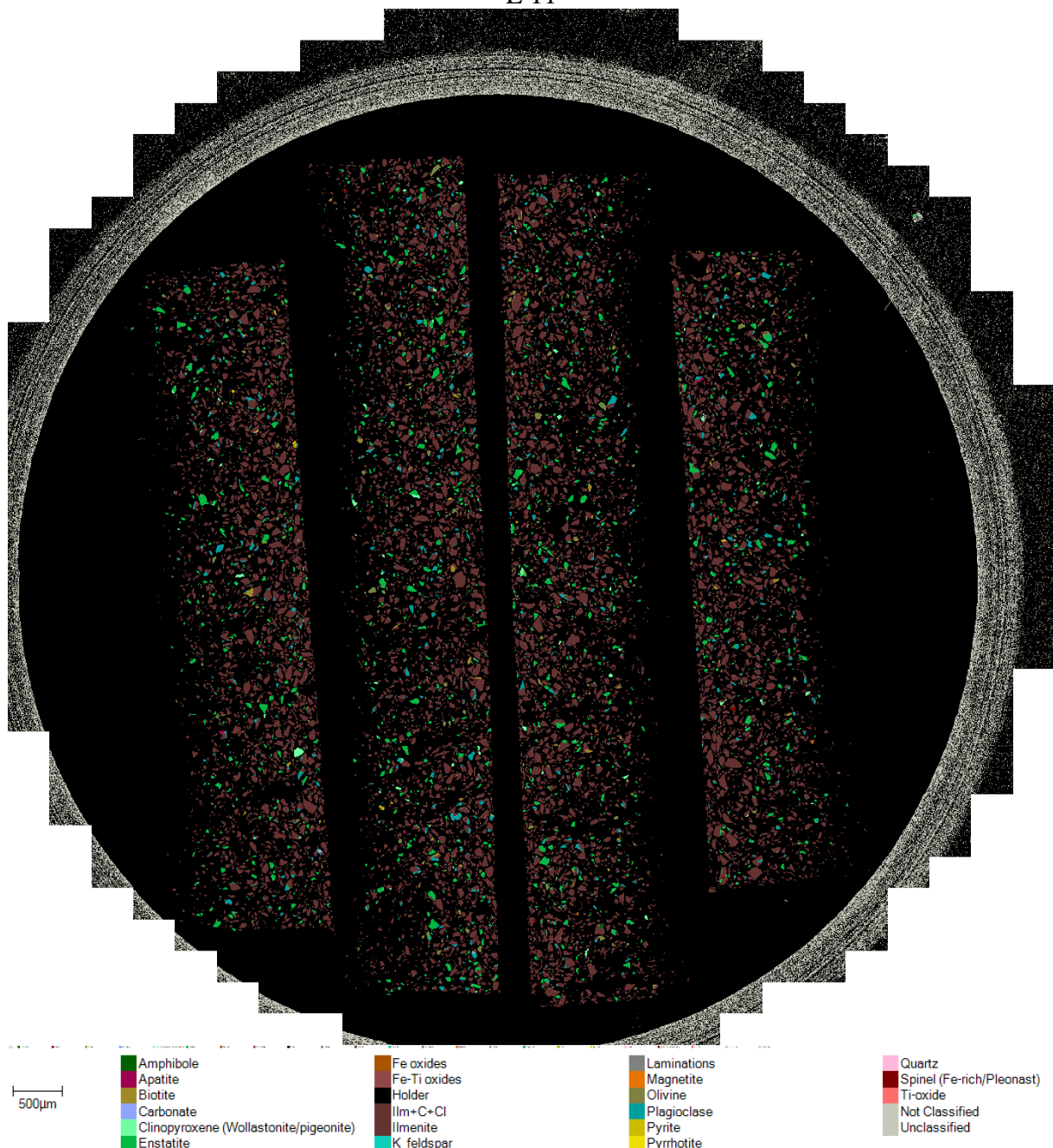


E 10

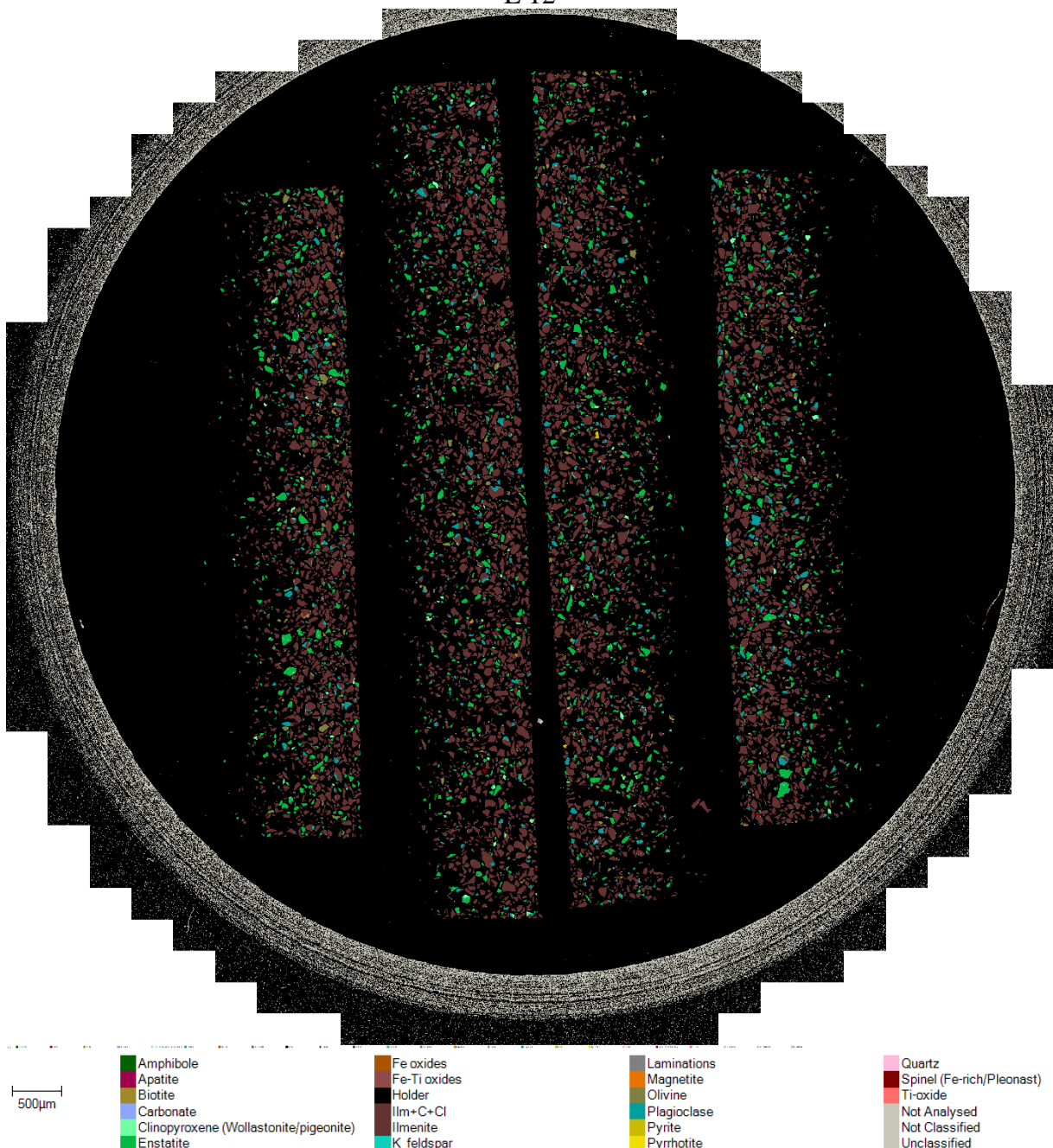


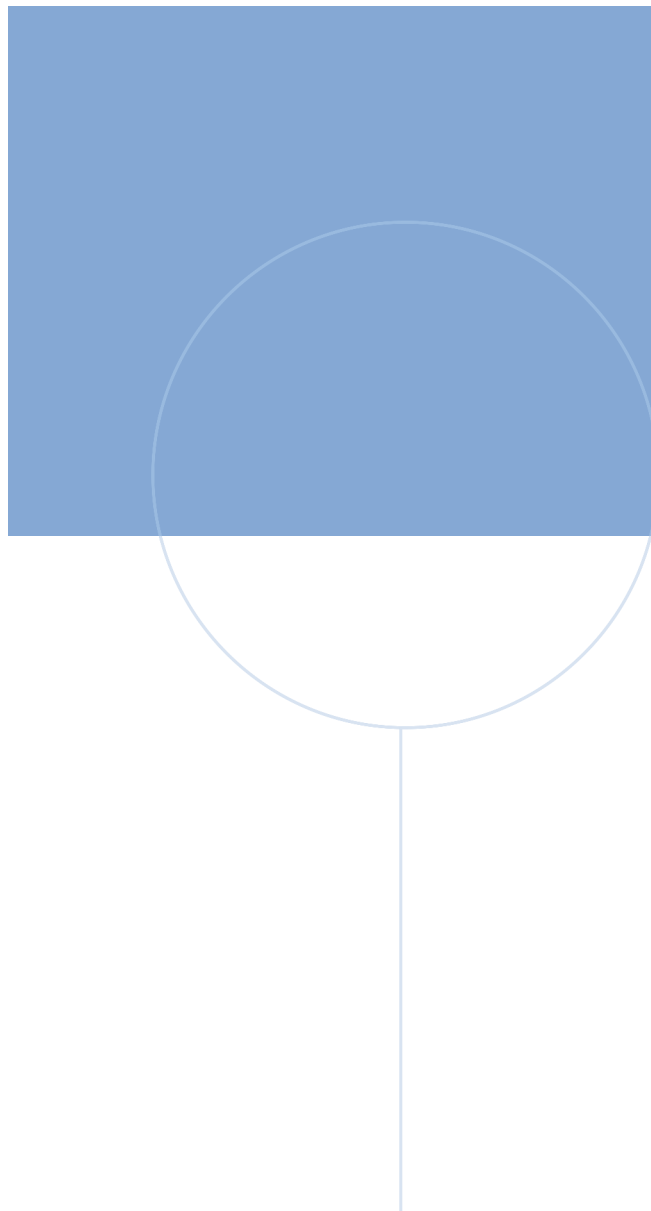
500 μm

E 11



E 12





NTNU
Norwegian University of
Science and Technology